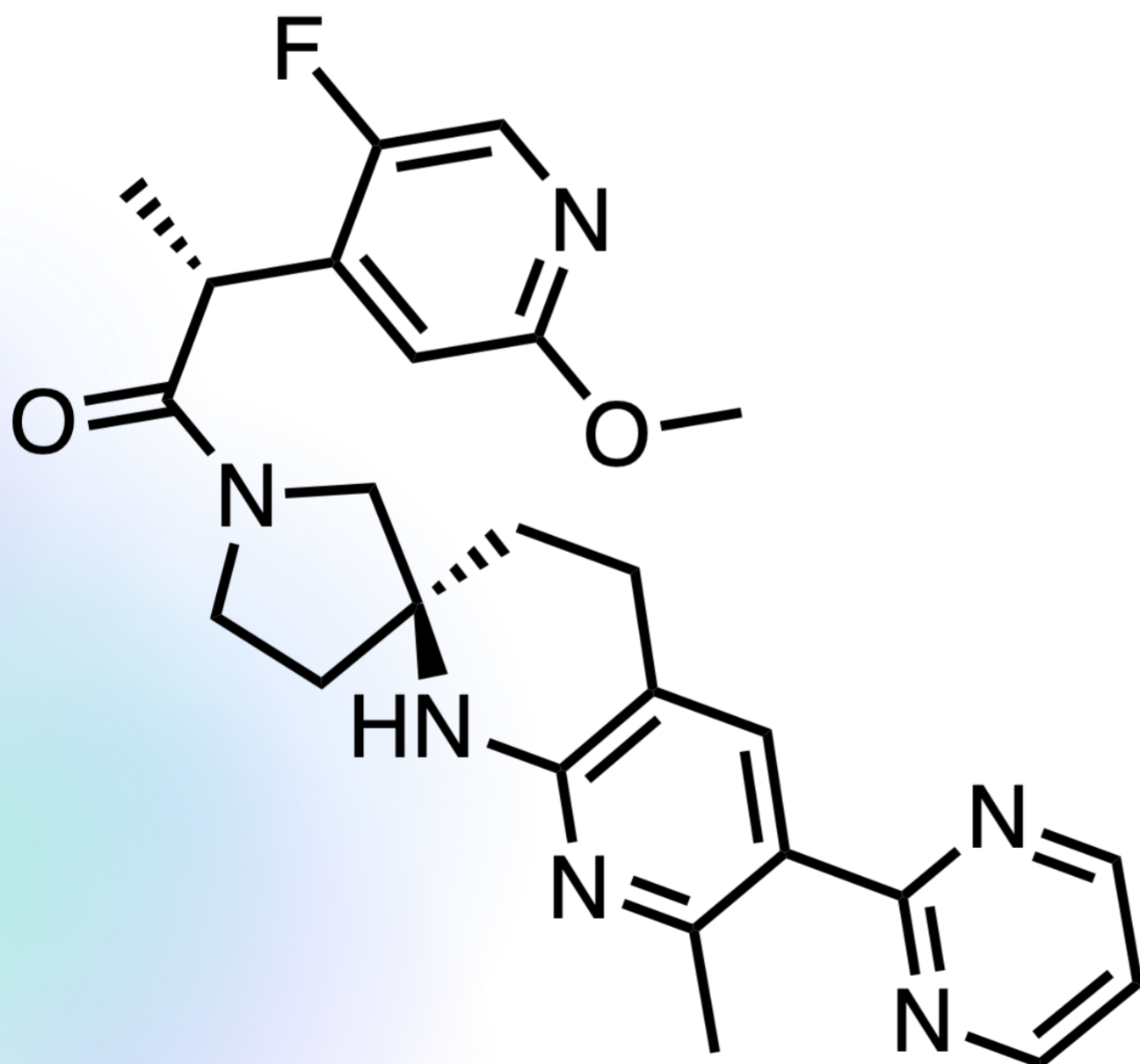


drughunter.com

Small Molecules of the Month

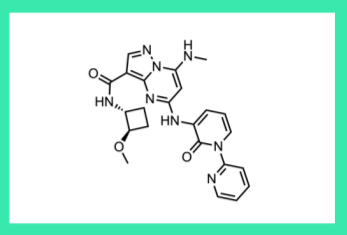
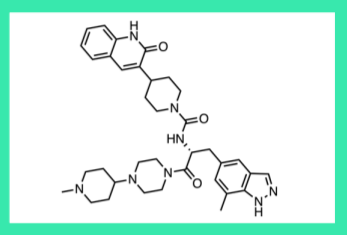
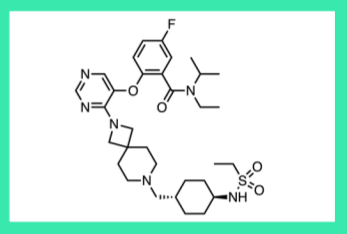
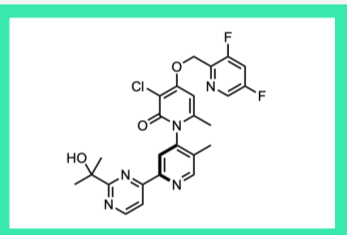
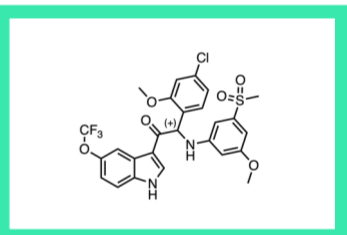
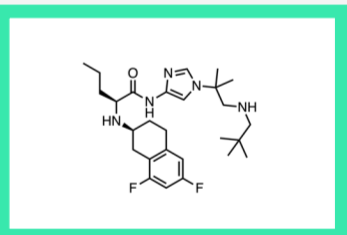
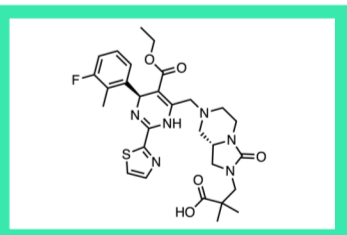
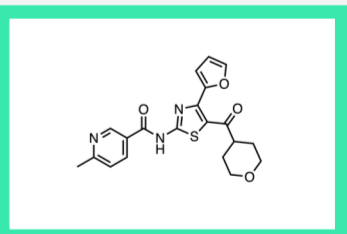
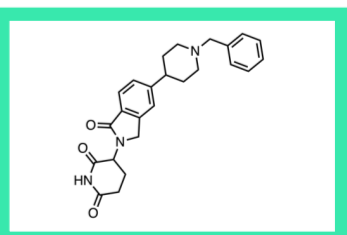
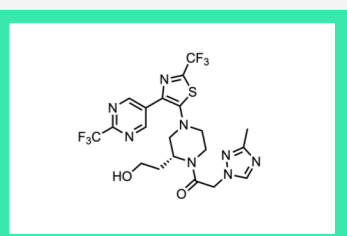
March 2023



drug
hunter

Table of Contents

March 2023

Page 3	TAK-279 TYK2	oral, once-daily, allosteric TYK2 inhibitor	Ph. IIb for moderate-to-severe plaque psoriasis	NIMBUS THERAPEUTICS, MA / TAKEDA, JP	
Page 6	zavegepant CGRP	CGRP receptor antagonist, first nasal spray	FDA-approved for acute migraines in adults	BRISTOL MYERS SQUIBB, NY / PFIZER, INC., NY	
Page 8	revumenib menin-KMT2A	oral menin-KMT2A inhibitor	Ph. I/II for r/r leukemia, CRC & solid tumors	VITAE, MADISON, NJ / SYNDAX, WALTHAM, MA	
Page 11	zunsemetinib MK2	oral p38α-MK2 inhibitor	Ph. IIa for hidradenitis suppurativa (failed)	CONFLUENCE, MO / ACLARIS THERAPEUTICS, PA	
Page 13	JNJ-1802 DENV	oral first-in-class DENV (NS3-NS4B) inhibitor	Ph. I for dengue	JANSSEN, BE + FR	
Page 15	nirogacestat gamma secretase	oral gamma secretase inhibitor	Ph. III for DT/AF + Ph. II for OvGCTs	PFIZER / SPRINGWORKS THERAPEUTICS, INC.	
Page 17	linvencorvir HBV core protein	allosteric HBV modulator	Ph. II for chronic hepatitis B (CHB)	ROCHE, SHANGHAI, CN	
Page 21	KW-6356 A _{2A} R	oral A _{2A} receptor antagonist/inverse agonist	Ph. II for Parkinson's Disease	KYOWA KIRIN CO., LTD., SHIZUOKA, JP	
Page 23	DKY709 IKZF2	oral IKZF2-selective molecular glue degrader	Ph. I/IIb for adv. solid tumors	NOVARTIS, CAMBRIDGE, MA	
Page 26	ACT-777991 CXCR3	oral reversible CXCR3 antagonist	Ph. I in healthy subjects	IDORSIA PHARMACEUTICALS LTD, CH	

March 2023

TAK-279

TYK2

oral, once-daily, allosteric TYK2 inhibitor

Ph. IIb for moderate-to-severe plaque psoriasis

FEP+-supported core hopping + VLS

w/ TYK2-JH2 Xtal structure

Press release, March 18, 2023

NIMBUS THERAPEUTICS, MA / TAKEDA, JP

article link:

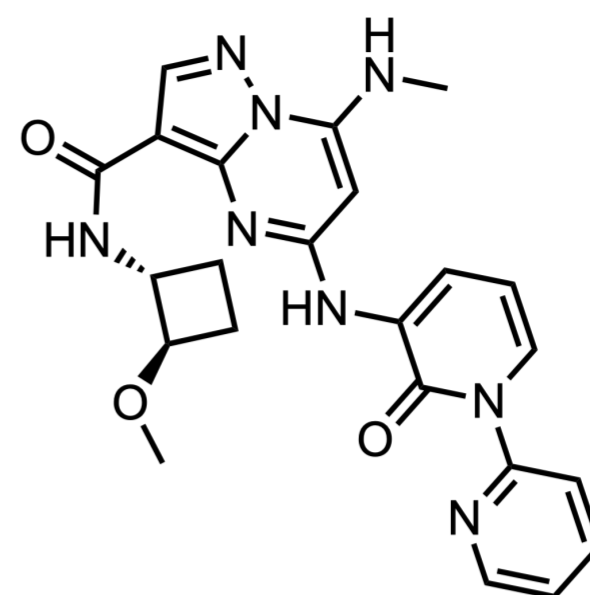
<https://www.takeda.com/newsroom/newsreleases/2023/takeda-announces-positive-results-in-phase-2b-study-of-investigational-tak-279>

[View Online](#)

A potential next best-in-class allosteric TYK2 inhibitor exhibits strong Ph. II results for plaque psoriasis. Takeda Pharmaceuticals has [announced positive results for TAK-279](#) in Ph. IIb for the treatment of moderate-to-severe plaque psoriasis (PsO). [Just disclosed last year](#), TAK-279 (formerly known as NDI-034858) was acquired by [Takeda from Nimbus in a recent \\$4 billion dollar deal](#). This oral, allosteric TYK2 inhibitor reduced the severity of PsO for [~68% of patients](#) at a 15 or 30 mg once-daily dose, enabling a 75% resolution in disease severity at 12 weeks based on PASI score ([NCT04999839](#)). TAK-279 was designed to specifically target the catalytically inactive pseudokinase [JH2 domain](#), which has less homology across the JAK family than between the orthosteric JH1 domains of TYK2 and the JAKs. Inhibitors of the JAK/TYK2-JH1 active site notoriously come with [black-box warnings](#) and, although therapeutically effective, can cause [adverse events](#) including but not limited to serious infections, major cardiovascular events, hematological abnormalities (increased levels of HDL, LDL, triglycerides), and liver toxicity, potentially due to IL-6 inhibition. Selectively targeting the JH2 domain is expected to provide for a more favorable safety profile in the clinic, which is especially crucial for a chronically dosed treatment outside of oncology. Even further, TAK-279's impressive exposures (IC₉₀ coverage for 24 hours) make it suitable for QD dosing and may allow for stronger efficacy than deucravacitinib, which only covers [IC₅₀ for 9 hours](#).

Remarkable selectivity for TYK2-JH2 over JAK-JH2 for a better safety profile, allowing greater efficacy. The hope for Takeda is that TAK-279 will prove to be more efficacious and with a better safety profile than BMS's expected blockbuster, allosteric TYK2 inhibitor and [2022 Molecule of the Year](#), [deucravacitinib \(SOTYKTU®\)](#). TAK-279 is [~1,500,000X selective](#) for the TYK2-JH2 pocket than the JAK1-JH2 pocket (K_d = 0.034 nM vs. 5000 nM), while deucravacitinib shows [~50X selectivity](#) (K_d = 0.009 nM vs. 0.43 nM), Ventyx's [VTX958 is ~4,000X](#) more selective (K_d = 0.058 nM vs. 240 nM), and BMS's [BMS-986202 is ~40X](#) more selective (IC₅₀ = 0.19 nM vs. 7.8 nM). For comparison, first-in-class deucravacitinib reduced psoriasis severity in [53 and 58%](#) of Ph. III patients at 16 weeks (PASI 75 response, [NCT03624127](#), [NCT03611751](#), 6 mg QD), albeit direct comparator trials have not been performed. This stark improvement in selectivity for TAK-279 may allow it to be dosed at consistently higher target coverage levels than the less TYK2-JH2-selective deucravacitinib, allowing an assessment of the efficacy/safety profile at stronger coverage levels.

High demand for oral therapies to treat chronic immunological diseases. More than 8M people in the US have psoriasis and [125M people worldwide](#) (2-3% of population). 60% of those psoriasis patients report it to significantly affect their daily life, with ~40% developing psoriatic arthritis. Where the immunology market has largely been dominated by biologic injectables with clean safety profiles (TNA-a antagonists, IL-12/IL-23 antagonists, IL-23



antagonists, IL-17 antagonists), there has been [great demand for oral treatments](#) that don't require regular injections for the long-term. Oral therapies that have been investigated include TYK2 inhibitors, JAK inhibitors, PDE4 inhibitors, RORγt inhibitors, RIPK1 inhibitors, A3AR agonists, CXCR2 antagonists, and AhR modulators, among others. There has been recent progress toward this goal with the approval of Amgen's PDE4 inhibitor, [OTEZLA®](#) (acquired from a forced sale from Celgene after BMS's acquisition), followed by BMS's allosteric selective TYK2 inhibitor, [SOTYKTU®](#). However, there remains a demand for increased efficacy and improved safety profiles for oral treatments.

The role of TYK2 in psoriasis. TYK2 is a member of the JAK family and is a key component of the JAK-STAT pathway. Increased activation of proinflammatory enzymes in this pathway is associated with several autoimmune diseases, including [psoriasis](#). Specifically, TYK2 is a mediator between IL-23-induced production of pro-inflammatory cytokine IL-17 in Th17 cells, which is thought to be the [primary cytokine responsible](#) for the chronic inflammation in PsO and PsA.

Impressive initial attempts at a TYK2-selective JH1 active site inhibitor. The first generation of TYK2 molecules pursued by Nimbus were [JH1 active site inhibitors](#). The team recognized that orthosteric pan-JAK inhibitor tofacitinib bound to JAK1-3 and TYK2 with a very high degree of similarity, with the gatekeeper methionine conserved across the JAK family. Utilizing proprietary crystal structures and [Schrödinger's Free Energy Perturbation \(FEP\) method](#), a quantitative selectivity model was developed in conjunction with the medicinal chemistry campaign, based upon the FEP-predicted- and measured K_d's of synthesized compounds. Ultimately, the team achieved a [~560X kinome selectivity breakthrough](#) for TYK2 over JAK2 with early lead compound, [NDI-031232](#), by taking advantage of additional interactions with non-conserved residues in the model, along with simultaneous optimization for biochemical and cellular activities. While the selectivity achieved was impressive, it paled in comparison to what was ultimately found with JH2-domain inhibitors, highlighting how the choice of starting point can make all the difference in a program.

A new JH2-selective starting point from a virtual screen. Nimbus disclosed the discovery story of TAK-279/NDI-034858 at the [ACS Fall meeting](#) last year (2022), highlighting the crucial computational chemistry collaboration with Schrödinger that enabled it. One can speculate that it was the tremendous success of this and other Nimbus programs that encouraged Schrödinger to recently enter drug discovery on its own. The starting point (compound 6) for the new program was identified using a virtual screen based on multiple TYK2-JH2 crystal structures. The pyrazolo-pyrimidine had submicromolar affinity for TYK2-JH2 (246 nM), but with >10,000-fold selectivity over JAK1/2/3-JH1.

March 2023

TAK-279

TYK2

oral, once-daily, allosteric TYK2 inhibitor

Ph. IIb for moderate-to-severe plaque psoriasis

FEP+-supported core hopping + VLS

w/ TYK2-JH2 Xtal structure

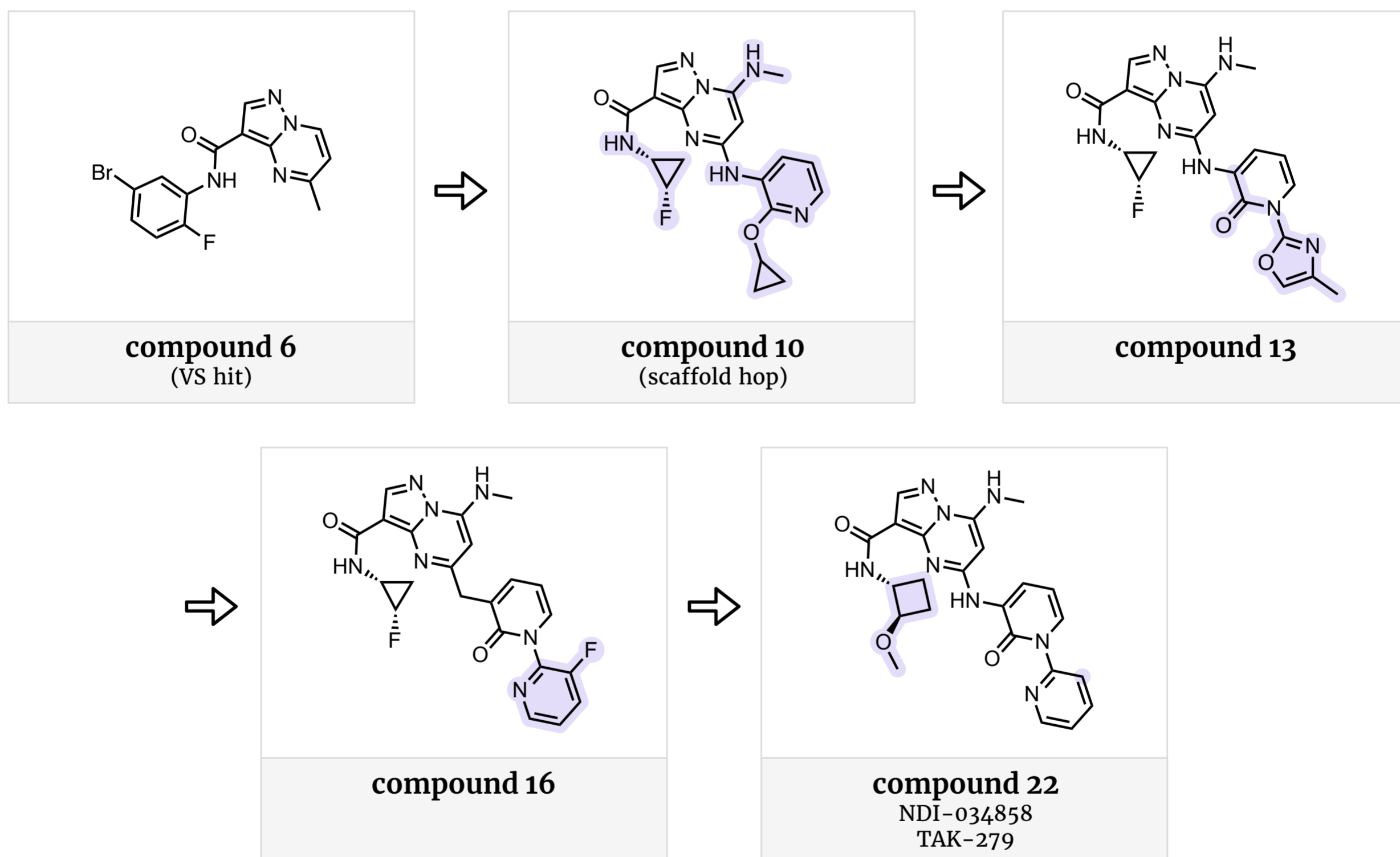
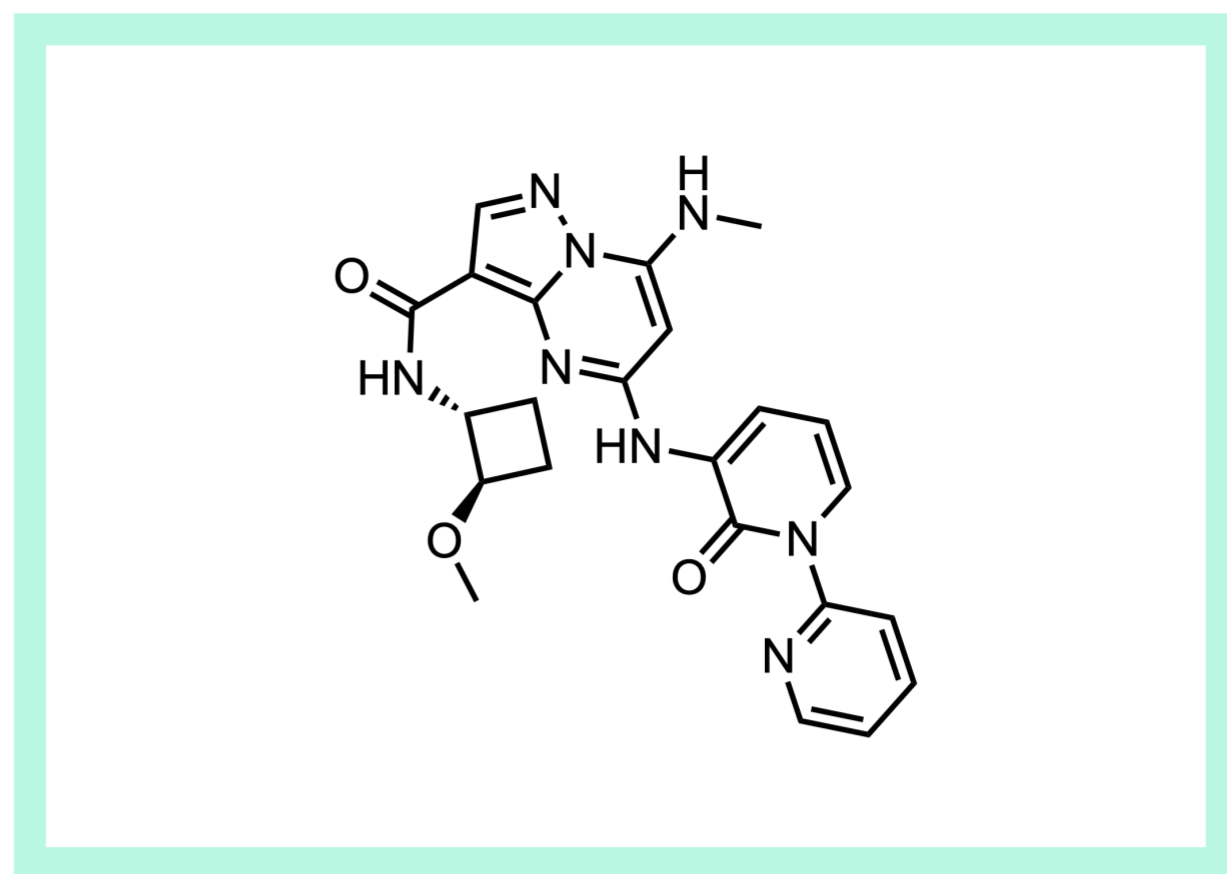
Press release, March 18, 2023

NIMBUS THERAPEUTICS, MA / TAKEDA, JP

article link:

<https://www.takeda.com/newsroom/newsreleases/2023/takeda-announces-positive-results-in-phase-2b-study-of-investigational-tak-279>

[View Online](#)



Computationally-assisted optimization for TYK2-JH2 selectivity. The FEP+ computational approach helped prioritize designs that were likely to be potent, allowing the team to focus on addressing other drug properties. A scaffold hop followed by optimization to mitigate PDE4 off-target activity afforded compound 10 with significantly improved potency (0.059 nM) and ~25,000X selectivity for TYK2-JH2 over PDE4. Cellular potency, PDE4 selectivity, and metabolic stability were generally more favorable when the amino pyridine was replaced with a *N*-(methyloxazole)pyridone (compound 13), while permeability and solubility were improved by an additional swap of the methyloxazole for a fluoro-pyridine (compound 16). While compound 16 had impressive in vitro properties, the projected human dose needed to cover human whole blood IC₅₀ was high (200 mg BID, or >1 g QD). Replacement of the terminal amide with the methoxycyclobutane of compound 22 led to a significant increase in biochemical potency (from 68 pM to 3.8 pM) while maintaining lipophilicity (ALogP = 2.1 for both compounds), contributing to an

increase in whole blood potency (from 330 nM to 51 nM) and metabolic stability (HHep Cl_{pred} from 2 to 0.69 mL/min/kg). Even further, the [projected human dose](#) to cover IC₉₀ for 24 hours was only 50 mg QD.

JH2-selectivity enabled by a single amino acid. The [binding mode](#) of TAK-279 was confirmed using an in-house X-ray crystal structure at 1.83Å (K_d = 0.0038 nM) and indicated the structural basis for selectivity was attributable to a single amino acid in the allosteric binding pocket. An isoleucine (Ile597 for JAK1 and Ile559 for JAK2) is present in the JAK enzymes which is not present in TYK2, causing a steric clash that allows for the significant selectivity over JAK1-JH2 (PDB - [4L00](#), K_d = 5,000 nM) and JAK2-JH2 (PDB - [5UT6](#)). TAK-279 can be technically considered a [Type IV allosteric binder](#) of TYK2 overall, even though its binding to JH2 is reminiscent of a Type I binder, with the pyrazolopyrimidine acting as the hinge binder.

March 2023

TAK-279

TYK2

oral, once-daily, allosteric TYK2 inhibitor

Ph. IIb for moderate-to-severe plaque psoriasis

FEP+-supported core hopping + VLS

w/ TYK2-JH2 Xtal structure

Press release, March 18, 2023

NIMBUS THERAPEUTICS, MA / TAKEDA, JP

article link:

<https://www.takeda.com/newsroom/newsreleases/2023/takeda-announces-positive-results-in-phase-2b-study-of-investigational-tak-279>

[View Online](#)

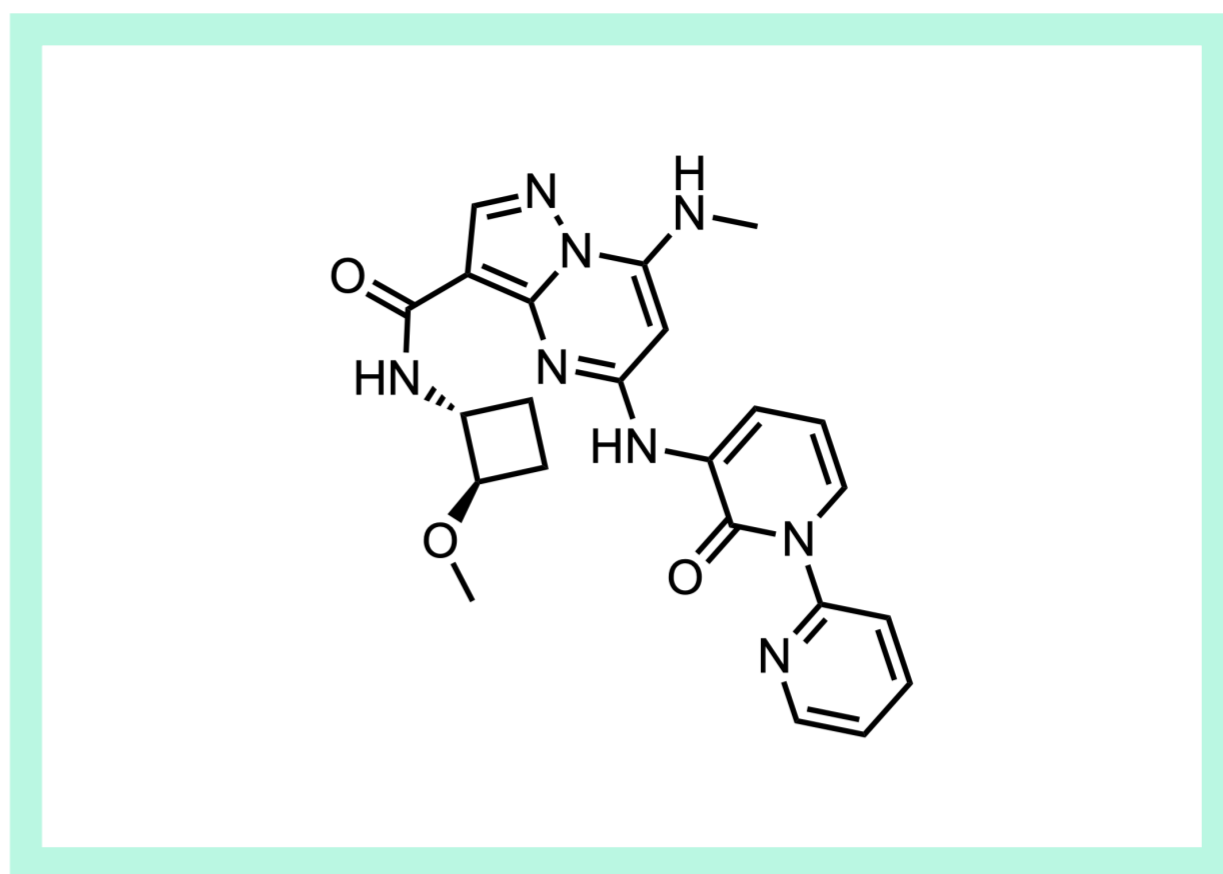
TYK2-JH2 binders	compound 6	compound 10	compound 13	compound 16	compound 22
hTYK2-JH2 K _d	246 nM	0.059 nM	0.082 nM	0.068 nM	0.0038 nM
kinetic solubility (pH 7.4)	-	-	2.5 μM	30 μM	32 μM
hWB IFN α IP-10 IC ₅₀	-	-	428 nM	330 nM	51 nM
projected human dose				200 mg BID or >1 g QD (IC ₅₀)	50 mg QD (IC ₉₀ , 24h)

Preclinical ADME and PK summary. The [final properties](#) for compound 22 (NDI-034858, TAK-279) were:

- ALogP/ pred Log RRCK P_{app} = 2.1 / -5.50
- TYK2-JH2 K_d = 3.8 pM
- TYK2 PBMC IL-12 pSTAT4 IC₅₀ = 8.4 nM
- hWB IFN α IP-10 IC₅₀ = 51 nM
- Kinetic solubility (pH 7.4) = 32 μM
- Caco-2 (A-B P_{app}) = 15 x 10⁻⁶ cm/s
- Caco-2 Efflux Ratio = 1
- Rat/Human Hep Cl_{pred} (mL/min/kg) = 30 / 0.69* (*generated from Hepatopac co-culture)
- PK Cl_{p,obs} (M/R/D/C/H) 1 mg/kg IV = 16 / 26 / 14 / 7 / 1.7-7.5 mL/min/kg
- F% (M/R/D/C) (M/R/D = 10 mpk PO, C = 5 mpk PO) = 70% / 37% / 47% / 47%
- PPB F_u (M/R/D/C/H) = 8% / 15% / 23% / 23% / 23%
- t_{1/2} (M/R/D/C) = 2.0 / 1.2 / 5.3 / 3.8 h
- V_{ss} (M/R/D/C/H) = 1.3 / 1.6 / 4.0 / 1.9 / 1.2-10 L/kg
- Good absorption across species (FaSSIF / FeSSIF = 13 / 70 μg/mL, w/ 32 μM kinetic solubility)
- Low DDI perpetrator potential (IC₅₀ for CYP3A4 (M) = 2 μM, CYP3A4 (T), CYP2C19 = >8μM, others >30 μM; no CYP TDI, low pXR activation (26% of rifamycin control at 30 μM)

In a [rat PD model](#), IL-12/IL-18-induced IFN γ signaling was reduced by all dose levels relative to vehicle, by 16% (1 mg/kg), 77% (3 mg/kg), 87% (10 mg/kg), and 100% (30 mg/kg). TAK-279 also showed a [dose responsive suppression of disease](#) in a Rat Adjuvant Induced Arthritis Efficacy Model, nearly on par with dexamethasone at 30mg/kg BID. Low metabolism of the inhibitor was observed overall and elimination was primarily oxidative by multiple CYP450s, followed by conjugation.

Efficacy and a clean safety profile demonstrated in Ph. I and II. TAK-279 reduced the severity of PsO for ~68% of patients at a 15 or 30 mg once-daily dose, with a 75% resolution in disease severity at 12 weeks based on PASI score, meeting the trial's primary endpoint (2, 5, 15 or 30 mg QD, n = 259, [NCT04999839](#)). Secondary endpoints were also achieved for patients receiving doses \geq 5 mg based upon PGA 0/1 (physician's global assessment of clear or almost clear), PASI-90, PASI-100, and change from baseline in DLQI (dermatology life quality index), all at week 12. Moreover, [one-third of patients](#) experienced total clearance of skin lesions at the highest 30 mg dose (PASI score of 100).



The oral T_{1/2} in human healthy volunteers was consistent across doses (16.5–30.7 hours), and both C_{max} and AUC were approximately dose-proportional from 5–75 mg.

Overall, TAK-279 was well-tolerated and showed a clean safety profile with generally low incidence of serious adverse events. Mild dermatologic events consistent with deucravacitinib like acne and rash were commonly observed in health volunteers in both single and multiple dose groups (which resolved without intervention), but interestingly were not observed in psoriasis patients. In Ph. II, at the highest dose, only 3 patients (6%) experienced Grade 3+ AEs, while the most common AEs were COVID-19 infection (13.5%), acne (3.8%), or acneiform dermatitis (5.8%). There was one patient that experienced Grade 3+ AEs of neutropenia, CPK elevation, triglyceride elevation at week 12. But, there were otherwise minimal changes in hematological, hepatic, renal or lipid parameters for the patients in this study.

What's next? Given these strong Ph. IIb results, Takeda will be taking TAK-279 into Ph. III for PsO later this year. The candidate is also in an ongoing Ph. IIb trial for active psoriatic arthritis (PsA) with topline data to be released by the end of this year ([NCT05153148](#)). Plus, Takeda has plans to take this candidate into Ph. II for the treatment of systemic lupus erythematosus (SLE) and inflammatory bowel disease (IBD) also by YE 2023, and plans for other indications to follow. Regulatory filing is expected by 2025–2027, based on the current timelines.

Relevant patents. "TYK2 inhibitors and uses thereof" ([US10196390B2](#), 2015) ([US11396508B2](#), 2017) ([US20210238198A1](#), 2016) ([US20220106306A1](#), 2019) ([US20230074228A1](#), 2016) ([US20230056447A1](#), 2018) ([US20220073528A1](#), 2020) ([US20220073527A1](#), 2017). "Tyk2 inhibitor and application thereof" ([US11040967B2](#), 2018)

4/24/23 NOTE: The original version of this article omitted the fact that the TYK2 research program was started by Nimbus in collaboration with Celgene. Additional context has been added to the introduction: "The Nimbus TYK2 research program was started to compete with BMS's deucravacitinib in a [research collaboration with Celgene](#), including a Joint Steering Committee and Celgene scientists contributing, but after BMS's acquisition of Celgene, Nimbus had to firewall Celgene and [sue for rights back to the molecule](#)." Thanks to readers for pointing out this omission.

March 2023

zavegepant

CGRP

CGRP receptor antagonist, first nasal spray

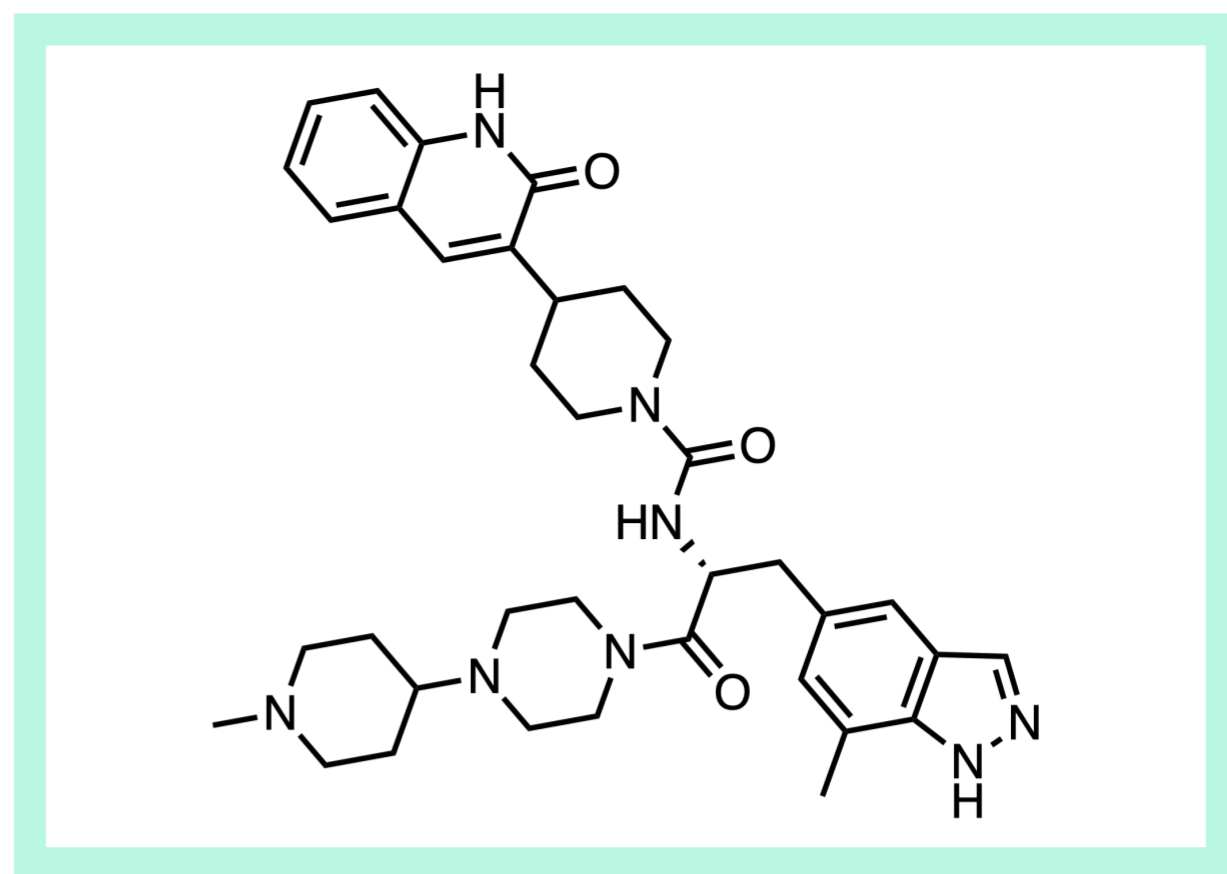
FDA-approved for acute migraines in adults

rational design based on known CGRP antagonists

FDA approval, March 10, 2023

BRISTOL MYERS SQUIBB, NY / PFIZER, INC., NY

article link: <https://www.pfizer.com/news/press-release/press-release-detail/pfizers-zavzpretm-zavegepant-migraine-nasal-spray>



View Online

The first approved CGRP receptor antagonist nasal spray for the treatment of migraine. Pfizer has announced the [FDA-approval](#) of zavegepant ([ZAVZPRET™](#), BHV-3500) for the treatment of acute migraine in adults based on positive Ph. II/III results. As the first and only [calcitonin gene-related peptide \(CGRP\) receptor antagonist](#) nasal spray for migraine treatment, zavegepant was statistically superior to placebo on the co-primary endpoints of 'pain freedom' and 'freedom from most bothersome symptom' at 2 hours after dosing ([NCT04408794](#)). This pivotal study also demonstrated pain relief as early as 15 minutes in a secondary endpoint, as compared to placebo. The rapid action for the intranasal delivery and the lack of needing to swallow a pill for relief for migraine patients, especially those with emesis, could make this attractive to patients.

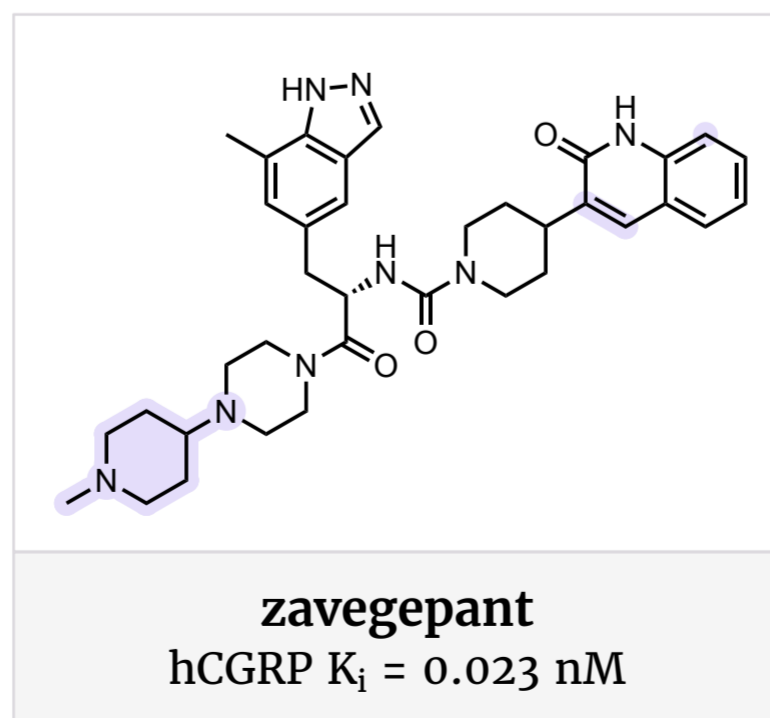
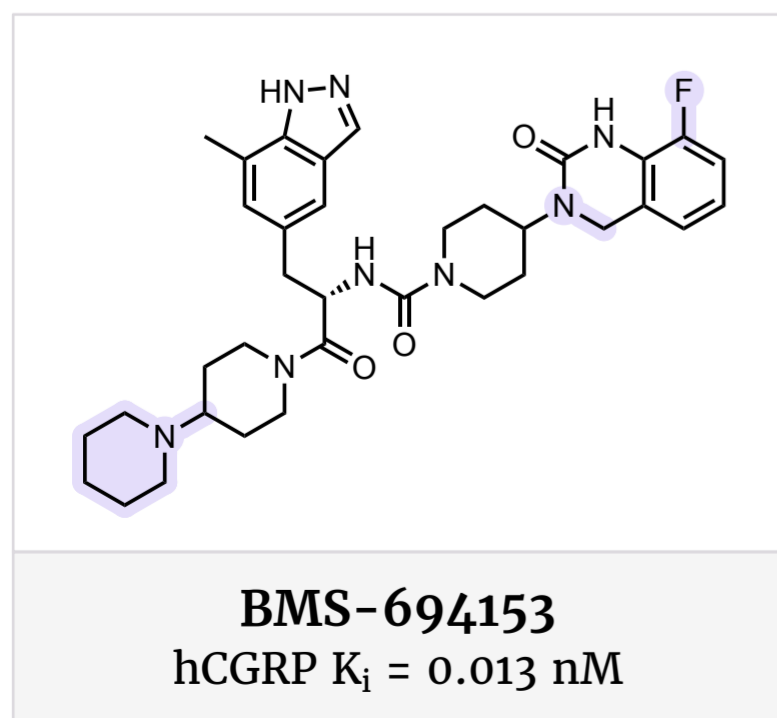
CGRP as a relatively new target for migraines. [CGRP](#) has emerged within the past few years as a novel therapeutic modality for the treatment of migraine. Rimegepant ([NURTEC®](#)) was the first approved product for Biohaven Pharmaceutical Holding Company Ltd, and is the only oral CGRP receptor antagonist FDA-approved for both acute ([2020](#)) and preventive use ([2021](#)). The orally disintegrating tablet was also [EMA-approved](#) for both of these indications as [VYDURA®](#) last year, in 2022. In 2021, Pfizer entered into a [\\$500M arrangement](#) (cash + equity) with Biohaven to have the rights to commercialize rimegepant and next-generation Ph. III candidate, zavegepant, in all regions outside the US. However, both of these assets and a portfolio of preclinical CGRP assets were [acquired by Pfizer](#) the following year for ~\$11.6 billion. The spin-off, Biohaven Ltd., retained all non-CGRP pipeline compounds not in development. Both rimegepant and zavegepant [were licensed by Biohaven](#) from [BMS](#), the originator, a few years prior, in 2018, for an upfront payment of \$50M.

The advantages of intranasal spray delivery of a CGRP receptor modulator. Other approved oral CGRP receptor antagonists for the treatment of migraines include AbbVie's ubrogepant ([UBRELVY®](#)) for [acute use](#) in 2019, and atogepant ([QULIPTA®](#)) for [preventive use](#) in 2021, also covered in our [approval deep-dive](#) on atogepant. BMS has reported on several other orally-active CGRP antagonists, including [BMS-846372](#)

in 2012 and a related [analog](#) with higher bioavailability (17% in rat) in 2020. In addition, several injectable monoclonal antibodies targeting CGRP have also been approved, including [erenumab](#), [eptinezumab](#), [fremanezumab](#), and [galcanezumab](#). However, patient compliance is often a challenge for injectable therapies, and most patients would prefer a non-injection option to treat pain. In contrast, third-generation CGRP receptor antagonist zavegepant is dosed as an [intranasal \(IN\) spray](#), which offers several distinct advantages over even oral administration. IN delivery allows for a more rapid onset of migraine relief than oral therapies, while still harnessing the power of CGRP receptor antagonism. Furthermore, the common migraine symptoms of nausea and vomiting can make swallowing and retaining oral medications challenging. However, very strong unbound receptor potency and very high aqueous solubility are all requirements for an API intended for IN delivery.

Nasal sprays have been developed for migraine in the past, such as with approved [TRUDHESA™](#) nasal spray, which has the 5-HT_{1D} receptor agonist, [dihydroergotamine](#), as the active ingredient. However, this promiscuous agonist also has high affinities for other serotonin receptors, as well as noradrenaline and dopamine receptors, and has therefore been associated with serious side effects.

Rational design and optimization for improved oxidative stability. Starting from [BMS-694153](#) and a literature survey of common structural motifs of known CGRP antagonists, the team found the 7-methylindazole moiety to be key for excellent potency in CGRP binding assays ($K_i = 0.013$ nM) with reduced CYP3A4 inhibition ($IC_{50} = 26$ μM) compared to other analogs. The benzylic methylene in the dihydroquinazolinone was replaced with an electron-deficient sp²-carbon to [improve the oxidative stability](#) of the compound in aqueous solution as required for IN delivery, while retaining its excellent in vitro potency. Modification of the piperidinyl piperidine to a piperidinyl piperazine afforded zavegepant with diminished nasal irritancy as compared to the parent and greatly improved oxidative stability.



March 2023

zavegepant

CGRP

CGRP receptor antagonist, first nasal spray

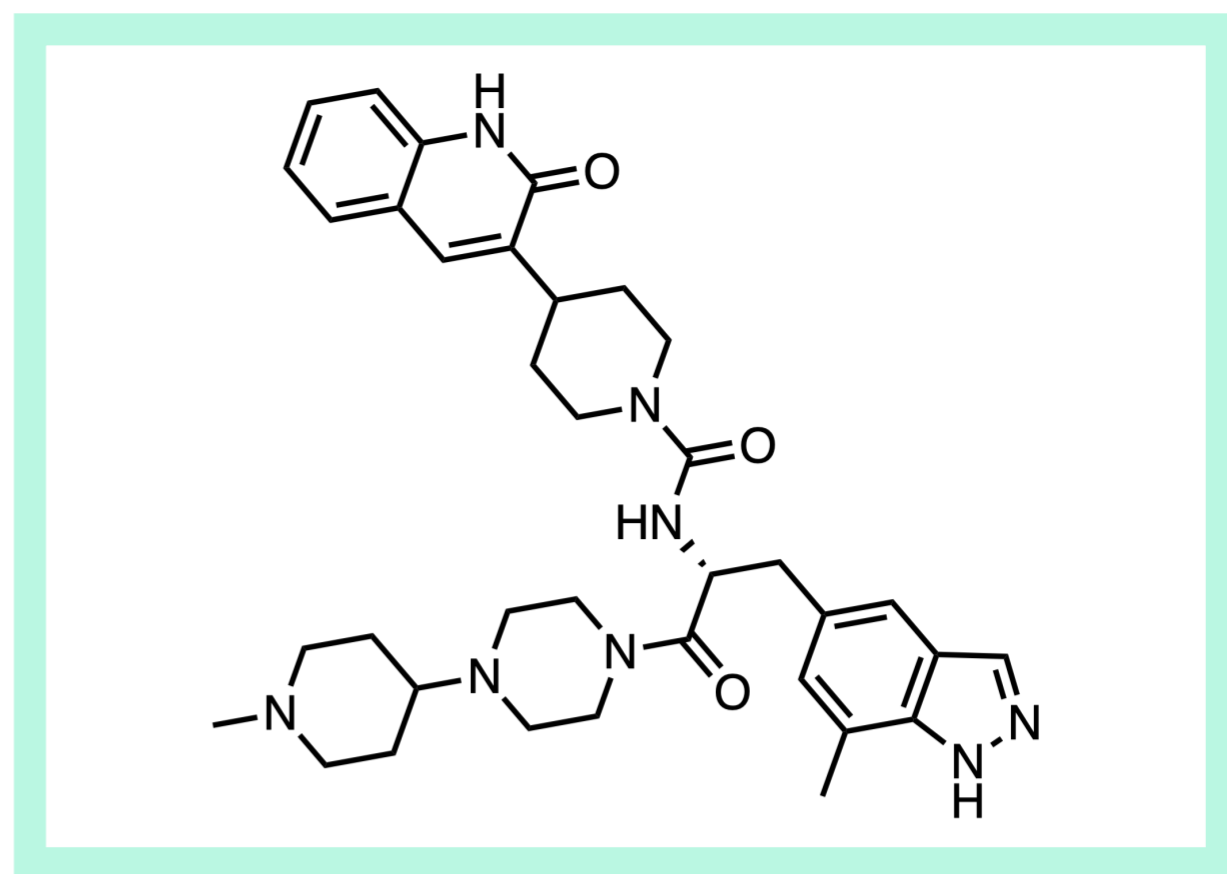
FDA-approved for acute migraines in adults

rational design based on known CGRP antagonists

FDA approval, March 10, 2023

BRISTOL MYERS SQUIBB, NY / PFIZER, INC., NY

article link: <https://www.pfizer.com/news/press-release/press-release-detail/pfizers-zavzprettm-zavegepant-migraine-nasal-spray>



View Online

Zavegepant displayed >10,000-fold selectivity for CGRP over other calcitonin receptors. The compound had no CYP inhibition, low hERG activity, and no significant off-target activity was observed in a panel of receptor and ion channel binding and enzyme activity assays (at 10 μ M). In vitro safety studies suggested low potential for hepatic, cardiovascular or genotoxic liabilities, and no toxicity issues (e.g., olfactory epithelial atrophy) or nasal irritation were observed in a 7-day rat study.

Binding mode. While an x-ray co-crystal structure of zavegepant with CGRP is not available, the structure of other approved CGRP antagonists, such as olcegepant, is known (PDB: [6ZIS](#)).

In vivo activity with intranasal dosing. Zavegepant inhibited CGRP-stimulated formation of cyclic AMP in SK-N-MC cells ($K_b = 22$ pM), and also potently reversed CGRP-induced dilation of ex vivo human intracranial arteries ($EC_{50} = 880$ pM). Zavegepant treatment didn't result in active contraction of human coronary arteries ex vivo up to 10 μ M concentration, suggesting an anti-dilatory effect for this MOA and that it won't have cardiovascular liabilities of triptans as nonselective vasoconstrictors, such as sumatriptan (ImitrexTM). Minimal degradation (0.3%) was observed after 3 months in open air pH 6 buffer solution at 40 °C, suggesting that the aerobic oxidative liability of the dihydroquinazolinone moiety in the parent BMS-742413 in solution had been properly mitigated (40 mg/mL concentration). Zavegepant also had very high aqueous solubility of 105 mg/mL at pH 8.5 and >300 mg/mL at lower pH, which is critical due to the small volume of dose required for nasal delivery.

In vivo studies with a non-invasive marmoset recovery model, dosing at 0.03 mg/kg (SC) produced 48% inhibition of CGRP-induced increases in marmoset facial blood flow upon subcutaneous (SC) dosing at 15 minutes post-dose and 80% at 60 minutes. Marmosets are the only animal reported to have human-like CGRP receptor pharmacology. Low oral bioavailability was observed in cynomolgus monkey ($F = 0.3\%$) and mouse ($F = 1.4\%$), but the compound was rapidly absorbed after IN dosing in rabbit with T_{max} at 15-20 min. Interestingly, the bioavailability increased when the concentration of the dosing solution was changed from 10 mg/mL (13%) to 100 mg/mL (30%).

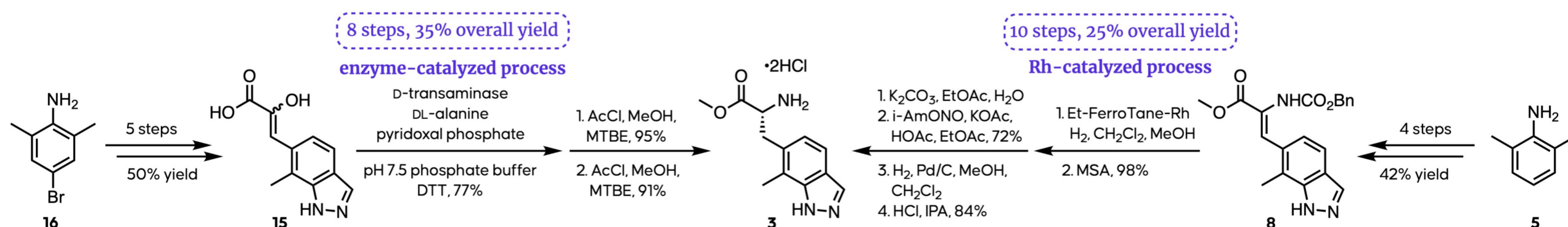
Positive Ph. III results support FDA-approval. The Ph. II/III study demonstrated statistically significant superiority to placebo at a variety of time points, including 5- and 30-minute pain relief, return to normal function at 30 min and 2 h, and durable sustained pain freedom at 2-48 hours ([NCT04408794](#)). Two hours after the treatment

dose, more participants had pain freedom (24% vs 15%) and freedom from their most bothersome symptom (40% vs 31%) as compared to placebo. The dose of 10 mg IN up to 8x per month for up to a year was well tolerated, and the most common adverse reactions were dysgeusia (21%), nasal discomfort (4%), and nausea (3%). A Ph. II/III study investigating zavegepant as an oral treatment for migraine prevention (Ph. II/III, [NCT04804033](#), n = 1440, est. completion 12/2027) and for allergic asthma are currently underway (Ph. Ib, [NCT04987944](#), n = 24, est. completion 5/2023).

A serendipitous Pd/Rh removal process on-scale. Two enantioselective routes toward the chiral aminoester intermediate were explored in the [process development](#) of zavegepant. A rhodium-catalyzed asymmetric hydrogenation of an enamide intermediate was optimized to a 0.25% catalyst loading of [Et-FerroTane-Rh](#) for a reaction time of 1 hour, and produced 14 kg of amino ester **3** overall in a 96% yield and >99.8% ee following polish filtration, solvent exchange and precipitation as the MSA salt. However, the hydrogenolysis step was plagued with variable yield upon scale-up, ranging from 50 to 89%, and there were also several issues encountered for the subsequent Pd-catalyzed Cbz deprotection. The steps prior to the deprotection were the result of a serendipitous find. In a prior route, they utilized a nitrosation which happened to remove colored impurities that correlated to the residual Pd and Rh. To replicate that process in this newer route, they neutralize the MSA salt with base, and then treat with isoamyl nitrite to remove those impurities. Overall, this route delivered the bis-HCl salt of **3** in 25% yield over 10 steps and in >99.9% ee.

A biocatalysis-enabled commercial-scale route. An alternate route using an enzyme-catalyzed transamination produced the aminoester **3** in 34% yield over 8 steps. The [enzymatic reaction](#) proceeded in 79% yield and >99.7% ee, and was catalyzed by a transaminase purified from soil organism *Bacillus thuringiensis* that was cloned and expressed in *E. coli*. This serves as yet [another example](#) of a biocatalytic process being preferred on-scale over metal-mediated processes. Whereas the proprietary rhodium catalyst had limited availability, was highly oxygen sensitive and required very pure substrate input for good TON, the enzymatic route mitigated the extra steps required for Pd- and Rh-removal and the associated downstream impurities, the enzyme catalyst was readily available and non-oxygen sensitive, and the substrate purity was less critical for the reaction to proceed well. Even though the biocatalysis reaction added more steps to the overall route, the overall yield was higher and was ultimately the route chosen for commercial support.

Patents. "CGRP receptor antagonist" [US8481546B2](#) (2013). "Dual treatment of migraine" [WO2022251752A2](#) (2022). "Pharmaceutical compositions of CGRP inhibitors and methods of their use" [WO2022165291A1](#) (2022).



March 2023

revumenib

menin-KMT2A

oral menin-KMT2A inhibitor

Ph. I/II for r/r leukemia, CRC & solid tumors

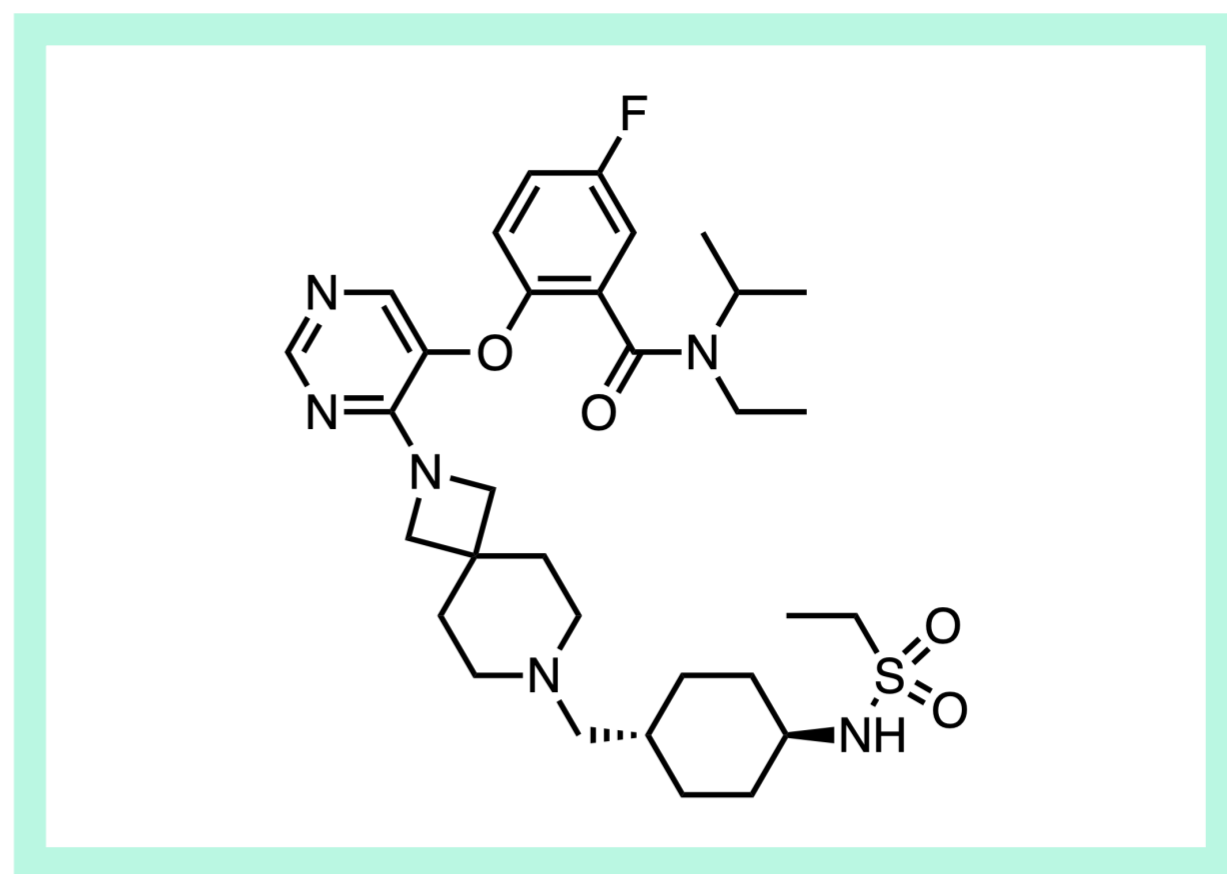
discovery not disclosed

Nature, March 15, 2023

VITAE, MADISON, NJ / SYNDAX, WALTHAM, MA

paper DOI: <https://doi.org/10.1038/s41586-023-05812-3>

[View Online](#)

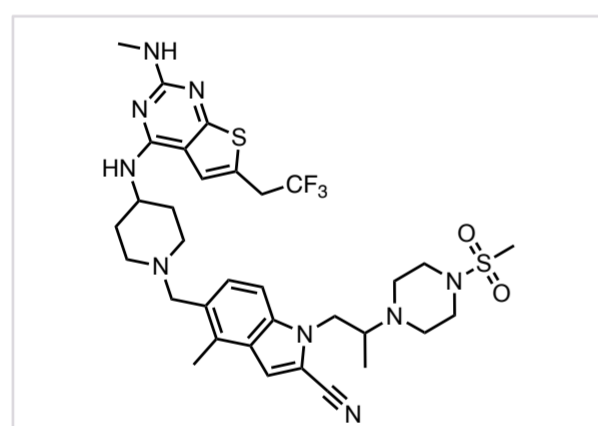


Revumenib: a novel Menin-MLL1 inhibitor in Ph. II for AML. [Acute myeloid leukemia](#) (AML) remains difficult to treat, with few novel therapies approved in the last three decades. A subset of these aggressive leukemias, [mixed lineage leukemias](#), are driven by fusions between the *MLL1* gene (“Mixed Lineage Leukemia”, or KMT2A) and more than [80 different fusion partners](#). MLL fusion proteins form part of a [protein complex](#) that upregulates the transcription of the leukemogenic *HOXA* and *MEIS1* genes, which drive proliferation and block differentiation of hematopoietic cells, ultimately leading to the acute lymphocytic leukemia (ALL) or acute myelogenous leukemia (AML). The histone lysine methyltransferase [Menin](#) is a key member of the complex, connecting transcription factors to chromatin. Hence, [targeting the protein-protein interaction](#) between Menin and MLL could disrupt leukemogenic gene transcription. Revumenib has

recently demonstrated [impressive](#) early activity in a [Ph. I trial](#), furthering Menin’s status as a target to watch.

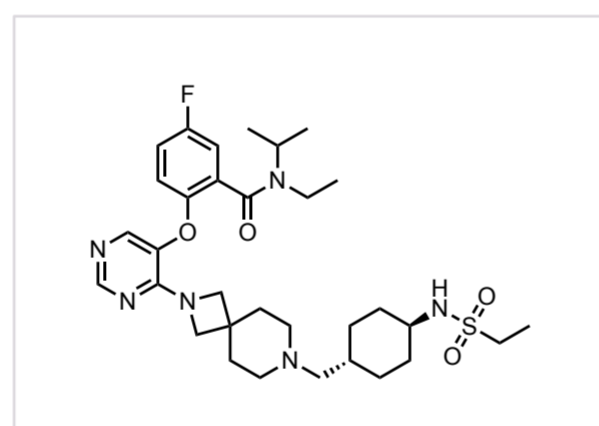
Menin-MLL1 inhibitors in the clinic. Although there are no drugs specifically approved for acute leukemia with MLL1/KMT2A rearrangements or mutated NPM1, a [number of Menin inhibitors](#) have entered clinical development for these leukemias, including [revumenib](#) ([NCT05761171](#)), [ziftomenib](#) ([NCT04067336](#)), [JNJ-75276617](#) ([3 trials](#)), [BMF219](#) ([NCT05153330](#)), [DS1594a](#) ([NCT04752163](#)), and [DSP-5336](#) ([NCT04988555](#)). More context can be found in our recent coverage of prior Molecule of the Month and Molecule of the Year, [ziftomenib here](#) and [here](#), which recently overcame a clinical hold from the FDA due to differentiation syndrome, which was in ways a positive sign for drug activity.

Clinical, small-molecule Menin-MLL PPI inhibitors



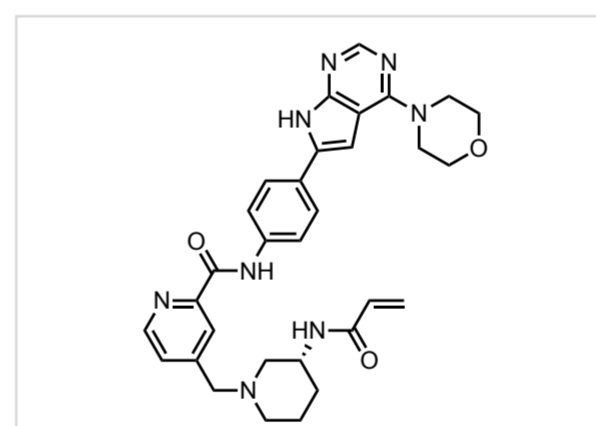
ziftomenib

(KO-539)
Kura Oncology
oral Menin-MLL1 (KMT2A) inhibitor
 IC_{50} = 11-49 nM (cell)
Ph. I/IIa for R/R AML



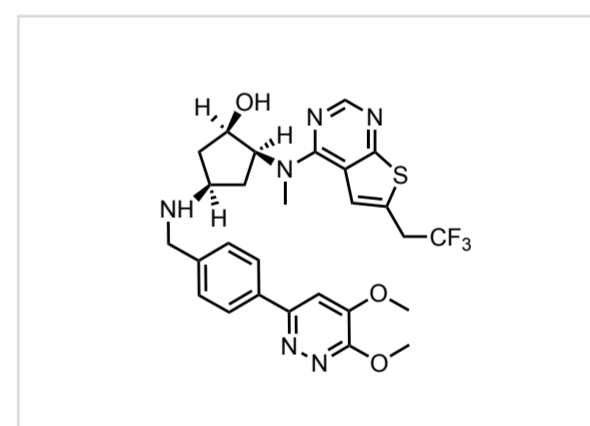
revumenib

(SNDX-5613, VTP-50469)
Syndax Pharmaceuticals
oral/IV/IT Menin-MLL1 (KMT2A) inhibitor
 IC_{50} = 13-37 nM (cell)
Ph. I/II for R/R ALL, MPAL, AML
w/ KMT2Ar, NPM1 mutations



BMF219

Biomea Fusion
oral, covalent Menin inhibitor
 IC_{50} = ~300 nM (cell)
Ph. I for AML, ALL w/ KMT2A/MLL1r,
NPM1+ mutations



DS1594a

Daiichi Sankyo
oral, Menin-MLL1 inhibitor
 IC_{50} = 2.5-28.5 nM (cell)
Phase I/II for R/R AML, ALL, CML, MS

[structure not disclosed]

[structure not disclosed]

JNJ-75276617
Johnson & Johnson
oral Menin-MLL (KMT2A) inhibitor
 IC_{50} = “potent”(cell)
Ph. I for AML, ALL w/ KMT2A/MLL1r, NPM1 alterations

DSP-5336
Sumitomo Pharma
oral Menin-MLL1 (KMT2A) inhibitor
 IC_{50} = 10 -31 nM (cell)
Ph. I/II for R/R AML, ALL w/ or w/o MLL1r or NPM1 mutations

March 2023

revumenib

menin-KMT2A

oral menin-KMT2A inhibitor

Ph. I/II for r/r leukemia, CRC & solid tumors

discovery not disclosed

Nature, March 15, 2023

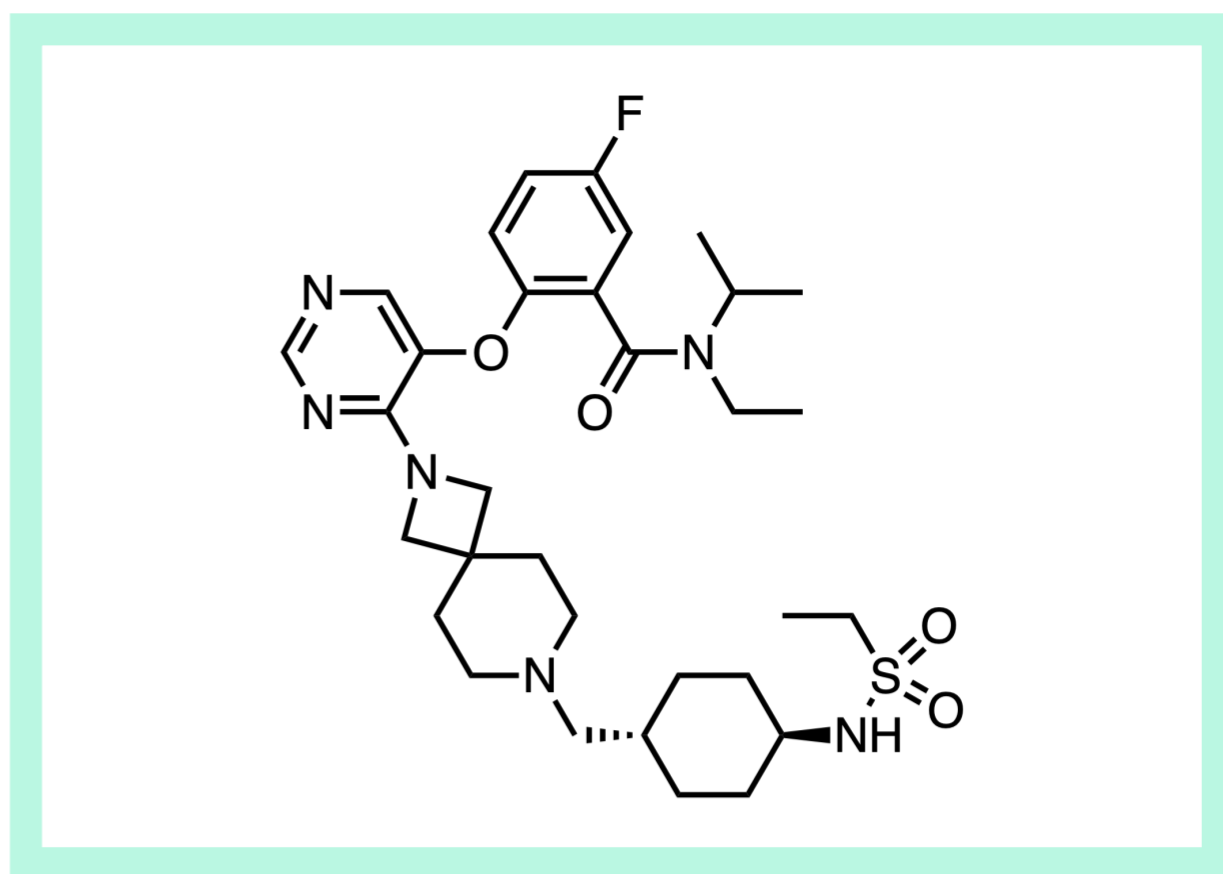
VITAE, MADISON, NJ / SYNDAX, WALTHAM, MA

paper DOI: <https://doi.org/10.1038/s41586-023-05812-3>

[View Online](#)

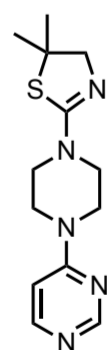
Structure-based design from ziftomenib's starting fragment. Revumenib was discovered through [iterative SBDD](#) utilizing the same starting chemical series ([MI-2](#)) that led to the first Menin-MLL1 clinical candidate, ziftomenib - a piperazinyl pyrimidine fragment, "compound 1". The goals for the optimization were to maintain optimal distance and geometry for the pyrimidine's H-bond to Tyr²⁷⁶, fill the hydrophobic pocket (Phe²³⁸), extend across the MLL binding pocket to incorporate an anchoring distal H-bond, and introduce a basic protonated amine to exploit a cation- π interaction in the bridging structure, and also improves aqueous solubility. Toward this end, a 4-fluorophenyl aniline was added to the pyrimidine ring, utilizing branching to fill the hydrophobic pocket, yielding "compound 2" ($K_i = 97$ nM). The 4-fluorophenyl was further elaborated with an aromatic side chain and a spirocyclic piperazine bioisostere was installed in place of the piperazine to afford "compound 3" with a ~30-fold increase in potency ($K_i = 2.9$ nM). The tertiary amine of this spirocycle does form distinct cation- π interactions with two tyrosine residues, Tyr³¹⁹ and Tyr³²³.

Key cation- π interactions with a spirocyclic piperazine bioisostere. The team noted that "compound 3" suffered from off-target activity, a CYP3A4 liability, and poor pharmacokinetic properties, although no further data was provided. A substituted amide replacement of the phenyl ring retained key hydrophobic interactions, while improving physical properties and reducing off-target activity. Finally, optimization of the spirocyclic linker and addition of a

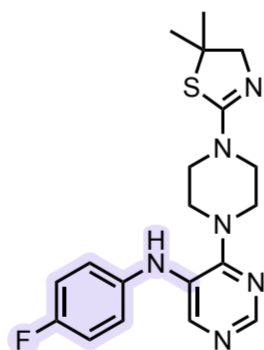


cyclohexyl sulfonamide in place of the tetrahydropyran resulted in revumenib. An x-ray co-crystal structure of the compound bound to Menin revealed that the pyrimidine and sulfonamide formed those key anchoring H-bonds to Y²⁷⁶ and W³⁴¹, respectively, along with the aforementioned cation- π interactions with the Y³¹⁹ and W³²³ side chains (PDB: [6PKC](#)).

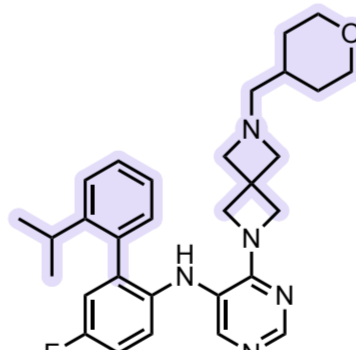
In vitro suppression of MLL target gene expression. Revumenib [displayed](#) concentration-dependent antiproliferative activity in a variety of cell lines carrying MLL rearrangements (MLL-r) with IC₅₀ values in the low nM range (13-37 nM) as measured by live cell counts, CellTiter-Glo, or MTT assay. Revumenib was confirmed to disrupt Menin incorporation into high-molecular-weight Menin-containing complexes based on experiments in MOLM13, RS4,11, and ML2 cells. The compound also suppressed MLL fusion target gene expression, as both the genetic loss of *MEN1* and treatment with revumenib resulted in reduced expression of an overlapping group of 34 genes. Though its pharmacological profile has not been completely elucidated, these results indicated that Menin inhibition mediates a major portion of the cellular effects of this agent. The team also assessed the chromatin occupancy of Menin and other chromatin-associated proteins and histone modifications important in MLL-r leukemia. These studies revealed that while loss of Menin on chromatin does not lead to a global loss of MLL chromatin binding, it does cause MLL and DOT1L binding loss, H3K79me2, and the associated gene expression decreases at a specific subset of MLL fusion target genes.



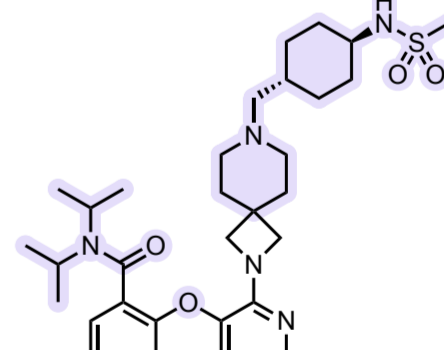
compound 1
MI-2, fragment
 $K_i = \sim 10^3$ nM



compound 2
 $K_i = 97$ nM



compound 3
 $K_i = 2.9$ nM



revumenib
SNDX-5613, VTP-50469
 $K_i = 104$ pM

March 2023

revumenib

menin-KMT2A

oral menin-KMT2A inhibitor

Ph. I/II for r/r leukemia, CRC & solid tumors

discovery not disclosed

Nature, March 15, 2023

VITAE, MADISON, NJ / SYNDAX, WALTHAM, MA

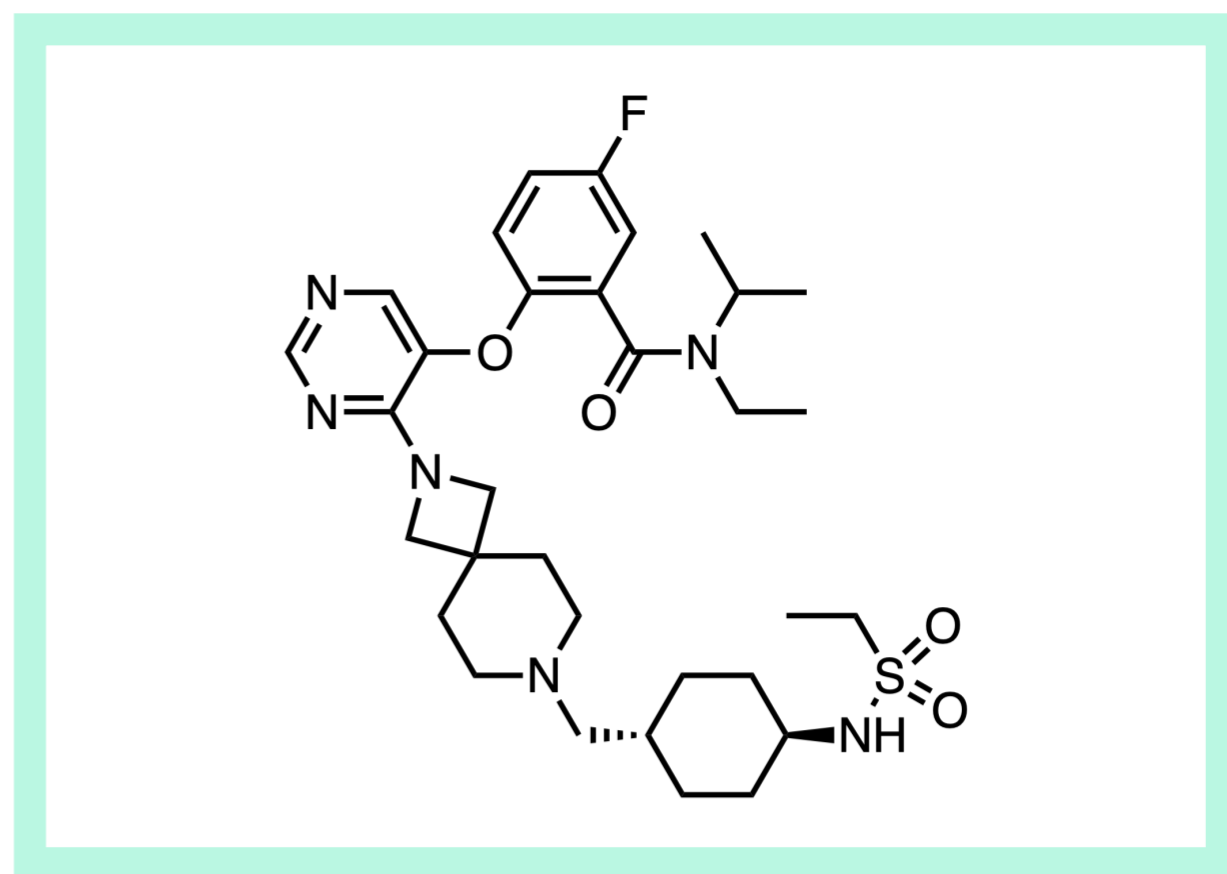
paper DOI: <https://doi.org/10.1038/s41586-023-05812-3>

[View Online](#)

In vivo activity in patient-derived xenograft models. In a xenotransplantation model, revumenib was highly efficacious in mice at 15–60 mg/kg. Treatment with revumenib in a variety of patient-derived xenograft (PDX) models indicated a dose-dependent decrease in subcutaneous tumor size over 4 days with an in vivo plasma IC_{50} of 109 nM (1.2, 6 or 30 mg/kg dosing), and a 28 day-treatment of 120 mg/kg led to almost complete eradication of leukemia cells in bone marrow, peripheral blood, and spleen of the mice. In vivo global gene expression was also investigated in vivo, revealing that the genes that lose MLL1n and Menin occupancy, including MLL-fusion target genes, decrease in expression, and these changes strongly correlate with the in vivo response to revumenib.

A 64% cytogenetic response in clinical AML patients with KMT2Ar, as compared to 9% for placebo. [Clinical studies](#) of revumenib were carried out in a heavily pretreated population with a median of four previous lines of therapy and almost half (46%) of the patients had relapsed after an allogeneic stem cell transplant. Most patients had relapsed or refractory AML (82%), while the remainder had ALL (16%) or mixed-phenotype acute leukemia (2%) ([NCT04065399](#)). The majority of patients had KMT2Ar (68%) or NPM1 (21%) mutations, although some had neither (12%). The rate of complete remission or complete remission with partial hematologic recovery (CR/CRh) was 30%, while the overall response rate was 53%. The rate of complete cytogenetic response in patients with KMT2Ar who achieved morphologic clearance of their myeloblasts was 64%. [In contrast](#), the rate of CR or complete remission with incomplete count recovery in relapsed KMT2Ar AML patients after two previous lines of therapy is 9%. The results with Menin-MLL inhibitors in AML is particularly notable given how challenging AML is to treat at baseline, combined with the fact that the patients in these trials have the worst forms of the disease (relapsed-refractory after many difficult treatments typically including aggressive chemotherapy).

Clinical DDI studies. Because revumenib is a substrate of cytochrome P450 3A4 (CYP3A4), two parallel dose-escalation cohorts were conducted with or without strong CYP3A4 inhibitors. Pharmacokinetic studies showed that



dose-proportional exposure was achieved in both cohorts, although the half-life was shorter in the arm without strong CYP3A4 inhibitors ($t_{1/2}$ = 3 h vs. 8 h).

Adverse events. The most common treatment-emergent adverse events of grade 3 or higher were febrile neutropenia (31%), thrombocytopenia (19%) and sepsis (18%). The most frequent treatment-related adverse event was prolongation of the QT interval observed in 53% of patients. Dose-limiting toxicity due to this effect was observed in 10% of patients across both arms of the study. In addition, grade 2 [differentiation syndrome](#) (DS) was reported in 16% of patients, which is commonly observed with [differentiation therapy](#) and is a positive sign of drug activity. DS is thought to result from a severe systemic inflammatory response mediated by increased expression of cytokines, chemokines, and adhesion molecules (e.g., integrins).

Other clinical biomarkers and resistance mutations. Assessment of transcriptional changes using RNA-seq of bone marrow cells from patients showed that a variety of leukaemogenic target genes were downregulated upon treatment with revumenib, including *MEIS1*, *HOXA9*, *PBX3*, and *CDK6*, while expression was increased for genes associated with differentiation such as *CD11b* and *CD14*. A [separate report](#) identified somatic mutations in *MEN1* in patients treated with revumenib that were associated with resistance to the drug at the revumenib-menin interface. Ultimately, this indicates that a chromatin-targeting therapeutic drug induces sufficient selection pressure in patients to drive the escape mutant evolution, leading to sustained chromatin occupancy and implies a common mechanism of therapeutic resistance.

Ongoing studies. Revumenib is currently being studied in a number of Phase I and Phase II clinical trials: [NCT04065399](#), [NCT05326516](#), [NCT05406817](#), [NCT05731947](#), [NCT05761171](#).

Patents. "Inhibitors of the menin-mlt interaction" [US20210053974A1](#) (2021). [US20230021684A1](#) (2023).

March 2023

zunsemetinib

MK2

oral MK2 inhibitor

Ph. IIa for hidradenitis suppurativa (failed)

designed to selectively inhibit the p38 α -MK2 complex

Press release, March 6, 2023

CONFLUENCE, MO / ACLARIS THERAPEUTICS, PA

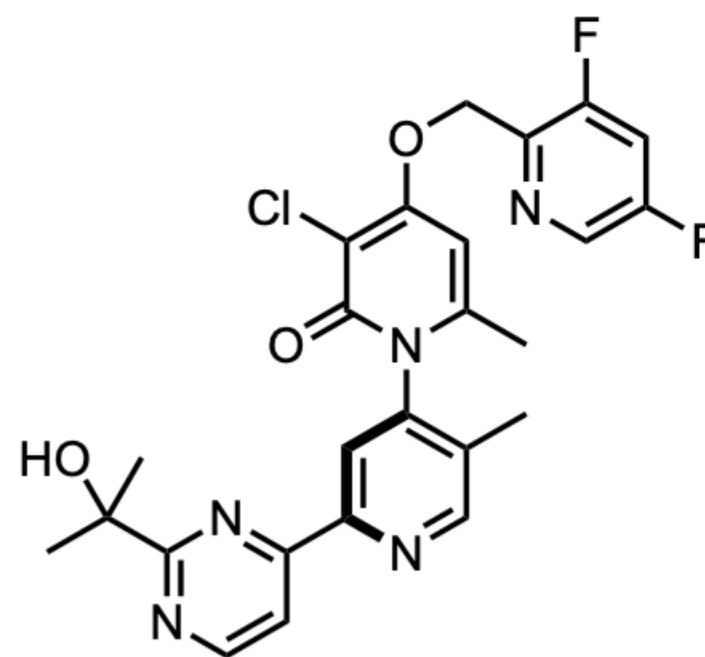
article link: <https://investor.aclaristx.com/news-releases/news-release-details/aclaris-therapeutics-announces-preliminary-topline-data-12-week>

[View Online](#)

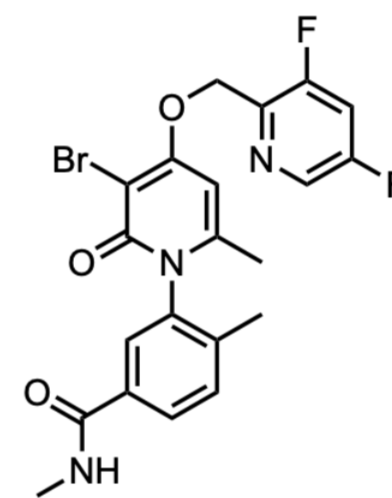
A p38 α -MK2 kinase complex inhibitor for inflammation. Zunsemetinib (ATI-450, CDD-450) is a p38 α -MK2 complex inhibitor discovered by Confluence Technologies and developed by Confluence spinout, [Aclaris Therapeutics](#). The molecule binds to a [site formed from the modified p38MAPK ATP binding pocket and MK2](#) when the two proteins interact, inhibiting the heterodimeric complex. The complex inhibitor represents one of the more promising attempts to [drug p38 \$\alpha\$](#) , a kinase which has been [long pursued in a range of indications but challenging to target](#) due to [systemic toxicities](#) (hepatotoxicity, CNS- and cardiac toxicities), and tachyphylaxis (loss of efficacy over time). Unfortunately, the molecule [recently failed to meet endpoints](#) in a Ph. IIa trial for hidradenitis suppurativa ([NCT05216224](#)), an immune-mediated skin disorder, though the company noted that the placebo response was higher than that observed in other published studies. At 50 mg BID over 12 weeks, it did not reduce the occurrence of inflamed and swollen [nodules](#), despite PK/PD showing drug-dependent inhibition of plasma cytokines and chemokines. In contrast, Incyte's JAK1 inhibitor, [povorcitinib](#), recently [demonstrated positive results](#) on the same [endpoints](#) in hidradenitis suppurativa and is [moving to Ph. III](#). The molecule still serves as an interesting human proof-of-principle for kinase complex-selective inhibition, is a nice example of a kinase inhibitor being taken safely outside of oncology, and is a rare example of an atropisomeric clinical candidate.

A glue-like mechanism of action. Zunsemetinib has a unique [mechanism of action](#) (MOA) that was [designed](#) to target the p38 α MAPK and MK2 proteins when they form their complex. This MOA differs from most p38 α or MK2 kinase inhibitors, which are traditional ATP-competitive active site inhibitors (see for example [another recent Molecule of the Month](#), a covalent ATP-competitive MK2 kinase inhibitor from BMS). Zunsemetinib [binds at an interface](#) formed between MK2 and a modified P38 α MAPK ATP binding pocket, effectively holding MK2 in an inactive conformation. This prevents the p38-dependent phosphorylation and subsequent activation of MK2. Although a [crystal structure of the p38 \$\alpha\$ -MK2 complex without zunsemetinib is available](#), there is no published crystal structure explicitly showcasing this interaction (though an image of how zunsemetinib/CDD-450 binds is available in [part C of the supporting information of this article](#) and in Aclaris company presentations).

Complex-selective mechanism of action may contribute to drug selectivity while preserving desired activity. Interestingly, the molecule binds with a [higher affinity for the complex than for either protein on their own](#), resulting in selective inhibition of pharmacology mediated through the complex, compared to other inhibitors that may affect p38 α or MK2 individually. For example, the molecule is at least 700x more potent for inhibiting p38 α -MK2 than other p38 α complexes like p38 α -PRAK or p38 α -ATF2, whereas classical p38 α kinase inhibitors like CDD-110 (*rac*-[PH-797804](#), from which zunsemetinib appears to be derived) have similar potency across these complexes. Zunsemetinib is also [>350x-selective across 193 kinases](#)



tested across the kinome as a result of this unique binding mode. Importantly, the anti-inflammatory effects of p38 α -MK2 inhibition are comparable to global p38 inflammation in rats and human patient cells, and the selectivity of the mechanism may help avoid the tachyphylaxis that [may be attributed to non-MK2 substrate inhibition](#).



rac-PH-797804

Likely derived from a traditional ATP-competitive starting point. While the discovery and optimization campaign around zunsemetinib is not disclosed, the molecule is structurally related to ATP-competitive molecule PH-797804, from which it is likely derived. This represents an interesting example of modification of a traditionally ATP-competitive inhibitor into a complex-selective inhibitor, which could potentially be applicable to other targets in the future.

Zunsemetinib has persistent activity in animal models in contrast to a global p38 α inhibitor. In genetically engineered neonatal-onset multisystem inflammatory disease (NOMID) mice with tamoxifen-inducible NLRP3 activation, zunsemetinib achieved sustained >60% inhibition of LPS-induced TNF- α expression. [In contrast to a global p38 \$\alpha\$ inhibitor \(CDD-111\), this effect persisted for up to 4 weeks after dosing.](#)

Zunsemetinib has in vitro activity in cells from patients with a genetic autoinflammatory syndrome. In human peripheral blood monocytes (PBMCs) isolated from a patient with [cryopyrin-associated periodic syndromes \(CAPS\)](#) caused by NLRP3 gain-of-function mutations, zunsemetinib reduced IL-1 β secretion and promoted IL-1 β mRNA instability, and inhibited LPS-induced production of TNF- α and IL-1 β with IC₅₀ values in the 1-10 nM range. It also inhibited IL-6 production with an IC₅₀ value in the 100 nM range. The actions of CDD-450 were specific to P38 α MAPK-MK2 blockade, as IKK2, JNK, and ERK1/2 pathways were not affected.

March 2023

zunsemetinib

MK2

oral MK2 inhibitor

Ph. IIa for hidradenitis suppurativa (failed)

designed to selectively inhibit the p38 α -MK2 complex

Press release, March 6, 2023

CONFLUENCE, MO / ACLARIS THERAPEUTICS, PA

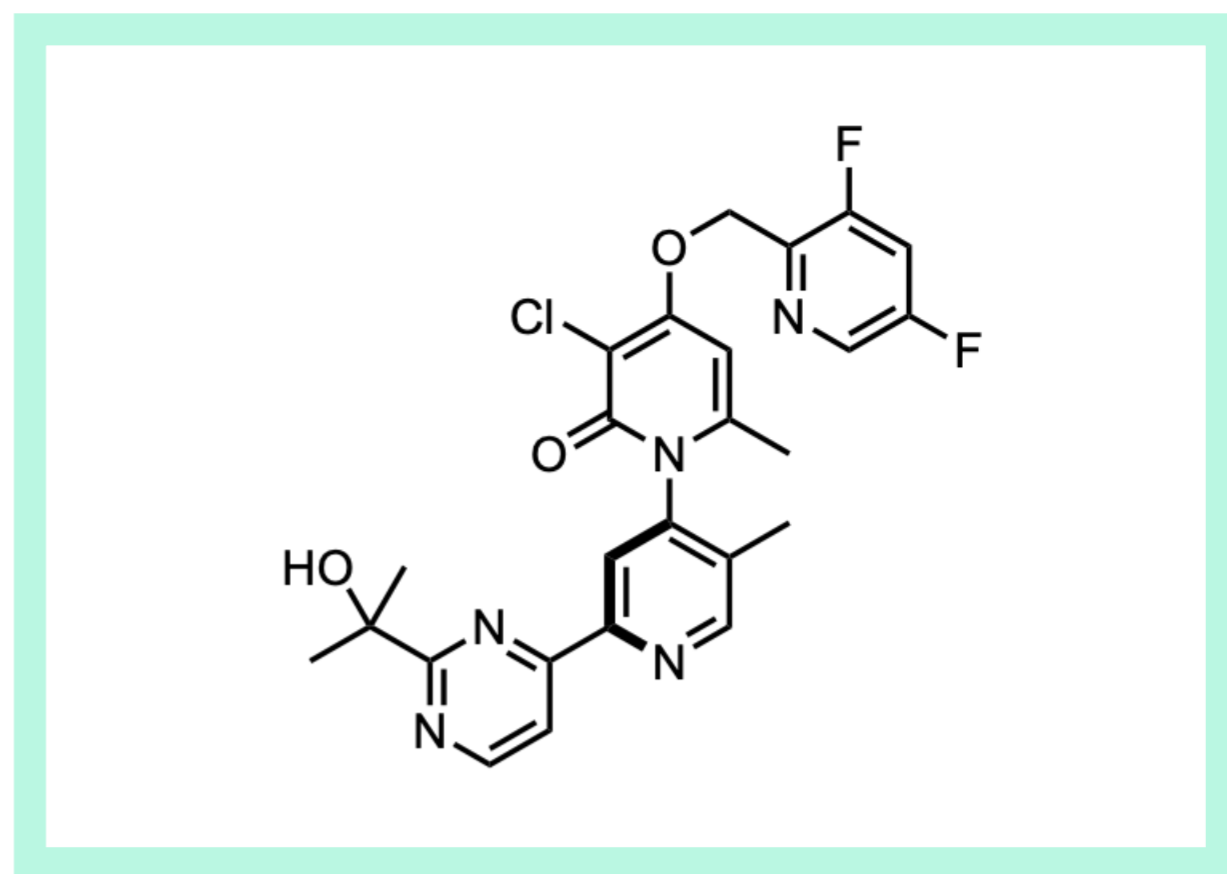
article link: <https://investor.aclaristx.com/news-releases/news-release-details/aclaris-therapeutics-announces-preliminary-topline-data-12-week>

View Online

DMPK and ADMET. Preclinically, zunsemetinib possesses favorable cross-species PK, with allometric scaling supporting QD or BID human dosing ([from the supporting information of this article](#)), and passed standard safety studies suggesting it would be well-tolerated at high exposures:

- Microsomal CL_{int} (M/R/H) = 38 / 11 / 6 mL/min/kg
- In vivo CL_{int} (M/R/D) = 59 / 28 / 6.3 mL/min/kg
- F% (M/R/D) = 111% / 52% / 45%
- hERG inhibition (QT prolongation) = negative
- Ames negative
- In vitro micronucleus genotoxicity negative
- 44 receptor selectivity screen = all >10 μ M
- Kinome selectivity screen (194 kinases) = 350x selective
- Rat 14-day IVT - 2 week reversal = NOAEL-determined therapeutic index >30x

Human PK/PD. In a [Phase I](#) clinical trial, PK studies indicated a terminal half-life of 9-12 hours in a multiple ascending dose cohort after 7 days (n = 24), and blood plasma concentrations of zunsemetinib reached steady state after two days of treatment. At 50 mg BID, trough drug levels were 1.4-2.4x greater than the IC₈₀ for TNF α , IL-1 β , IL-8, and p-HSP27. Maximum inhibition of



>96% was observed for TNF- α , IL-6, and downstream target heat shock protein 27 (p-HSP27), and 74% for IL-1 β and 57% for interleukin-8 (IL-8).

Zunsemetinib demonstrates safety but failed to meet endpoints in a Phase II trial. The [Phase I](#) clinical trial determined that zunsemetinib was well tolerated, with the most common treatment-emergent adverse events (TEAEs) being headache (20%), dizziness (12.5%), upper respiratory tract infection (6.3%) and constipation (6.3%). Unfortunately, a 12-week [Phase IIa](#) study examining zunsemetinib treatment (50 mg BID) in moderate-to-severe hidradenitis suppurativa (HS), a chronic inflammatory skin disorder, failed to meet its primary endpoint of reducing inflammatory nodules, despite PD being consistent with earlier studies. However, study [safety outcomes](#) again indicated that zunsemetinib was well tolerated (n = 95) supporting the selectivity hypothesis. While the efficacy is disappointing, this still serves as an interesting proof-of-principle for selective kinase complex inhibition, which may prove valuable in other settings.

An example of an atropisomeric drug. The synthesis of zunsemetinib can be found in the patent filed on December 11, 2014 ([WO2014197846A1](#), example 49). The drug itself is a stable atropisomer, and in the patent was separated by chiral SFC.

March 2023

JNJ-1802

DENV

oral first-in-class DENV (NS3-NS4B) inhibitor

Ph. I for dengue

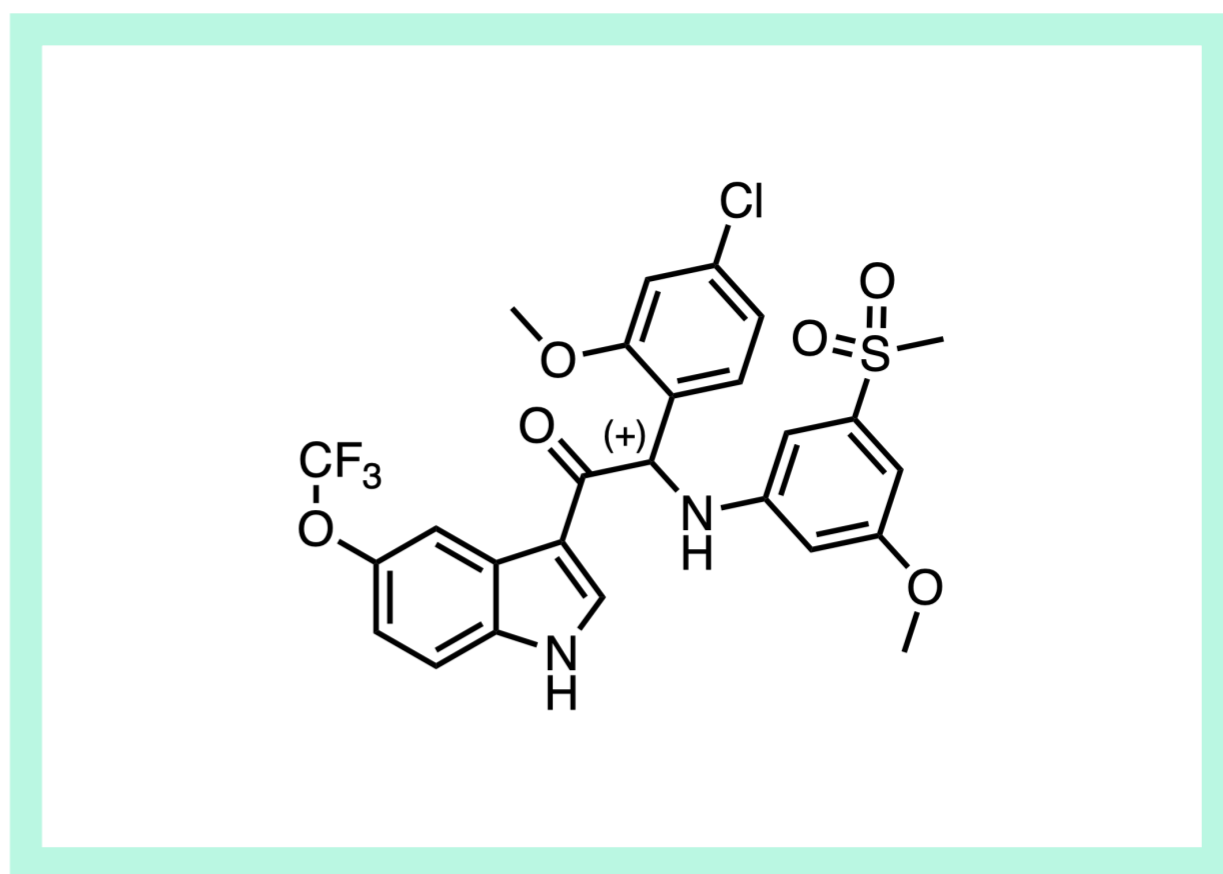
from a DENV-2 phenotypic antiviral screen

Nature, March 15, 2023

JANSSEN, BE + FR

paper DOI: <https://doi.org/10.1038/s41586-023-05790-6>

[View Online](#)



The first dengue NS3-NS4B inhibitor to enter the clinic. Recently disclosed in *Nature*, Janssen's [JNJ-1802](#) is the first dengue virus NS3-NS4B protein-protein interaction inhibitor to enter the clinic. The molecule is derived from a related chemical series to [JNJ-A07](#), which was also disclosed in *Nature* in 2021 and highlighted as a [Molecule of the Month in Oct. 2021](#), but [binds to a different site](#) than Novartis's NS4B inhibitor [NITD-688](#), which was also discovered via phenotypic screening. JNJ-1802 has completed a Ph. I study in healthy volunteers and is currently in [three actively recruiting Ph. II trials](#) including for the treatment of confirmed dengue fever in Singapore (NCT04906980) and prevention of dengue infection in Brazil (NCT05201794). There are still no small molecule treatments approved for dengue.

The growing need for a pan-serotype small molecule therapy for dengue fever. More than 50% of the global population is at risk of [DENV infection](#), and there are approximately 96 million symptomatic infections, 2 million severe diseases cases, and 21k deaths per year caused by dengue. It is predicted that [60% of the world population](#) will be at risk of contracting the mosquito-borne dengue virus by 2080. There are [four DENV serotypes](#) (DENV-1 to DENV-4), and each is capable of inducing the full disease. [Vaccine development](#) is challenged by the requirement that a balanced immune response [must be elicited across all four DENV serotypes](#), or else [antibody-dependent enhancement can cause a more serious secondary infection](#).

Until Takeda's recent [QDENG A approval](#) (with estimated peak sales of \$2B), Sanofi's [Dengvaxia](#) was the only available dengue vaccine, which had [limited efficacy and safety issues](#) (including antibody-dependent enhancement). A pan-serotype small molecule could be highly impactful for this growing global need, but achieving pan-serotype activity is challenging given the limited homology between serotypes, and several NS4B-targeting antivirals lacking pan-serotype activity have already been discontinued (e.g. Novartis Singapore's [compound 14a](#) and [NITD-618](#), Janssen's [JNJ-1A](#)).

An indole starting point from a phenotypic screen for DENV antivirals. The starting point ('Compound 1'; EC₅₀ = 0.078 μM), an indole derivative, was [identified](#) through a medium-throughput phenotypic antiviral screening against the [CD3 compound library](#). A cytopathic effect reduction assay was used, with testing done against the DENV-2 'Rega' lab strain. A significant reduction in viral RNA was observed at nontoxic concentrations, implying that the activity was selective for the viral biology and not due to adverse effects on the host cell.

Identification of NS3-NS4B protein-protein interaction as a novel mechanism of action through resistance screening. Target deconvolution through selection of drug-resistant variants, resulted in the identification of the [non-structural protein NS4B](#) as a target, which showed that multiple

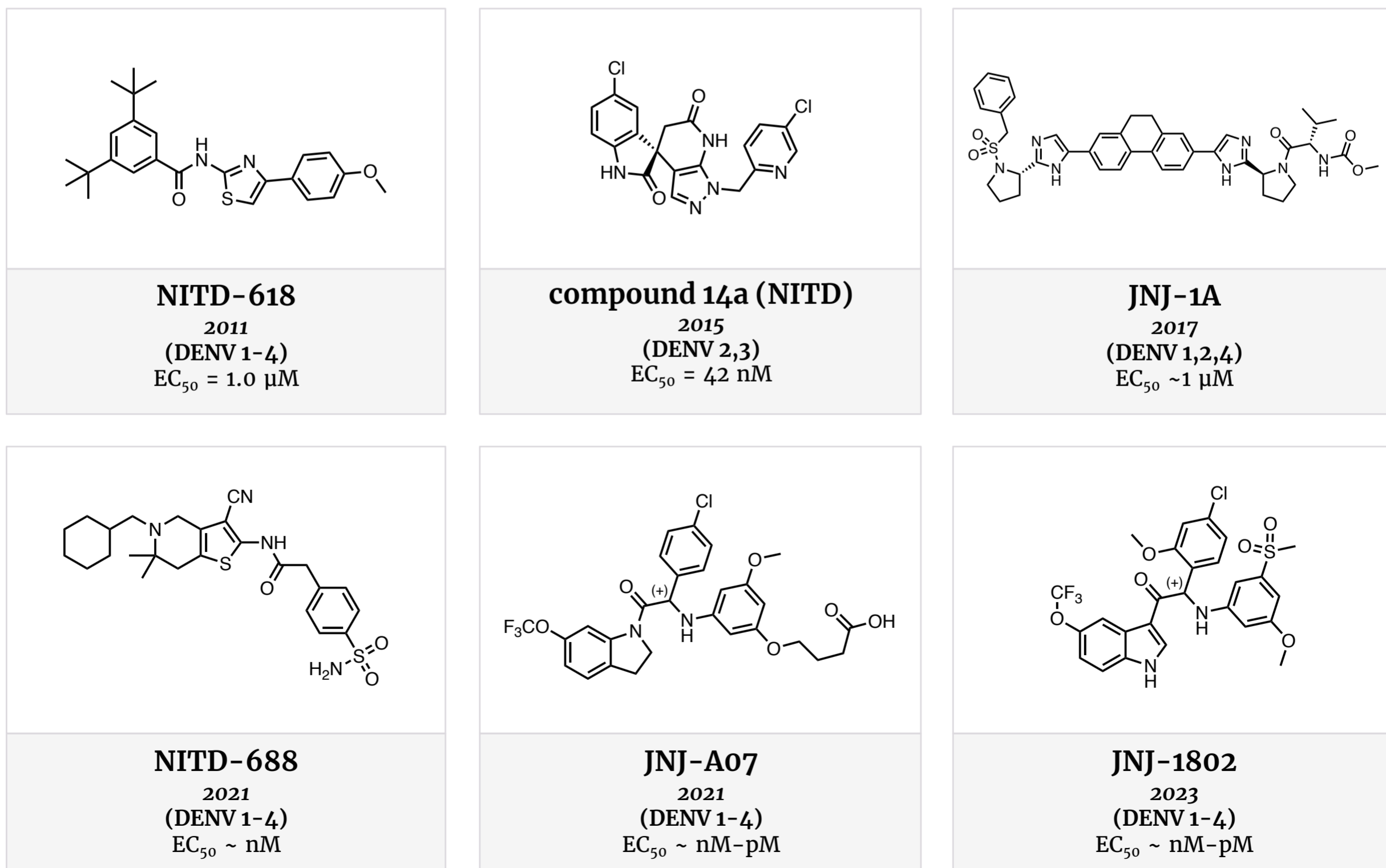


Fig. 1. Representative [NS4B inhibitors](#) over time. The most promising molecules come from Novartis and Janssen, with pan-serotype activity, strong potency, and promising PK.

March 2023

JNJ-1802

DENV

oral first-in-class DENV (NS3-NS4B) inhibitor

Ph. I for dengue

from a DENV-2 phenotypic antiviral screen

Nature, March 15, 2023

JANSSEN, BE + FR

paper DOI: <https://doi.org/10.1038/s41586-023-05790-6>

[View Online](#)

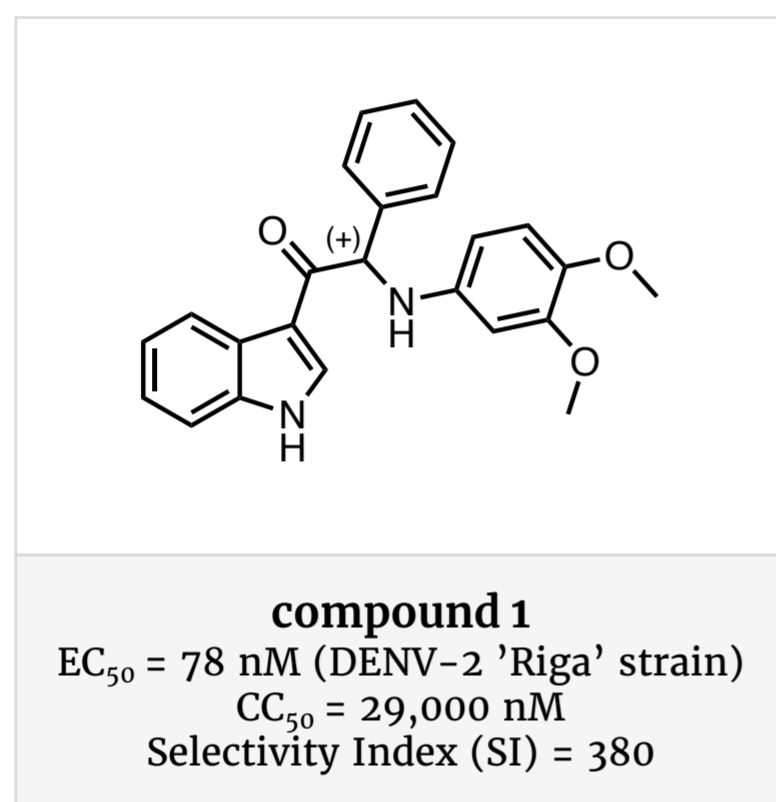


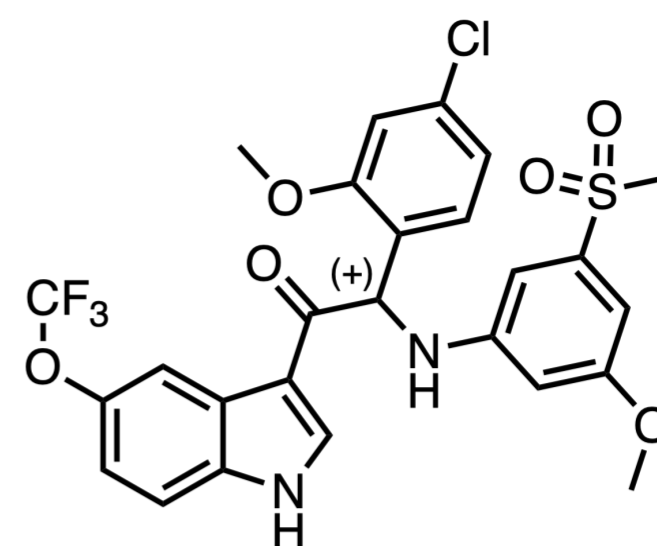
Fig. 2. Chemical starting point for JNJ-1802.

mutations in the viral NS4B gene were needed together to result in resistance. A molecule from the series, JNJ-A07, [decreased co-precipitation of NS4B captured by NS3](#), demonstrating that the series inhibits the NS4B-NS3 interaction. The 7 non-structural (NS) DENV proteins mediate viral assembly, replication, and immune evasion during dengue progression and pathogenesis. [NS3](#), an enzyme, contains protease activity at the N-terminus and helicase activity at the C-terminus, while [NS4B](#), a transmembrane protein with no enzymatic activity, is a key component of the replication complex on the cell membrane. DENV inhibitors targeting either [NS4B](#) or [NS3](#) had been described, but not [NS4B-NS3 PPI](#) inhibitors. The DENV NS4B-NS3 PPI was [first reported in 2006](#) and supported by [subsequent studies](#) that have implicated the complex in viral replication through [regulation of NS3 helicase activity](#). JNJ-1802 [targets](#) NS4B and blocks the NS3-NS4B PPI, impacting viral replication by preventing NS3 from achieving [optimal helicase activity, which requires NS4B](#). However, already established NS3-NS4B complexes are not impacted by the inhibitor.

A picomolar inhibitor in human DENV target cells from optimization of cell-based activity. Given the non-enzymatic role of NS4B, and the lack of a solved structure of the membrane-associated protein, a [cell-based DENV-2 virus yield reduction assay with a RT-qPCR readout was used to guide initial optimization](#). Limited details are available about the SAR leading to the final compound, but after the synthesis of ~2000 analogues, [JNJ-A07, a representative compound from the series](#), was found to exhibit potent pan-genotype and pan-serotype activities (nanomolar-picomolar) in various cell lines and against various clinical isolates. JNJ-1802 was ultimately identified with strong potency across settings, DENV genotypes and serotypes, with picomolar EC₉₀'s in human DENV target cells and nanomolar potency in mosquito cells:

- Cellular antiviral EC₅₀ (Vero monkey kidney cell line, DENV-2/16681/eGFP) = 59 pM
- Cellular antiviral EC₉₀ (Vero, DENV-2/16681/eGFP) = 161 pM
- Cellular CC₅₀ (Vero) = 2.61 uM (44,000x selectivity index)
- Cellular antiviral EC₅₀ w/ 50% human serum (Vero, DENV-2/16681/eGFP) = 1.4 nM
- Cellular antiviral EC₉₀ w/ 50% human serum (Vero, DENV-2/16681/eGFP) = 4.8 nM
- Cellular antiviral EC₅₀ (C6/36 mosquito cell line, DENV-2/RL) = 1.24 nM
- Cellular antiviral EC₅₀ (THP-1/DC-SIGN human DENV target cells, DENV-2/16681/eGFP) = 173 pM
- Strong pan-genotype and pan-serotype potency (EC₅₀: <0.04 nM to 1.8 nM) against a panel of 20 DENV strains with diverse genotypes across the 4 serotypes
- Inactive against other flaviviruses (West Nile Virus, JEV, Zika); EC₅₀ from 0.25-1.1 uM

Both therapeutic and prophylactic oral efficacy in rodents and non-human primates. In preclinical studies in immunocompromised [AG129 mice](#) to evaluate prophylactic efficacy, BID



dosing at 0.2 – 60 mg/kg/day for 3 days led to decreased mean viral RNA from a range of 3.8log₁₀ to 1.0log₁₀ copies/ml. Initiation of JNJ-1802 treatment at 6 or 60 mg/kg BID before viral challenge with DENV-1, DENV-3 or DENV-4 led to a 100% survival rate, with animals in the treatment group remaining disease-free till end of the study; in the vehicle group, the survival rate was 0% in most studies. Efficacy was also observed in non-human primates (NHPs) based on biomarkers such as viral RNA load and IgM/IgG response, since NHPs are susceptible to dengue and have competent immune systems, but [do not present with clear infection symptoms](#). The combined results suggest that JNJ-1802 has the potential to be effective in both prophylactic and therapeutic settings in humans.

Excellent PK leads to consistent coverage of the 3x pbaEC₉₀. JNJ-1802 also had an [excellent PK profile](#) in both mice and NHPs, with high oral bioavailability and a long half-life (see below). The predicted efficacious concentration vs. DENV-2/16681 was estimated at 3x the protein-binding adjusted 90% effective concentration (3x pbaEC₉₀) or 14 nM (8.2 ng/mL), [a measure which has been used to estimate efficacious concentrations against other viruses such as HCV](#). At 3 mg/kg/day, exposure values were well above (40-230 fold) 8.2 ng/mL at 24 h after the first dose. At 0.18/mg/kg/day, exposure values were just above 8.2 ng/mL, translating to an intermediate effect. 0.01 mg/kg/day resulted in exposure levels below the 3x pbaEC₉₀ and was less efficacious.

- 3x pbaEC₉₀ = 14 nM (8.2 ng/mL)
- Mouse / NHP PPB > 99.9%
- Mouse / NHP CL_p (2.5/1 mg/kg) = 5.0/1.7 mL/min/kg
- Mouse / NHP T_{1/2} (2.5/1 mg/kg) = 6.2 h / 50 h
- Mouse F% (1/3/10 mg/kg) = 46%/59%/>100%
- NHP F% = 18-27%

A high barrier to drug resistance. There appears to be a high barrier for resistance to JNJ-1802, as the first highly resistant triple mutants only emerged after [35 or more passages](#) of increased drug concentrations (6 mo. of in vitro culture), which is in contrast to HCV protease inhibitors and RNA polymerase inhibitors which develop mutants in 10 cell passages or less. The biology of dengue virus may also help, as viraemia lasts for only a week resulting in a short treatment period that may not allow for drug-resistant variants to emerge. Furthermore, even if drug-resistant mutants were to emerge, they may not be viable in mosquitoes, which would be needed for transmission of a resistant mutant.

Preclinical safety. Limited data is available, though it is stated that no adverse drug effects were observed in NHPs, and that [JNJ-1802 was selected over JNJ-A07 as a clinical candidate due to a better preclinical safety profile](#).

First dengue-specific antiviral small molecule to complete a first-in-human study. JNJ-1802 (JNJ-64281802) has been evaluated in a [completed Ph. I study in healthy volunteers \(NCT05201937\)](#), a suspended Ph. II study in a dengue human challenge model in healthy adults ([NCT04480736; recruitment paused](#), reason unknown), and is being evaluated in 3 ongoing Ph. II studies. These include a study in participants with no evidence of DENV infection (prophylactic study; [NCT05201794](#)), a study in those with confirmed DENV infection ([NCT04906980](#)) and a study in healthy individuals challenged with DENV-3 infection ([NCT05048875](#)). In the completed Ph. I safety and tolerability study, no deaths, serious adverse events (AEs) or AEs leading to treatment discontinuation were [observed](#). In humans, the drug has a long terminal t_{1/2} of 6.3-9.2 days, and in the Ph. II study for dengue prevention, the high dose regimen involves a 400 mg BID loading dose over two days followed by a 150 mg QD maintenance dose, and the low dose regimen involves a 150 mg BID loading dose for two days followed by a 50 mg QD maintenance dose. Though [non-specific antivirals](#) have been explored for dengue without success, [no other dengue-specific antiviral small molecule appears to have completed a human clinical study to date](#).

Patents:

- “Substituted indoline derivatives as dengue viral replication inhibitors”: [US10689340B2](#) (2020), [US10913716B2](#) (2021)
- “Mono- or di-substituted indole derivatives as dengue viral replication inhibitors”: [US10696632B2](#) (2020)

March 2023

nirogacestat

gamma secretase

oral gamma secretase inhibitor

Ph. III for DT/AF + Ph. II for OvGCTs

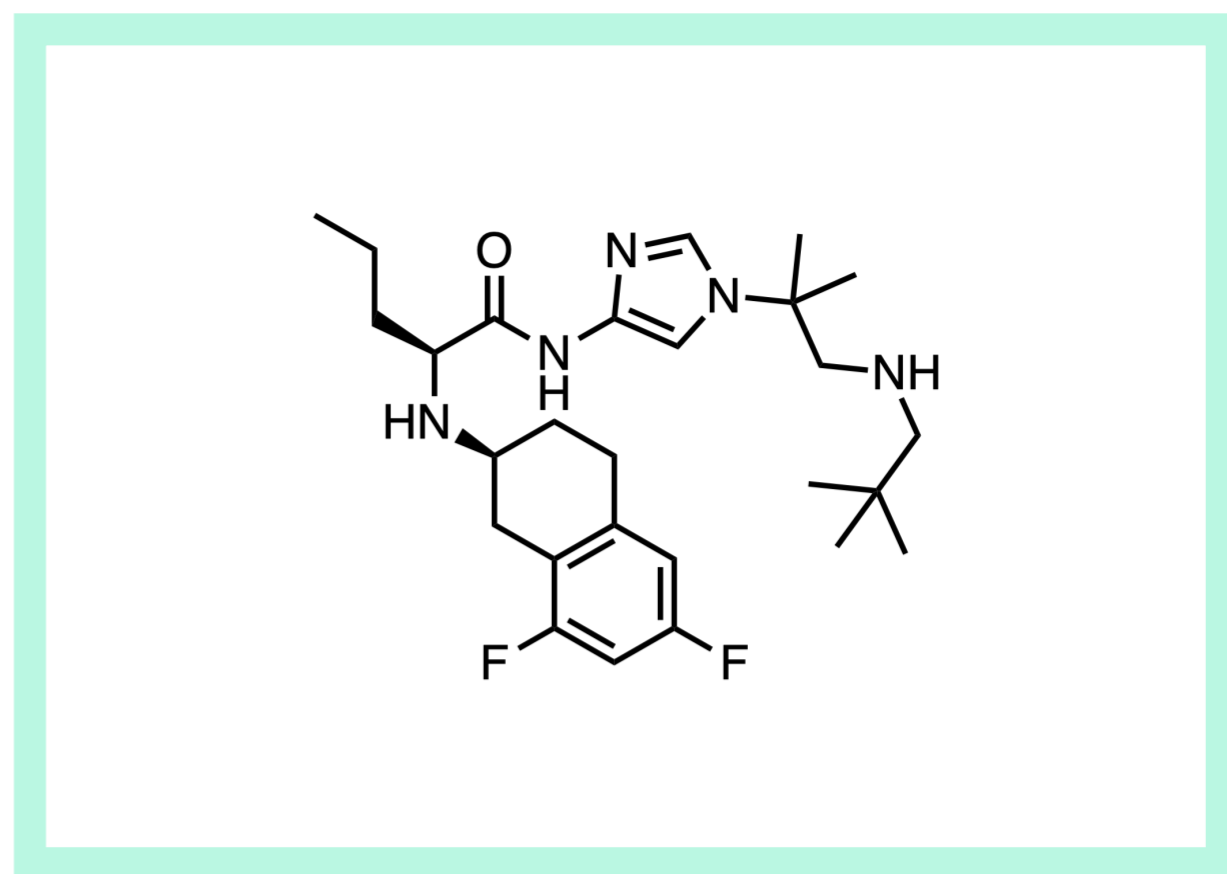
single-digit nanomolar potency for

A β reduction in vitro

Press release, February 27, 2023 / NEJM, March 9, 2023

PFIZER / SPRINGWORKS THERAPEUTICS, INC.

article link: <https://ir.springworkstx.com/news-releases/news-release-details/springworks-therapeutics-announces-fda-acceptance-and-priority>



View Online

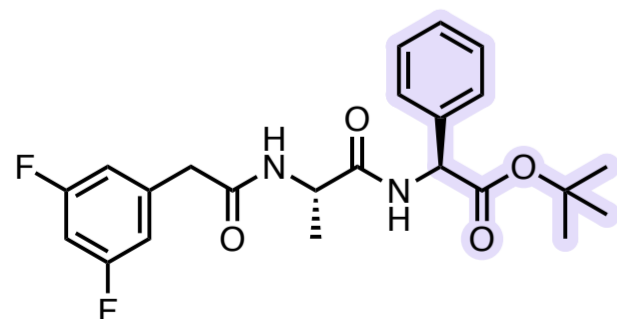
Upcycling a γ -secretase inhibitor for a potentially first- & best-in-class treatment for aggressive desmoid tumors. Nirogacestat was recently granted [FDA priority review](#) for rare, aggressive, locally invasive, soft-tissue desmoid tumors (DTs). This reversible, non-competitive gamma secretase inhibitor (GSI) draws its anticancer activity from its ability to block Notch signaling, and is the lead drug from a 2017 [Pfizer spinout](#), [SpringWorks Therapeutics](#). While not metastatic or life-threatening, [desmoid tumors](#) can compress vital organs, causing nerve damage, severe pain and intestinal complications, and there are no FDA-approved treatments. [Therapeutic approaches for DT](#) include robust chemotherapy, radiation and TKI treatments, but these are often poorly tolerated and inconsistently efficacious. For these reasons, nirogacestat has been granted Fast Track, Breakthrough Therapy and Orphan Drug designations from the FDA. This Ph. III candidate [reduced the risk](#) of disease progression by 71% and improved pain, other tumor-specific symptoms and physical functioning (150 mg BID, n = 142, [NCT03785964](#)), and the PDUFA date has been set to August 27th 2023.

Liabilities for Alzheimer's turned into a treatment strategy for aggressive tumors. Gamma-secretase is more commonly known as an [Alzheimer's Disease \(AD\) target](#), as inhibition of it rapidly reduces levels of amyloid- β (A β) peptide, the main component of damaging plaques associated with AD, and the cleavage product of amyloid precursor protein (APP). Pfizer [originally developed](#) nirogacestat, known as PF-3084014 at the time, for the treatment of AD, but early clinical trials indicated that it did not demonstrate adequate brain exposure. However, a known [on-target liability](#) at the time was hyperplasia of intestinal goblet cells and circulating B-cell reduction in preclinical models, which had been linked to modulation of another gamma-

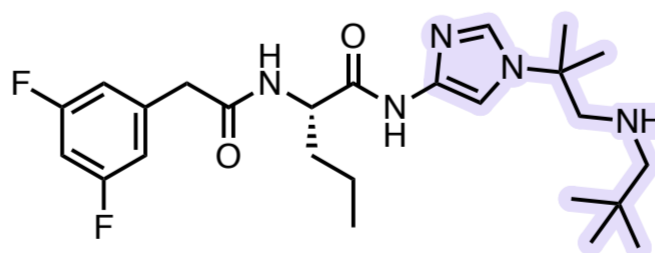
secretase substrate, [Notch](#). Notch inhibition has also been associated with [antitumor efficacy](#) in multiple models, which led to nirogacestat's repurposing for the treatment of desmoid tumors. Pfizer cited that the originally unintended, [peripherally-restricted exposure](#) of nirogacestat and its good human safety and tolerability profile positioned it well as a potentially best-in-class GSI for oncology indications.

Gamma-secretase's role in aberrant Notch1-signaling in cancers. Gamma secretase catalyzes the proteolytic [release of the Notch intracellular domain \(NICD\)](#), which plays a key role in Notch-dependent nuclear signaling. About 10% of all T-cell acute lymphoblastic leukemia (T-ALL) patients have deletions in the *Notch1* extracellular domain. These deletions result in constitutively-active Notch1 proteins and oncogenic Notch signaling. Even further, *Notch1* is the most commonly activated oncogene for T-ALL, with activating Notch1 mutations found in [>50% of patients](#). Activated Notch1 has also been identified in multiple myeloma, breast & pancreatic cancer, and melanoma tumors. These [mutations induce the production](#) of NICD via gamma-secretase cleavage or [increase NICD's half-life](#), leading to increased NICD levels and activation of Notch signaling in cells.

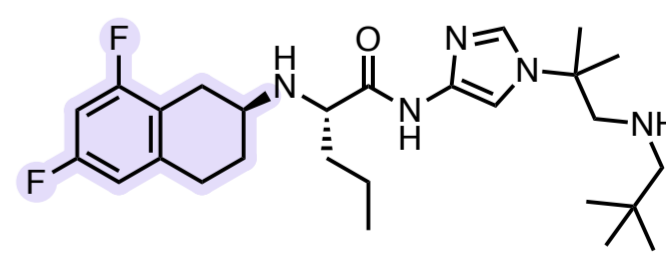
Desmoid tumors overexpress and are partly driven by Notch1 signaling. While the mechanism of action of nirogacestat in the treatment of desmoid tumors is [not fully understood](#), this tumor type is typically characterized by genetic mutations in the Wnt- β -catenin pathway (*CTNNB1*) and overexpresses Notch1. The crosstalk between these pathways is thought to drive the proliferation of desmoid tumors. By blocking Notch signaling and inhibiting γ -secretase-mediated cleavage of Notch receptors, tumor proliferation can be blocked.



DAPT
GS IC₅₀ (WCA) = 20 nM



compound 10h
GS IC₅₀ (WCA) = 0.4 nM
FTOC EC₅₀ = 1.2 μ M
MDR E_r = 8.4



nirogacestat
(PF-3084014, compound 14f)
GS IC₅₀ (WCA) = 1.2 nM
FTOC EC₅₀ = 1.8 μ M
MDR E_r = 1.5 (racemic)

GS = gamma secretase; WCA = whole cell assay; FTOC = fetal thymic organ culture; E_r = efflux ratio

March 2023

nirogacestat

gamma secretase

oral gamma secretase inhibitor

Ph. III for DT/AF + Ph. II for OvGCTs

single-digit nanomolar potency for

A β reduction in vitro

Press release, February 27, 2023

PFIZER / SPRINGWORKS THERAPEUTICS, INC.

article link: <https://ir.springworkstx.com/news-releases/news-release-details/springworks-therapeutics-announces-fda-acceptance-and-priority>

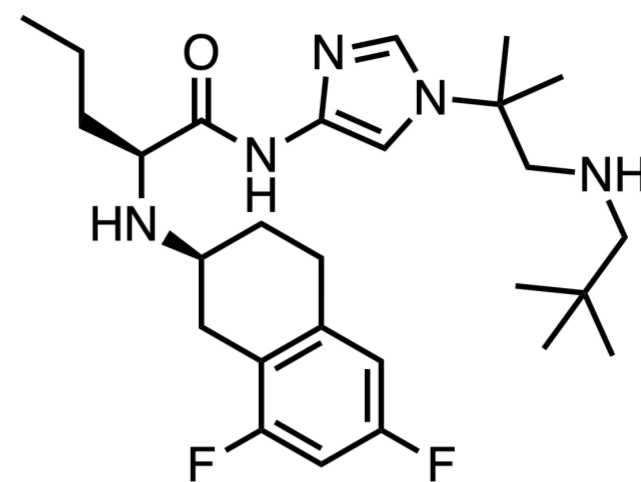
[View Online](#)

Optimization of DAPT for stability, selectivity and brain-penetration. The chemistry starting point for the team was GSI N-[N-(3,5-difluorophenacetyl)-l-alanyl]-S-phenylglycine t-butyl ester, or [DAPT](#), with 20 nM whole cell potency reported by Eli Lilly and Elan in 2001. The hydrolytic liability of the t-butyl ester led to the development of a [diamide amino imidazole series](#) in 2011. Varying the N-substituent on the imidazole ring led to the identification of “compound 10h” with excellent cellular potency that reduced A β in the brain, cerebrospinal fluid (CSF) and plasma in guinea pig models upon acute treatment. Optimization of the selectivity profile and mitigation of the significant P-gp-mediated efflux led to a tetralin replacement of the phenyl acetic acid moiety, resulting in the [discovery of PF-3084014](#) (nirogacestat, “compound 14f”). A thorough screen of other proteases, receptors, ion channels and kinases confirmed its selectivity for gamma-secretase. It is notable that nirogacestat is orally bioavailable and has low efflux in vitro despite being [dibasic](#), though brain penetration was not achieved in humans.

An initially misleading in vitro window between PF-03084014 A β activity and Notch activity. Originally intended to be developed for the treatment of Alzheimer’s Disease (AD), it was thought in [2010](#) that the separation between nirogacestat’s A β activity from its Notch activity would be beneficial for drug safety, given the well-known [gastrointestinal toxicities](#) related to Notch inhibition observed in mice. Nirogacestat (PF-3084014) reduced A β production with an IC₅₀ of 1.2 nM (whole cell assay) and inhibited Notch-related T- and B-cell maturation at an EC₅₀ of 2.1 μ M (in vitro thymocyte assay over 5 days). Dose-dependent reduction of A β in the brain, cerebrospinal fluid (CSF) and plasma was observed in mouse and guinea pig models upon treatment, and the extent and duration of A β reduction in these models exceeded the reductions in B-cell endpoints by 3- to 5-fold in CRND8 mice. Fortunately for its application to cancer treatment, it turns out that PF-03084014 is not actually selective for A β activity and Notch when measured in different ways.

In vivo studies and longer treatment times show PF-03084014 Notch inhibition is actually comparable to its activity on A β . However, [in vivo](#) studies with [osmotic minipumps](#) showed that the compound was relatively more active on Notch signaling in vivo than in the in vitro assay, and results unpublished at the time showed that Notch and A β activity were comparable after [longer treatment periods of 5-16 days](#). It turns out that cell cycle block and apoptosis are only evident after [7 days of treatment](#) (vs. the 5 days used in the thymocyte assay). In a cell-based functional assay looking at Notch receptor cleavage, the cell IC₅₀ was [13 nM](#), much more in line with activity on A β .

Complete responses in first-in-human studies support the NOTCH1-based therapeutic hypothesis. Nirogacestat was well-tolerated in a Ph. I dose-escalation study of patients, with [favorable PK and early evidence of clinical activity](#) (20-500 mg BID, n = 72, [NCT00878189](#)). Eight patients with T-ALL or T-LBL demonstrated complete response (CR) with full hematologic recovery that lasted for ~3 months (150 mg BID, 2 continuous cycles). Results from Sanger and deep sequencing of patient samples supported the hypothesis of a [leukemogenic role for NOTCH1-activating mutations](#) in T-ALL T-LBL demonstrated complete response (CR) with full hematologic recovery that lasted for ~3 months (150 mg BID, 2 continuous cycles). Results from Sanger and deep sequencing of patient



samples supported the hypothesis of a [leukemogenic role for NOTCH1-activating mutations](#) in T-ALL and the corresponding sensitivity to gamma-secretase inhibition. Favorable human PK was demonstrated, with a mean terminal t_{1/2} of 18 h and steady state achieved by day 8.

Ph. II studies in desmoid tumors suggest significant efficacy. Buoyed by early Ph. I clinical activity in liquid tumors, the molecule moved into [Ph. II studies](#) for the treatment of desmoid tumors and aggressive fibromatosis (AF). A 31% ORR and a notable extended progression-free survival (PFS) (150 mg BID, continuous 3w cycles, n = 17, [NCT01981551](#)) was observed, with most common adverse events of hypophosphatemia (76%), diarrhea (76%), nausea (65%), AST increase (65%), and lymphopenia (65%). The long response duration and lack of tumor progressions supported moving nirogacestat into Ph. III.

Ph. III efficacy confers FDA priority review. In the Ph. III trial for the treatment of desmoid tumors in adults, the [primary endpoint](#) of significant PFS benefit over placebo was achieved, with a 76% likelihood of being event-free at 2 years, versus 44% for placebo (150 mg BID, n = 142, [NCT03785964](#)). There was a 41% ORR for tumor shrinkage (vs. 8%) with 7% CR rate (vs. 0%) and a median time to response of 5.6 months (vs. 11.1). Secondary endpoints of significant improvements in pain, physical functioning, disease-specific symptoms and overall quality-of-life were met. Nearly all adverse events remained grade 1 or 2, including diarrhea (84%), nausea (54%), fatigue (51%), hypophosphatemia (42%), and maculopapular rash (32%). Among female patients of childbearing potential, 27 of 36 (75%) had adverse events consistent with ovarian dysfunction, but this did resolve in 20 of those patients (74%).

What’s next? Nirogacestat is also in Ph. II for pediatric patients (<18 years) with desmoid tumors ([NCT04195399](#)), and for ovarian granulosa cell tumors in adults (OvGCTs, [NCT05348356](#)), which are likely susceptible to gamma secretase inhibition due to mutations in FOXL2. It is also in Ph. I for R/R MM in combination with linvolseltamab ([NCT05137054](#)).

Lessons learned. Overall, nirogacestat is a nice example showing how the originally intended indication for a drug or target may not be the one the drug is ultimately successful in. Several disconnects between experimental models were observed, from potency differences between in vitro assays, to differences in brain penetration between models and humans, highlighting the importance of using multiple readouts for key properties. Finally, nirogacestat is a good case study for the emerging trend of large pharma companies like Pfizer founding their own startups to help develop their assets in more focused areas.

Patents. “Methods of treating desmoid tumors with (s)-2-(((s)-6,8-difluoro-1,2,3,4-tetrahydronaphthalen-2-yl)amino)-n-(1-(2-methyl-1-(neopentylamino)propan-2-yl)-1h-imidazol-4-yl)pentanamide” [US20230049311](#) (2023). “A combination therapy with nirogacestat and a bcma-directed therapy and uses thereof” [WO2021183934A1](#) (2021). “Combination therapy with an anti bcma antibody and a gamma secretase inhibitor” [WO2020208572A1](#) (2020). “Imidazole compounds for the treatment of neurodegenerative disorders” [US7951958B2](#) (2010), [WO2005092864A1](#) (2005).

March 2023

linvencorvir

HBV core protein

allosteric HBV modulator

Ph. II for chronic hepatitis B (CHB)

opt. of known allosteric heteroaryl pyrimidine

core protein modulator

J. Med. Chem., March 10, 2023

ROCHE, SHANGHAI, CN

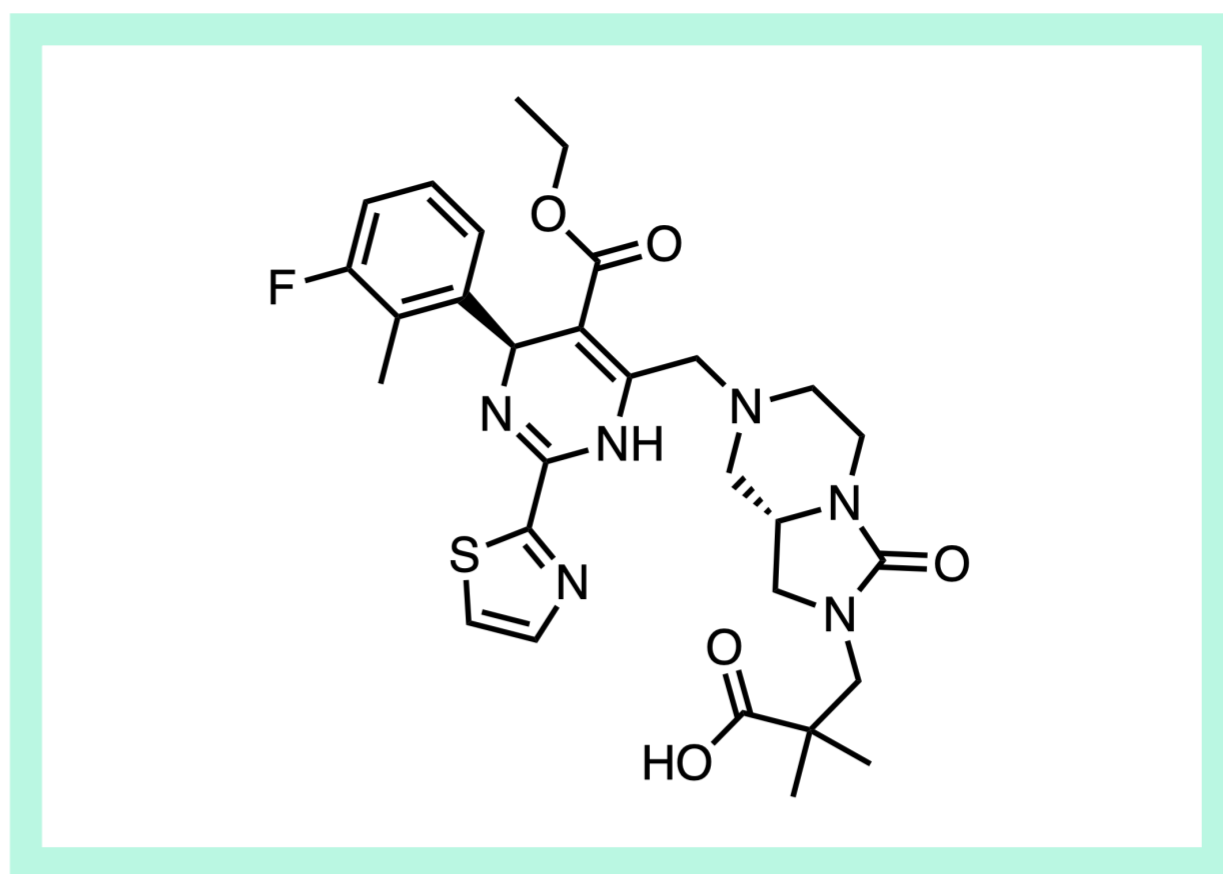
paper DOI:

<https://pubs.acs.org/doi/10.1021/acs.jmedchem.3c00173>

[View Online](#)

A Ph. II liver-targeting HBV core protein modulator optimized for ADMET properties. Linvencorvir (RG7907), a novel HBV core protein allosteric modulator, offers a promising treatment option for chronic hepatitis B which affects 296 million people globally. It possesses an interesting glue-like mechanism that causes the HBV core protein to aggregate into incompetent capsids, reminiscent of HIV capsid modulator [lenacapavir](#). Its potent anti-HBV activity, low CYP3A4 induction, favorable human PK, and promising safety have allowed it to reach Ph. II. The resolution of a CYP induction problem and a hERG issue aided by interesting co-crystal structures make this a valuable med chem case study, while the unmet need and mechanism of action make it a noteworthy pharmacological advance.

The unmet medical need in HBV. Currently, standard of [care](#) for HBV involves using interferons and nucleos(t)ides that are designed to reduce the virological response, measured by the loss of the HBV e antigen, [HBeAg](#), from plasma. However, HBV cannot usually be cured; chronic infection is signalled by the remaining presence of the surface antigen, [HBsAg](#), which is extremely difficult to completely remove. HBsAg is only spontaneously removed in <3% cases after 1 year of treatment, and <15% cases after 1 – 5 years treatment with nucleos(t)ides and pegylated interferon treatment. Therefore, chronically infected patients need continuous monitoring of HBV DNA levels in serum and potentially lifelong treatment. As interferon and nucleos(t)ide therapies

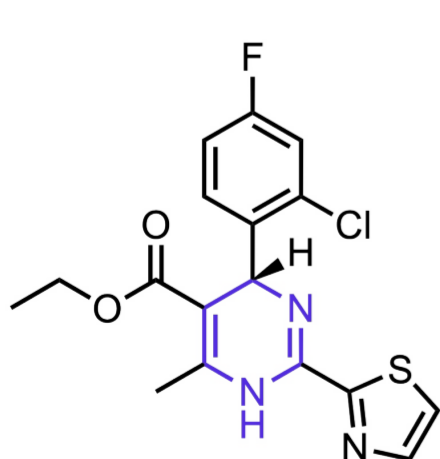


have significant side-effects, continuation on treatment for life poses significant burdens, not to mention risk of viral resistance. [Development of a drug](#) that can clear HBV infection, as measured by a reduction in HBsAg antigen, would be extremely useful and potentially lead to a higher cure rate for HBV. With favorable preclinical data and ongoing clinical trials, this innovative class of molecules represents a shot on goal to address the limitations of existing treatments, such as side effects, lifelong necessity, and viral resistance, though it may no longer be in development (see below).

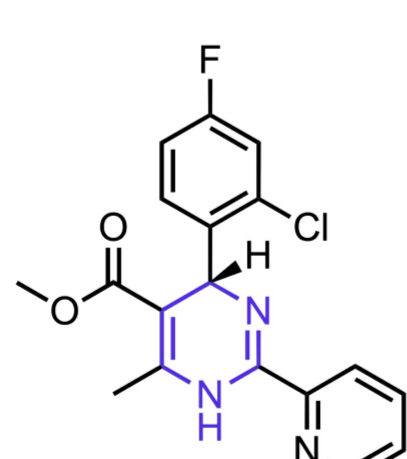
A HAP-based Class I HBV capsid assembly modulator. Linvencorvir, a Class I capsid assembly modulator (CAM), targets HBV core protein as an allosteric modulator, [inducing abnormal capsid formation](#). CAMs are categorized into two classes: Class I, including heteroaryldihydropyrimidines (HAPs), forms non-capsid polymers or large core protein aggregates, while Class II generates empty capsids lacking pgRNA. Despite distinct effects, both classes [bind the same hydrophobic pocket](#) within HBV core protein, with their different activities attributed to a unique [hydrophobic subpocket](#) occupied by the thiazole of Class I modulators.

- For mechanistic characterization of the HAP starting point, see [PNAS 2005](#).
- For a 2021 review on CAMs, [see here](#).
- For a 2023 review on approaches to HBV treatment, [see here](#).

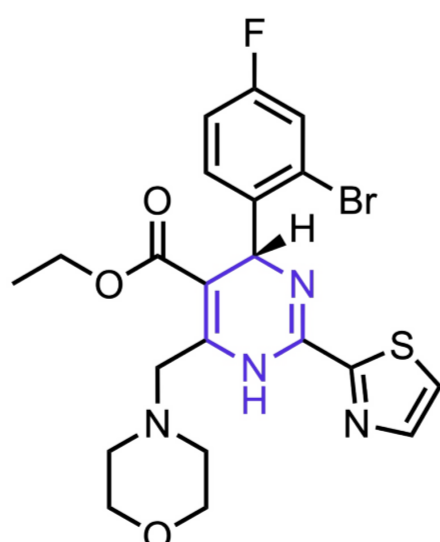
Class I CAM Examples:



BAY 39-5493
HBV cell IC₅₀ = 50 nM
cell CC₅₀ = 7 μM

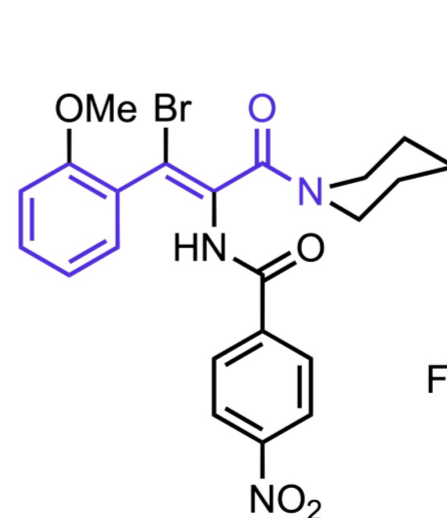


HAP-1
HBV cell IC₅₀ = 3 nM
cell CC₅₀ = >100 μM

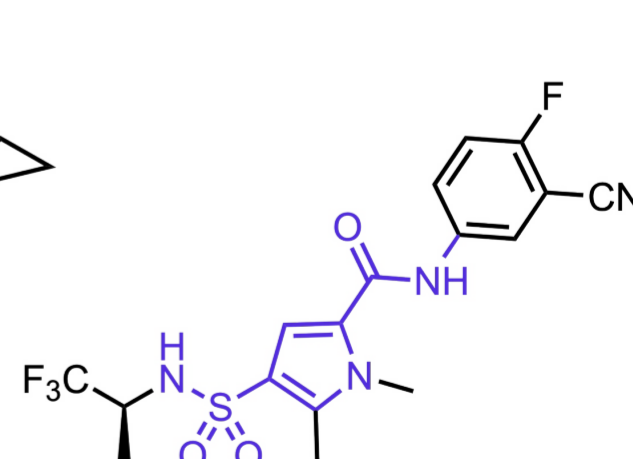


GLS4 (morphothiadin)
Entered Ph. II

Class II CAM Examples:



AT-130
Entered Ph. I



JNJ-56136379 (bersacapavir)
Entered Ph. II

March 2023

linvencorvir

HBV core protein

allosteric HBV modulator

Ph. II for chronic hepatitis B (CHB)

opt. of known allosteric heteroaryl pyrimidine

core protein modulator

J. Med. Chem., March 10, 2023

ROCHE, SHANGHAI, CN

paper DOI:

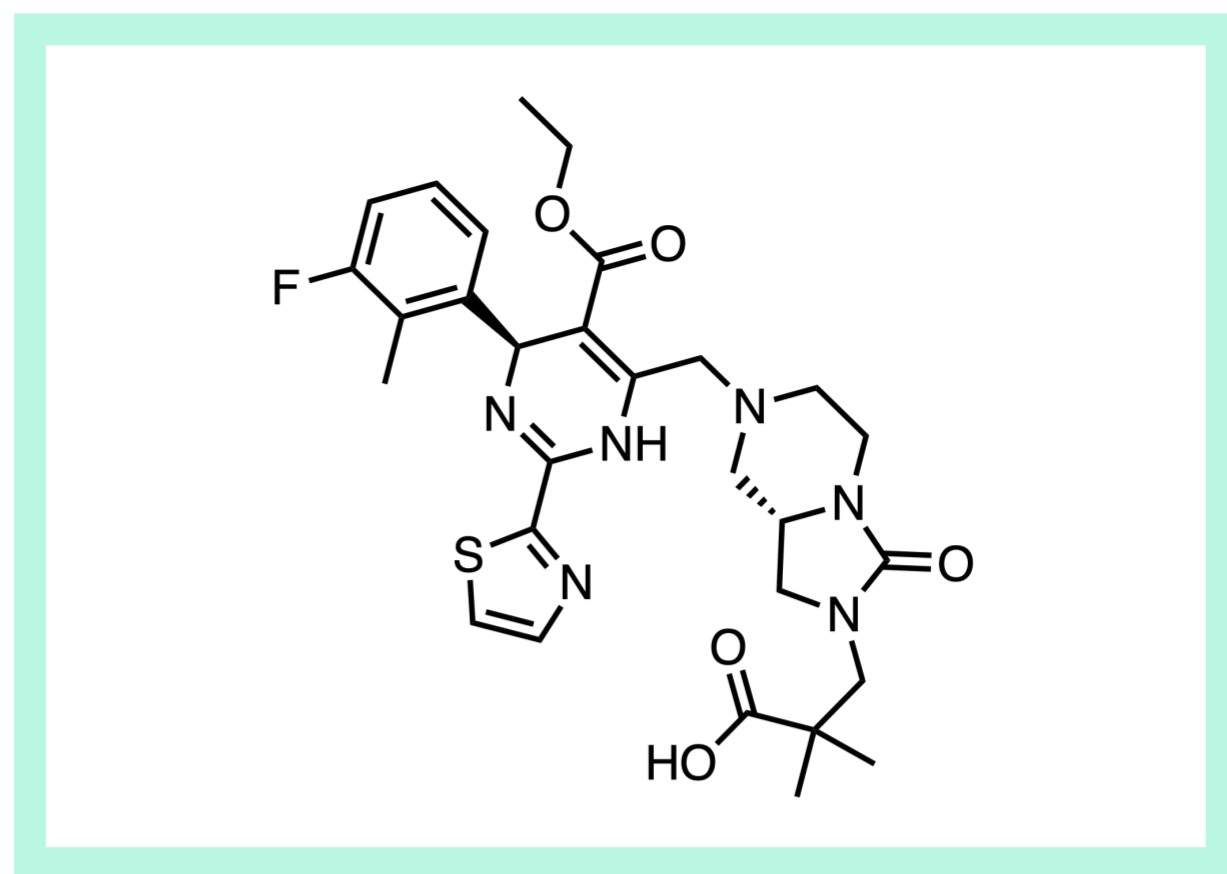
<https://pubs.acs.org/doi/10.1021/acs.jmedchem.3c00173>

[View Online](#)

From optimization of a Bayer scaffold discovered in the 2000's. Linvencorvir builds upon [dihydropyrimidine \(HAP\)-based scaffolds](#) which were [discovered by Bayer](#) and [entered Ph. I](#) in the early 2000's. The Roche Shanghai team successfully addressed CYP3A4 induction problem [endemic to the series](#) by adding a large, polar, rigid substituent at C-6.

- Bayer initial program disclosure ([Antiviral Res. 2002](#))
- Bayer HAP-scaffold disclosure ([Science 2003](#))
- Sunshine Lake Pharma clinical candidate (GLS4, morphothiadin) disclosure ([BMC 2017](#))
- Roche Shanghai's 2017 characterization of third-gen. HAP analogues w/ CYP induction ([JMC 2017](#))
- Roche Shanghai's 2017 disclosure of HAP_R01 and structural characterization of its mechanism ([Sci Rep 2017](#))
- Roche Shanghai's 2019 attempt to address CYP induction through dihedral angle modulation ([JMC 2019](#))

Mitigation of CYP3A4 induction by changing the polarity pattern of the C6 amine. CYP induction is attributed to [activation of the pregnane xenobiotic receptor \(PXR\)](#) nuclear receptor. The [PXR pharmacophore](#) is similar to the HAP pharmacophore, with lipophilic regions surrounding a hydrogen bond acceptor. [Introduction of polar groups to the ends of a PXR activator](#) to destabilize interactions with the lipophilic regions of PXR is a commonly employed tactic to get around CYP induction. Whereas

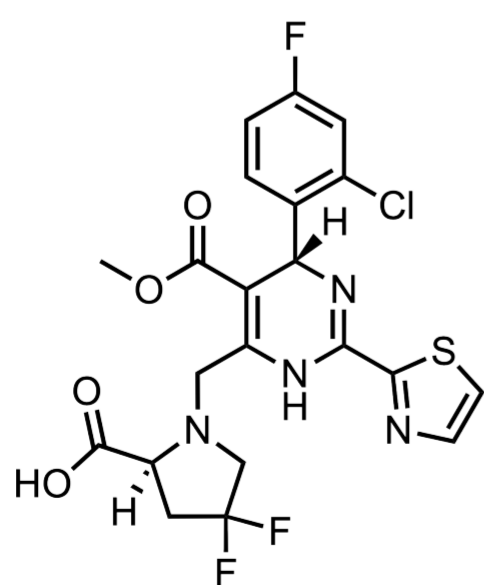


the non-polar C-2 and C-4 substituents are required for activity and located in hydrophobic pockets, the difluoropyrrolidine off of C-6 of [HAP_R01](#) binds in a solvent-exposed region of the HBV core protein ([PDB: 5WRE](#)), suggesting its replacement with groups of different polarity patterns could mitigate PXR activation and CYP induction. Screening and evaluation of several different amines at this region led to the finding that fused bicyclic amines like compound 11 retained potency while having significantly reduced CYP3A4 induction, as measured by reduced CYP3A4 mRNA level upon compound treatment at 10 μM relative to [rifampicin](#).

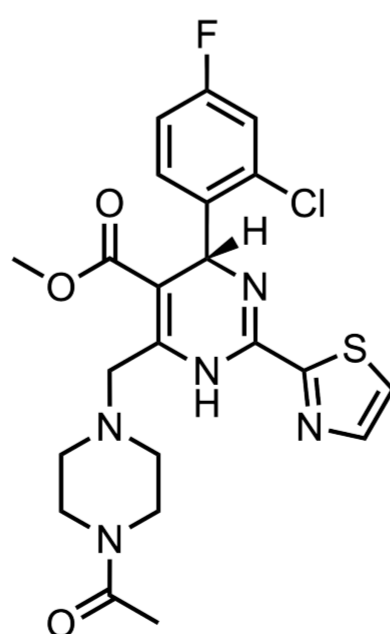
- See this excellent [2021 JMC review](#) from UCB on mitigation of PXR modulation through SBDD

Addressing a hERG liability through re-introduction of a carboxylic acid. Unfortunately, while CYP3A4 induction was mitigated, compound 11 exhibited modest human metabolic stability (HLM CL = 7.2 mL/min/kg) and significant hERG inhibition ($\text{IC}_{50} < 1 \mu\text{M}$). A classic [strategy for mitigating hERG inhibition](#) by amines is to generate a zwitterion through introduction of a carboxylic acid. However since unbranched carboxylic acids can lead to [acylglucuronides](#) or [thioethers](#) and thus pose an idiosyncratic toxicity risk, α -substituted carboxyls were prioritized. Indeed, acid-containing compounds like 19 were inactive on hERG ($\text{IC}_{20} > 10 \mu\text{M}$), were not CYP inducers (1% rel. to rifampicin at 10 μM), and were more metabolically stable (HLM CL = 0.4 mL/min/kg) with negligible acylglucuronide formation. Additionally, such acid-containing compounds were found to be more distributed to the liver, which could be beneficial for treating HBV, which manifests in the liver, with lower risk of systemic side effects.

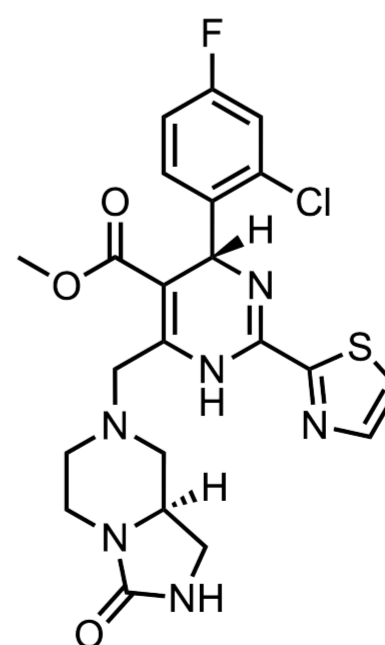
Mitigation of CYP3A4 Induction While Preserving HBV Activity:



HAP_R01
HBV cell $\text{IC}_{50} = 3 \text{ nM}$
cell $\text{CC}_{50} = >100 \mu\text{M}$
CYP3A4 induction = 110%



compound 2
HBV cell $\text{IC}_{50} = 50 \text{ nM}$
cell $\text{CC}_{50} = >100 \mu\text{M}$



compound 11
HBV cell $\text{IC}_{50} = 2 \text{ nM}$
cell $\text{CC}_{50} = 52 \mu\text{M}$
CYP3A4 induction = 17%
hERG $\text{IC}_{50} < 1 \mu\text{M}$
moderate metabolic stability

March 2023

linvencorvir

HBV core protein

allosteric HBV modulator

Ph. II for chronic hepatitis B (CHB)

opt. of known allosteric heteroaryl pyrimidine

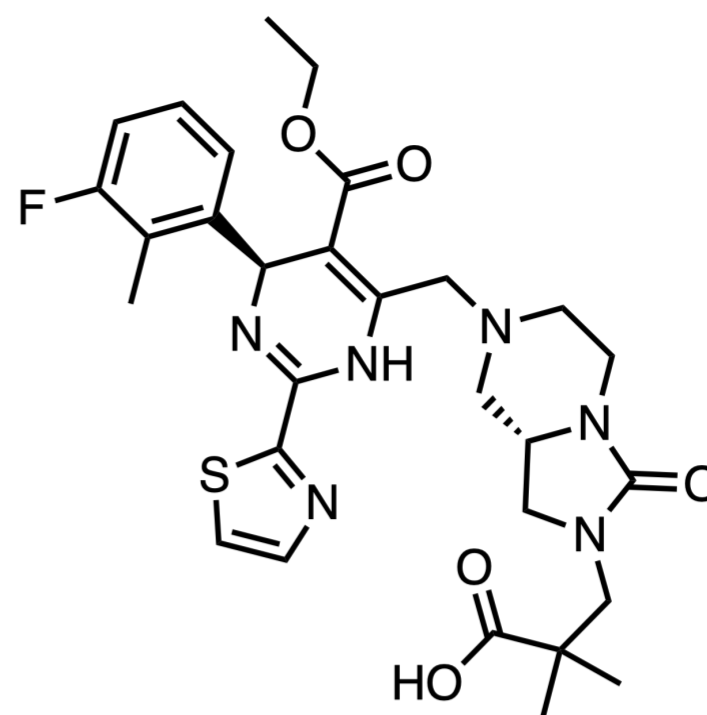
core protein modulator

J. Med. Chem., March 10, 2023

ROCHE, SHANGHAI, CN

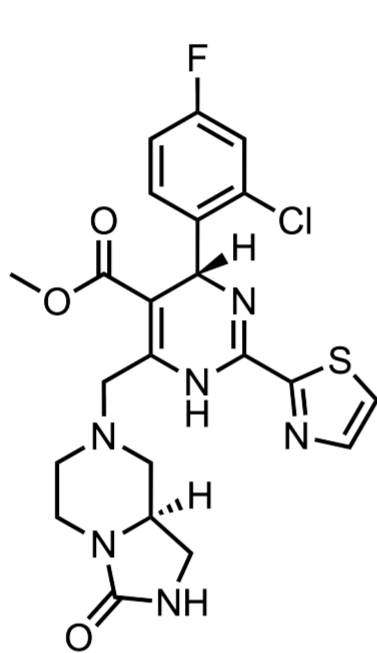
paper DOI:

<https://pubs.acs.org/doi/10.1021/acs.jmedchem.3c00173>

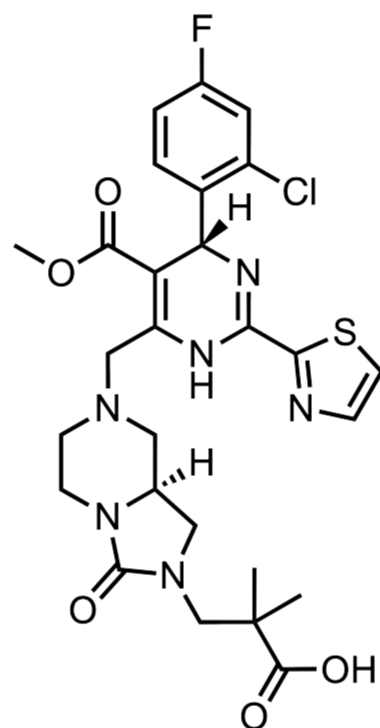


[View Online](#)

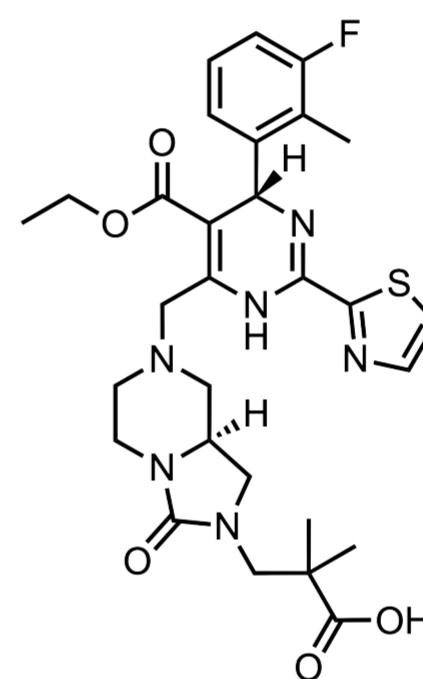
Re-introduction of Acid Mitigates hERG Inhibition and More:



compound 11
HBV cell IC_{50} = 2 nM
cell CC_{50} = 52 μ M
CYP3A4 induction = 17%
hERG IC_{50} < 1 μ M
moderate metabolic stability



compound 19
HBV cell IC_{50} = 3 nM
cell CC_{50} = >100 μ M
CYP3A4 induction = 1%
hERG IC_{20} > 10 μ M
HLM CL = 0.4 mL/min/kg



linvencorvir (39)
HBV cell IC_{50} = 6 nM
cell CC_{50} = >100 μ M
improved cross-species PK

Liver-targeting properties and PK of lincovir. Interesting, carboxylic acid compounds like 19 and lincovir were generally found to be much more distributed in the livers of mice than in plasma (e.g. >30x AUC in liver vs. plasma for lincovir in mice). Interestingly, total exposures and oral bioavailability both increased with increasing doses across preclinical species, with the most pronounced effect in rodents, and a stronger effect for males in some species and females in others. The molecule also had impressed preclinical safety margins, with an NOAEL of up to 350 mpk/day in minipigs. A summary of key pharmacological properties of lincovir appear below:

- $\log D$ = 1.75
- Cellular EC_{50} (HBV DNA reduction HepG.2.2.15 cells): 3 nM
- CC_{50} (toxicity vs. HepDE19 cells): >100 μ M
- Predicted Hep CL from hepatocytes (H/R) = 5.6 / 11 mL/min/kg
- CL Rat / Monkey / Minipig (2 mg/kg) = 30.5 / 23.6 / 24.1 mL/min/kg
- V_{ss} Rat / Monkey / Minipig (2 mg/kg) = 1.34 / 0.67 / 1.12 L/kg
- $t_{1/2}$ Rat / Monkey / Minipig (2 mg/kg) = 1.46 / 1.77 / 2.19 h
- F% Rat / Monkey / Minipig (3 mg/kg) (males) = 13.5% / 10.3% / 12.6%
- F% Rat / Monkey / Minipig (30 mg/kg) (males) = 50% / 25.8% / 20.6%
- F% Rat / Monkey / Minipig (3 mg/kg) (females) = 14.3% / 14.5% / 10.6%
- F% Rat / Monkey / Minipig (30 mg/kg) (females) = 105% / 18.6% / 12.4%

- Mouse plasma PO AUC = 275 μ g*h/L
- Mouse liver PO AUC = 8848 μ g*h/L
- Mouse AUC liver / AUC plasma (PO) = 32
- CYP3A4, 2D6, 2C9, 2C19, 1A2 IC_{50} : >50 μ M
- No signs of hERG, GSH adduction, mutagenicity (Ames), or clastogenicity (micronucleus)
- Rats and minipigs selected as rodent/non-rodent tox. Species based on metabolite coverage + PK
- GLP tox. NOAEL (28 d) = highest doses tested (250 mpk/day in rats, 350 mpk/day in minipig)

Dose-dependent decrease in both HBsAg and HBeAg levels in an HBV mouse model. In contrast to the nucleoside reverse transcriptase inhibitor (NRTI) HBV drug, [entecavir](#), lincovir not only reduced serum HBV DNA levels in an AAV-HBV mouse model, but also had a significant reduction upon the serum levels of HBV surface antigen (HBsAg) and HBV e antigen (HBeAg). The standard of care of HBV (interferons and nucleos(t)ides) are effective at reducing HBV DNA (virological response) and inducing loss of HBeAg, but are not effective at functionally curing HBV within a finite dosing time based on the complete loss of HBsAg.

March 2023

linvencorvir

HBV core protein

allosteric HBV modulator

Ph. II for chronic hepatitis B (CHB)

opt. of known allosteric heteroaryl pyrimidine

core protein modulator

J. Med. Chem., March 10, 2023

ROCHE, SHANGHAI, CN

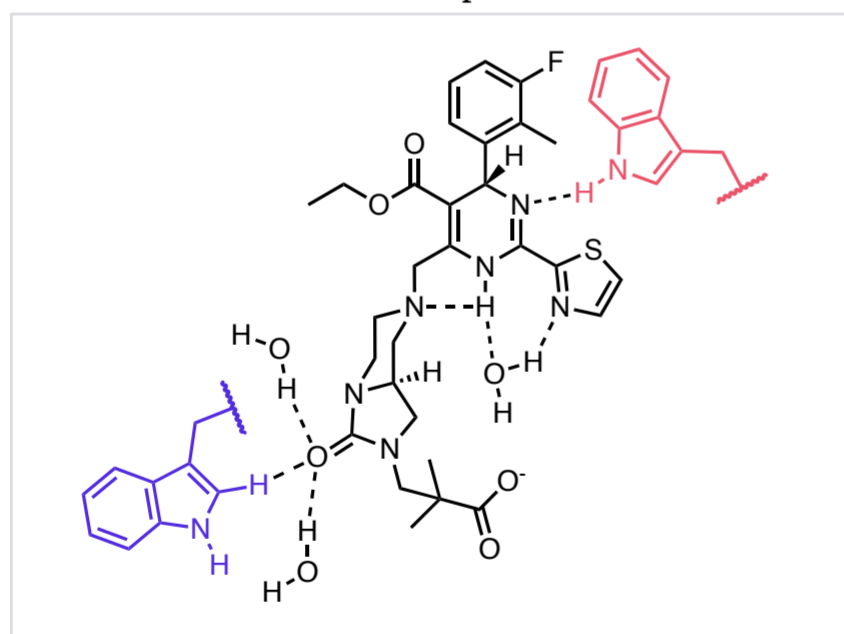
paper DOI:

<https://pubs.acs.org/doi/10.1021/acs.jmedchem.3c00173>

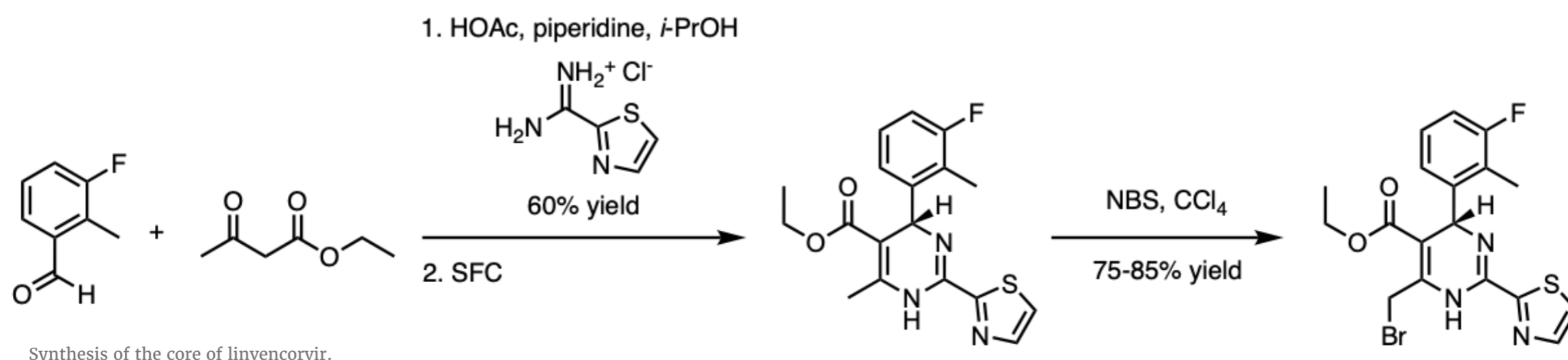
[View Online](#)

Binding mode. A co-crystal of HBV core protein Y132A mutant in complex with linvencorvir has been disclosed (PDB: [8I71](#) – be sure to look at the ligand between two monomers). For comparison, the HAP_R01 co-crystal structure is also available (PDB: [5WRE](#)). There are a few notable aspects within the crystal structure:

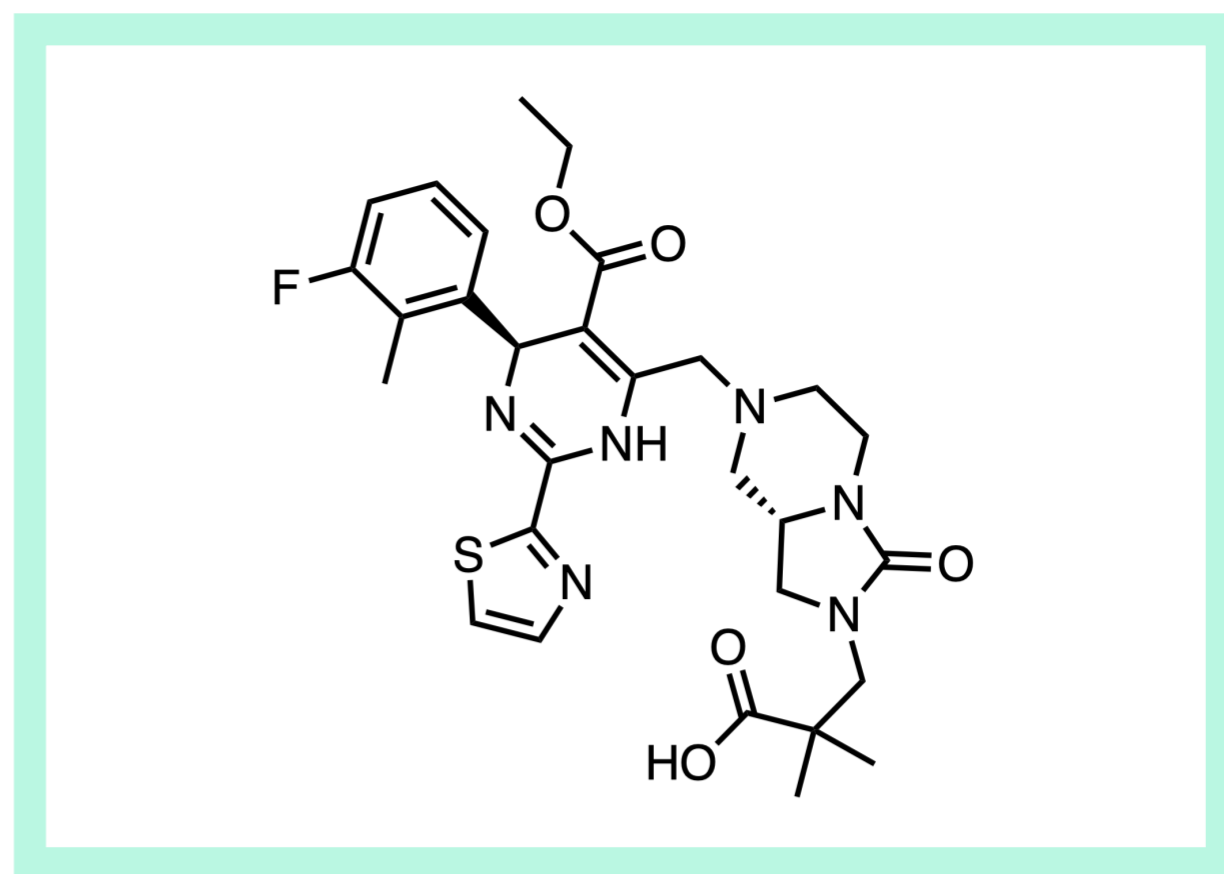
1. The ester binds intact to the target in the ester form (i.e. not a prodrug)
2. The thiazole, tertiary amine, and dihydropyrimidine all appear to coordinate to a single water
3. The molecule binds at an interface between two monomers, with the basic nitrogen on the dihydropyrimidine binding to the N-H of a tryptophan on one monomer, while the carbonyl group on C-6 of the bicyclic ring is said to undergo H-bonding with two water molecules and non-classical aromatic H-bonding with the C-H of Trp125 from the other monomer
4. The C-6 bicyclic component is in a narrow, lipophilic channel, rationalizing the difficulty in getting away from the CYP induction pharmacophore
5. The COOH extends toward a solvent-exposed area



Linvencorvir interestingly binds at the interface between two monomers, surrounded by lipophilic residues except in specific pockets where hydrogen bond acceptors/donors are accommodated by water molecules.



Synthesis of the core of linvencorvir.



Ph. I trials showed promising efficacy and safety; entered Ph. II but discontinued by Roche. Phase I clinical trials ([NCT02952924](#) and [NCT03570658](#)) assessed the efficacy of linvencorvir in healthy participants, with single (150–2,500 mg) and multiple (200–800 mg) dose cohorts. HBV DNA [decreased significantly](#) over 4 weeks in doses as low as the 200 mg QD group. The trials also [investigated drug-drug interaction](#) potential with [midazolam](#), a known CYP3A4 inhibitor. No adverse effects were reported, and absorption/elimination occurred rapidly in plasma, with <1% of the dose recovered from urine. Absorption was rapid and peak plasma concentration was achieved 1.25–3.0 hours post-administration under fasted conditions, and human $t_{1/2}$ ranged from 3.3 to 13.9 hours, and C_{max} was dose-dependent. While it is possible to measure human liver drug concentrations through [biopsies](#) to verify the liver-targeting phenomenon, [ethical and practical concerns](#) make this challenging. A Ph. II trial is still listed as in [progress](#), though the molecule was [removed from Roche's pipeline in Oct. 2022](#).

- Ph. I study [publication](#) from healthy volunteers in China
- Ph. I study [publication](#) from HBV patients
- Ph. I first-in-human study [publication](#) from healthy volunteers in New Zealand

Relevant patents. Novel 6-fused heteroaryldihydropyrimidines for the treatment and prophylaxis of hepatitis b virus infection ([WO2015132276A1](#), example 76), Roche Shanghai.

Synthesis highlights. The synthesis of the core uses a Bignelli-like 3-component condensation to form the dihydropyrimidine. Surprisingly, this core tolerates radical bromination with NBS to produce the key bromide intermediates used across the medicinal chemistry campaign in alkylation reactions with various amines.

March 2023

KW-6356

A_{2A}R

oral A_{2A} receptor antagonist/inverse agonist

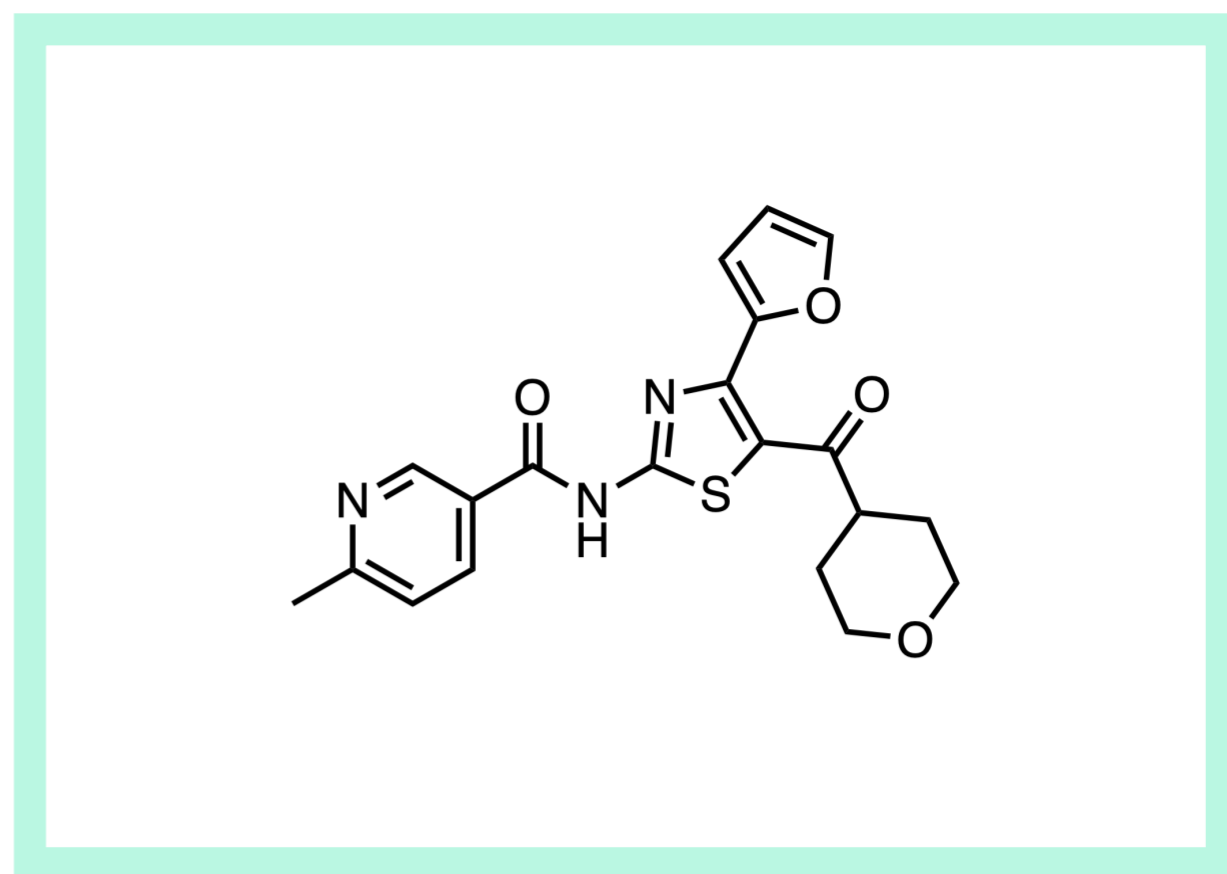
Ph. II for Parkinson's Disease

2nd gen. A_{2A} receptor antagonist

ASPET, March 9, 2023

KYOWA KIRIN CO., LTD., SHIZUOKA, JP

paper DOI: <https://doi.org/10.1124/molpharm.122.000633>

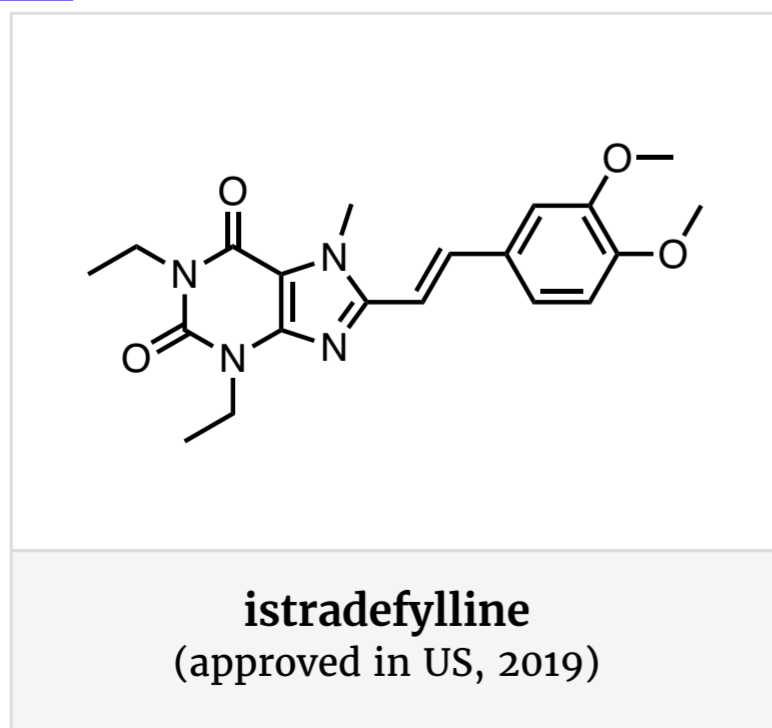


View Online

A furan-containing insurmountable antagonist and inverse agonist of the adenosine A_{2A} receptor for Parkinson's disease. Kyowa Kirin's KW-6356, or [sipagladenant](#), is a non-xanthine A_{2A} receptor intended to treat Parkinson's disease. Unlike Kyowa Kirin's recently US-approved neutral antagonist, istradefylline, the molecule is an insurmountable antagonist and inverse agonist, both of which may contribute to better efficacy. Unfortunately, despite positive clinical results, the molecule was discontinued for commercial reasons. The molecule is scientifically notable for the GPCR co-crystal structures which provide insight into GPCR insurmountable antagonism and inverse agonism.

Antagonism of the A_{2A} receptor is a clinically validated, non-dopaminergic approach to Parkinson's motor symptom relief. In PD patients, decreased dopamine signaling due to loss of dopaminergic neurons leads to an [increase in the excitability of the "indirect pathway,"](#) a series of neural connections involved in motor control. This leads to the motor dysfunction characteristic of Parkinson's disease. [A_{2A} receptor activation also increases the excitability of the indirect pathway;](#) hence, [blockade of A_{2A} receptor decreases excessive activation of the indirect pathway.](#) This provides a non-dopaminergic approach to symptomatic relief of Parkinson's disease. Despite considerable efforts in examining [non-dopaminergic drugs](#) for improving motor symptoms in PD, most have failed to show efficacy or have had undesirable side effects. A first-generation oral, selective A_{2A} receptor antagonist, [istradefylline](#), is approved in Japan (2013) and in the US ([2019](#)) for use as an adjunct treatment to levodopa/decarboxylase inhibitors in adults with PD experiencing OFF episodes or wearing-off phenomenon.

- For a 2022 review of the therapeutic hypothesis for A_{2A} receptor antagonism by Kyowa Kirin, [see here](#).
- For a 2020 review of how A_{2A} receptors regulate motor function by Kyowa Kirin, [see here](#).



- For a 2020 review of istradefylline's path to approval written with Kyowa Kirin, [see here](#).

A brief history of A_{2A} chemical matter. Though the discovery of KW-6356 (sipagladenant) has yet to be disclosed, it has a patent priority date as early as 2003 (see [US8889718B2](#)). The oldest known adenosine antagonists are xanthines including [caffeine](#) (rat A_{2A} K_i = 4.8 uM, human K_i = 18 uM). Non-xanthine, furan-containing A_{2A} antagonists such as [CGS 15943](#) were disclosed by CIBA-Geigy as early as 1988 (though discovered in 1983). Derivatives such as SCH-58261 (4) were reported by Schering-Plough in Italy as early as 1993, resulting in a furan-containing clinical candidate for PD (preladenant, [SCH-420814](#)) that was developed by Merck until its discontinuation in [2013](#). Given the orthosteric binding mode of KW-6356 and the fact that the furyl moiety binds in nearly the exact same position as ZM241385, KW-6356 is likely derived from ligand-based design of earlier-reported non-xanthine A_{2A} antagonists.

- For a 2011 review of chemical structures of A_{2A} antagonists, from JNJ Spring House, [see here](#).

Insurmountable antagonism by an orthosteric molecule on the A_{2A} receptor may lead to better efficacy. [Insurmountable antagonism](#) occurs when an antagonist is unable to be overcome by increasing the concentration of agonist, and can commonly be confused with irreversible or covalent inhibition, based on the time-dependent and apparently non-competitive nature of the phenomenon. In contrast to istradefylline, KW-6356 reduces the maximal response induced by selective A_{2A} receptor agonist CGS21680, a tell-tale sign of insurmountable antagonism. The likely most common cause of insurmountable antagonism is sustained receptor occupancy through slow dissociation (or long residence time) of the ligand on the receptor. Indeed, while KW-6356 reaches equilibrium association with the A_{2A} receptor within 45 min, binding remained for >3 h. Clinical studies have demonstrated that insurmountable antagonists such as valsartan (targeting AT₁R) are more effective long-term than surmountable antagonists such as losartan [in acute myocardial infarction](#), raising the possibility that insurmountable antagonist KW-6356 may also be more effective than the approved surmountable antagonist, istradefylline.

- See this 2002 review on [insurmountable antagonism](#) for more.

A structural basis for insurmountable antagonism in GPCRs? As the receptor for caffeine, A_{2A} is one of the most structurally well-studied GPCRs, with numerous complex structures available in the PDB. However, less is known about the structural basis of insurmountable antagonism, which this article explores further. Interestingly, the insurmountable AT₁ receptor antagonist olmesartan (PDB ID: [4ZUD](#)) has an imidazole group where the tetrahydropyran is situated in A_{2A} receptor antagonist KW-6356 (PDB ID: [8GNE](#)), suggesting that occupation and interaction this region of GPCRs may be important for achieving insurmountable antagonism. A comparison of the binding mode with the binding

March 2023

KW-6356

A_{2A}R

oral A_{2A} receptor antagonist/inverse agonist

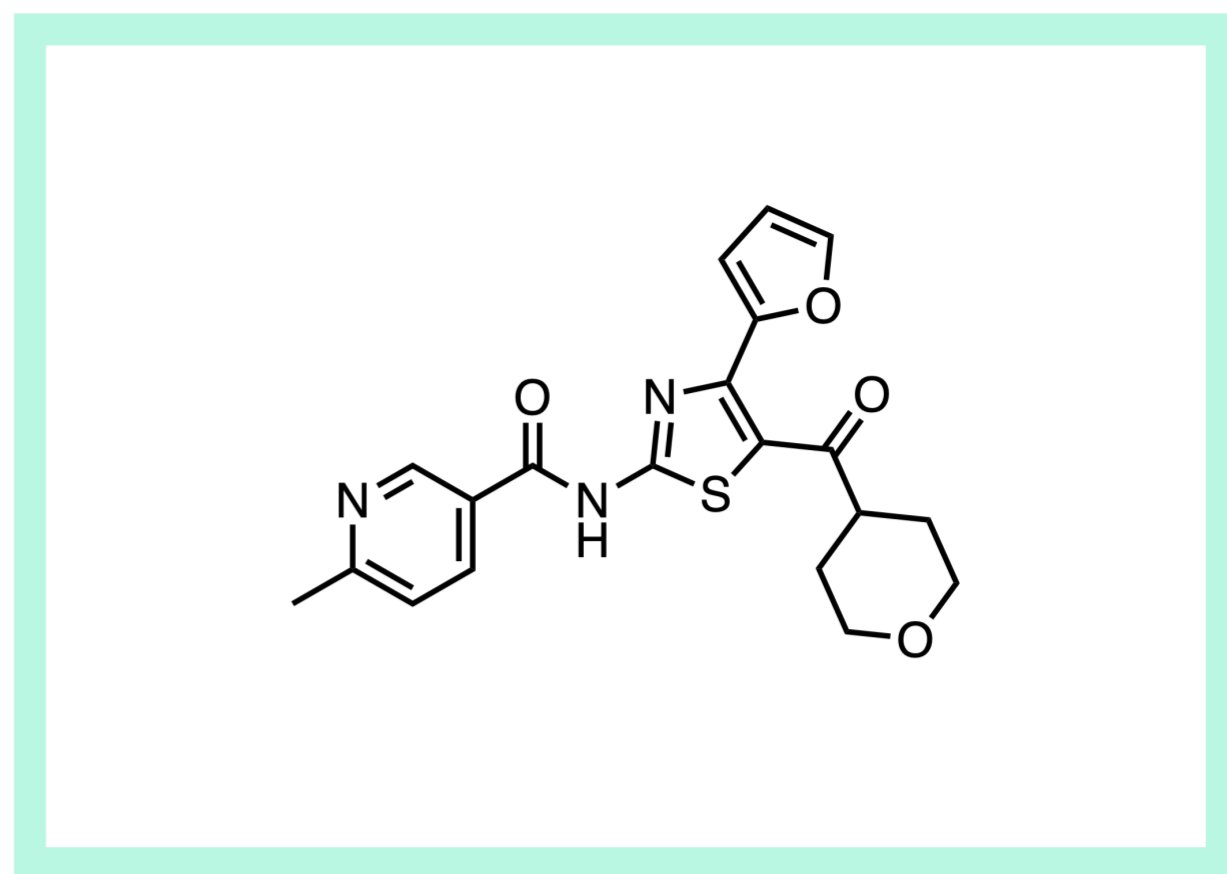
Ph. II for Parkinson's Disease

2nd gen. A_{2A} receptor antagonist

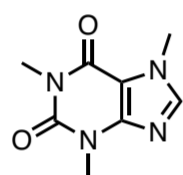
ASPET, March 9, 2023

KYOWA KIRIN CO., LTD., SHIZUOKA, JP

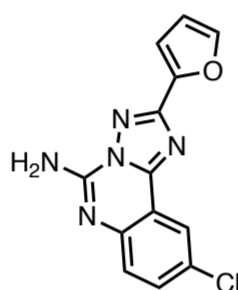
paper DOI: <https://doi.org/10.1124/molpharm.122.000633>



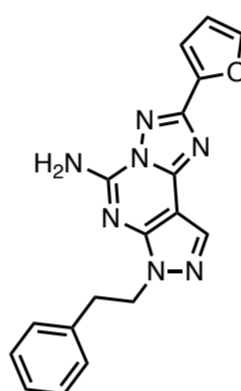
[View Online](#)



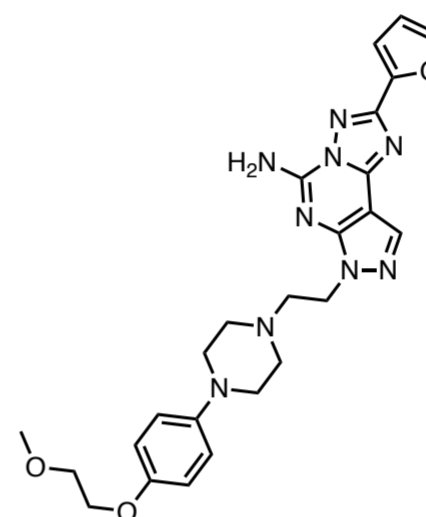
caffeine



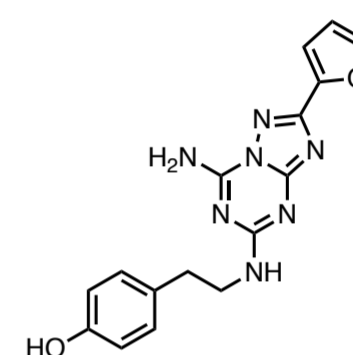
CGS 15943



SCH-58261



preladenant



ZM241385

mode of other long-residence-time molecules including a derivative of ZM241385 ("12x," from Heptares, [PDB ID: 5IUB](#)), or triazine derivative [4e](#) (Heptares, [PDB ID: 3UZC](#), [5OLZ](#)) further supports the idea that interacting with His264 and stabilizing the extracellular loops of the receptor may cause insurmountable antagonism of the A_{2A} receptor. This relationship between insurmountable antagonism and GPCR binding mode may be useful for those attempting to identify insurmountable antagonists in the future.

- See this [2016 JMC article](#) by Heptares for another interesting structure-residence-time relationship study.

A structural basis for Inverse agonism. In contrast to istradefylline which is a neutral antagonist, KW-6356 is also an inverse agonist, [blocking the constitutive activity of the receptor](#). The inverse agonism is attributed to the ability of KW-6356's furan group to reach the Trp246 "[toggle-switch](#)," stabilizing the receptor structure in an inactive state. Again from the AT1R blocker literature, inverse agonists such as valsartan appear to [differentiate clinically](#) from neutral antagonists such as losartan, which is attributed in part to the different mechanisms of action of the drugs. Hence, the inverse agonism of KW-6356 could potentially be another reason it could differentiate from istradefylline.

- For a review on inverse agonism in GPCRs, see [this 2006 Trends. Pharm. Sci. article](#).

An intramolecular S-O interaction, several CH- π interactions, and confirmation of furan binding. Notable aspects of the co-crystal structure of KW-6356 bound to A_{2A} include The authors note a CH- π interaction between Leu249 and the thiazole core, and note that the conformation of the thiazole scaffold is restricted to a plane thanks to an [intramolecular S-O interaction](#) between the sulfur of the thiazole and the carbonyl oxygen of the nicotinamide amide. The unique furyl group is stabilized by hydrophobic CH- π interactions with Met177 and His250, and the oxygen atom of the furyl group forms an H-bond with a water molecule. KW-6356 makes many more interactions than istradefylline, which may explain its significantly higher affinity and its selectivity against other receptors. The co-crystal structures of the furan-containing molecules are interesting confirmation of direct binding, as furans [have a bad reputation](#) during hit finding and lead ID [in part due to their oxidative instability](#).

- KW-6356 bound to the A_{2A} orthosteric site: ([PDB ID:8GNE](#))
- Non-xanthine, furyl- inverse agonist ZM241385 bound to the A_{2A} orthosteric site: ([PDB ID: 4E1Y](#))
- Xanthine antagonist istradefylline bound to the A_{2A} orthosteric site: ([PDB ID:8GNG](#))
- Caffeine bound to the A_{2A} orthosteric site ([PDB ID: 5MZP](#))

Efficacy and safety demonstrated in Ph. IIB, but discontinued for commercial reasons. Kyowa Kirin reported [positive Ph. IIB results](#) for KW-6356 in treating Parkinson's symptoms as adjunct to levodopa therapy in 2022. 167-168 patients were assigned to the 3 mg, 6 mg, and placebo groups, and in both dose groups, KW-6356 met the primary efficacy endpoint of reduction in motor symptoms based on the MDS-UPDRS Part III total score, and the secondary efficacy endpoint of a reduction in Mean OFF time/day. In the 6 mg group's post-hoc analysis, it also improved PD Sleep Scale-2 total score for patients with sleep problems at baseline.

The drug was well-tolerated and the Ph. I healthy volunteer study including doses up to 60 mg SAD and 24 mg QD multiple doses has been [published](#). The drug has a terminal elimination half-life of 18.4-43.1 h following single doses of 1-60 mg. Given estimated peak sales of <\$100M/yr by [Credit Suisse](#), and Kyowa Kirin's historical challenges in getting FDA approval from istradefylline, it is understandable that Kyowa Kirin announced [discontinuation](#) of development in 2022. Given the differentiating properties of the drug, it may be picked up by a smaller developer in the future.

Picomolar binding affinity and other preclinical pharmacology. Based on radiolabeled ligands including tritiated KW-6356, KW-6356 has a >100x stronger affinity for A_{2A}R than other adenosine receptor isoforms. The molecule has high affinity for A_{2A} across species (humans, marmosets, dogs, rats, mice) and hardly any activity against dopamine-related targets like MAO-A, MAO-B, and COMT. The molecule is highly selective against a panel of receptors, ion channels, and other targets at 10 μ M ([Table 2 here](#)).

- A_{2A} K_i = 0.117 nM
- A₁ K_i = 100 nM
- A_{2B} K_i = 32 nM
- A₃ K_i = 417 nM

Relevant patents. "Method for producing thiazole derivative." ([JP6770962B2](#), 2022). "Thiazole derivatives." ([US8889718B2](#), 2014, 2003 priority date).

March 2023

DKY709

IKZF2

oral IKZF2-selective molecular glue degrader

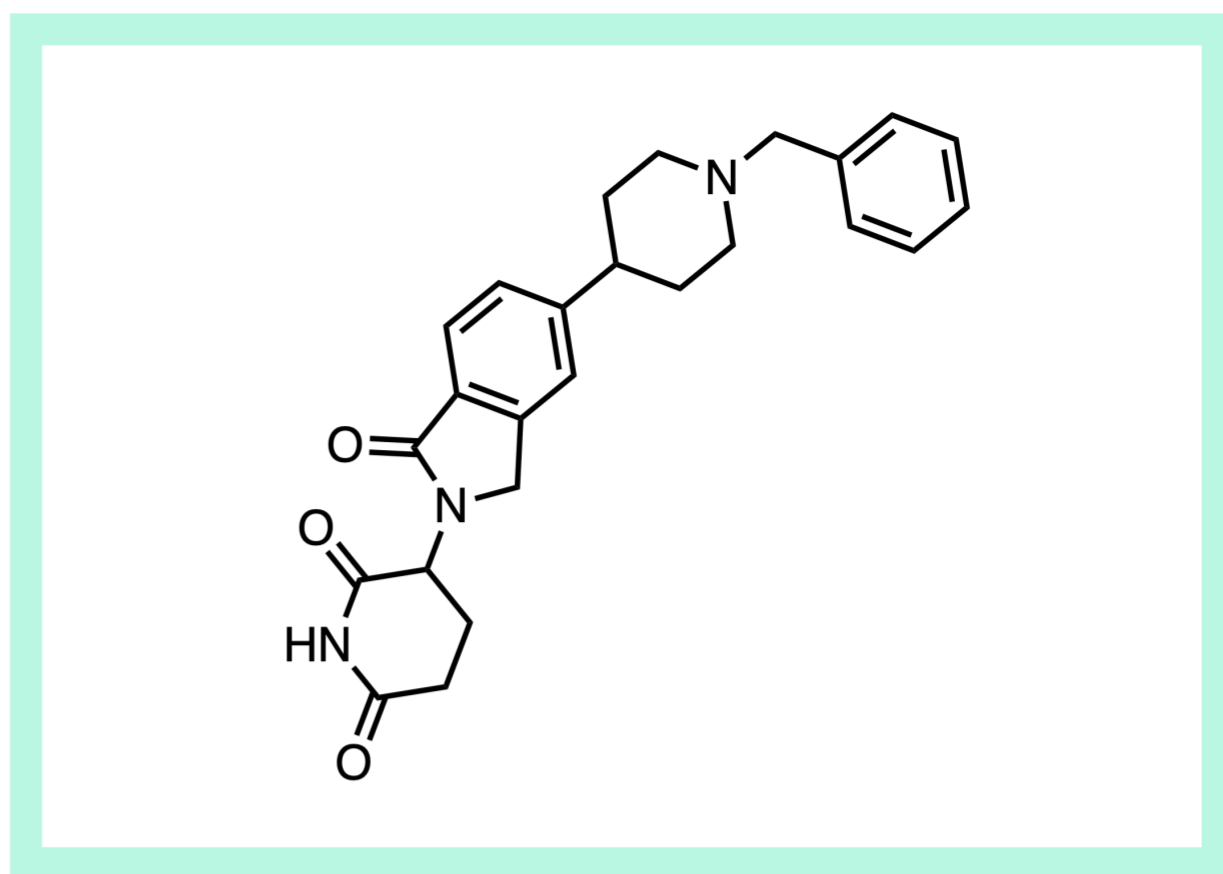
Ph. I/IIb for adv. solid tumors

opt. of pomalidomide analog

Cell Chemical Biology, March 1, 2023

NOVARTIS, CAMBRIDGE, MA

paper DOI: <https://doi.org/10.1016/j.chembiol.2023.02.005>



View Online

A T_{reg} -modulating IKZF2 (Helios) glue degrader for cancer immunotherapy. Tumors can evade the immune system [through the recruitment of regulatory T cells \(Treg\)](#) which limit the activation and expansion of effector T cells (Teff). IKZF2 (Helios) is an [Ikaros transcription factor family member](#) that is [expressed in a majority of Treg cells](#). NVP-DKY709 is a first-in-class selective [molecular glue degrader](#) of IKZF2 that makes Treg cells less immunosuppressive and Teff cells more active in vitro, while completely sparing the traditional pomalidomide targets IKZF1/3 from degradation. It has demonstrated significant and sustained IKZF2 degradation in a Ph. I clinical trial ([NCT03891953](#), not recruiting) and was [intended to be studied in combination with PD-1 antibody, spartalizumab in NSCLC or melanoma patients who had received prior anti-PD1/PD-L1 therapy](#), but [no longer appears](#) to be in development by Novartis as of Q1 2023.

Like most transcription factors, which are [mostly unstructured and lack good binding sites](#), IKZF2 is hard to drug traditionally, but contains the [C2H2](#) Zinc finger degnon that is recognized by the E3 ligase CRBN.

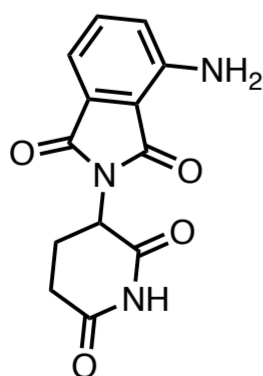
Obtaining IKZF2 selectivity over IKZF1/3 is a challenge. It is well-known now that IMiD drugs like pomalidomide and lenalidomide induce the degradation of the related IKZF1/3 transcription factors through recruitment of CRBN, but IKZF1/3 degradation leads to on-target hematopoietic toxicities including neutropenia and [myelosuppression](#). It has become clear that the target selectivity of IMiD-based drugs can be modified through structural changes, such as for [GSPT1](#) or [CK1 \$\alpha\$](#) . Though a [CRBN-based molecular glue degrader of IKZF2 had been disclosed with effects on Treg cells](#) (ALV2), it does not adequately spare IKZF1/3, potentially confounding the interpretation of the Treg effects. In order to identify an IKZF2-selective, the Novartis team needed to completely override the intrinsic selectivity of the IMiD drug class, which does not degrade IKZF2.

Guided by IKZF1/2 to CRBN recruitment assays rather than IKZF1/2 degradation. Since pomalidomide has no effect on IKZF2 protein levels up to 50 μ M, instead of relying on IKZF1/2 degradation assays, [NanoBiT](#) cellular assays were used to measure the recruitment of IKZF1/2 to CRBN. Although pomalidomide did not affect IKZF2 protein levels, it did induce an interaction between IKZF2 and CRBN in cells, which was measured by a split enzyme recruitment assay (A_{max} 460%). This interaction was only 4-fold weaker than that observed with IKZF1 (A_{max} 1,940%), suggesting that pomalidomide could be used to identify more potent molecules for recruiting IKZF2 to CRBN. This strategy of starting by optimizing for recruitment rather than degradation allows a broader range of starting points to be detected in targeted protein degradation programs, and is likely to be applied more broadly in other programs.

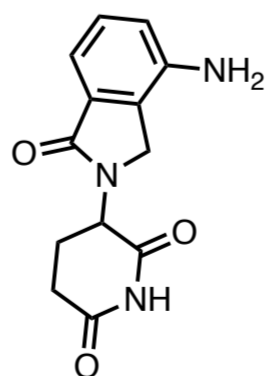
A single IKZF amino acid is responsible for IKZF1/2 degradation differences. Pomalidomide-bound CRBN [binds to a glycine \$\beta\$ -hairpin](#) in [zinc finger 2 of IKZF1](#). This hairpin differs in IKZF1 and IKZF2 by a single amino acid (Q146 versus H141):

- IKZF1 145 FQCNQCGASFTQKGNLLRHKLH 167
- IKZF2 140 FHCNQCGASFTQKGNLLRHKLH 162
- IKZF3 146 FQCNQCGASFTQKGNLLRHKLH 168
- IKZF4 187 FHCNQCGASFTQKGNLLRHKLH 209

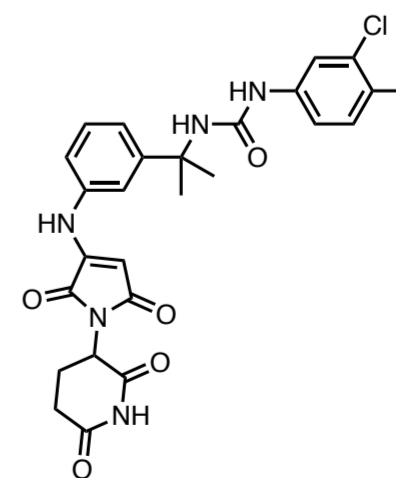
To ensure that a medicinal chemistry campaign wouldn't be a wild goose chase and that IKZF2 degradation by CRBN would ultimately be possible, tagged versions of full-length IKZF1, IKZF2, or IKZF2(H141Q) mutant were expressed. Treatment with pomalidomide led to equally efficient degradation of full-length IKZF2(H141Q) as full-length IKZF1 in cells, showing that the single amino acid difference is solely responsible for the inability of pomalidomide to degrade IKZF2 and that a compound that can accommodate the histidine in IKZF2 zinc finger 2 could be a competent IKZF2 degrader.



pomalidomide
IKZF1/3 degrader
no IKZF2 degradation



lenalidomide
IKZF1/3 degrader
no IKZF2 degradation



ALV-2
IKZF2/4 degrader w/ IKZF1/3 activity
max activity at ~10 μ M

March 2023

DKY709

IKZF2

oral IKZF2-selective molecular glue degrader

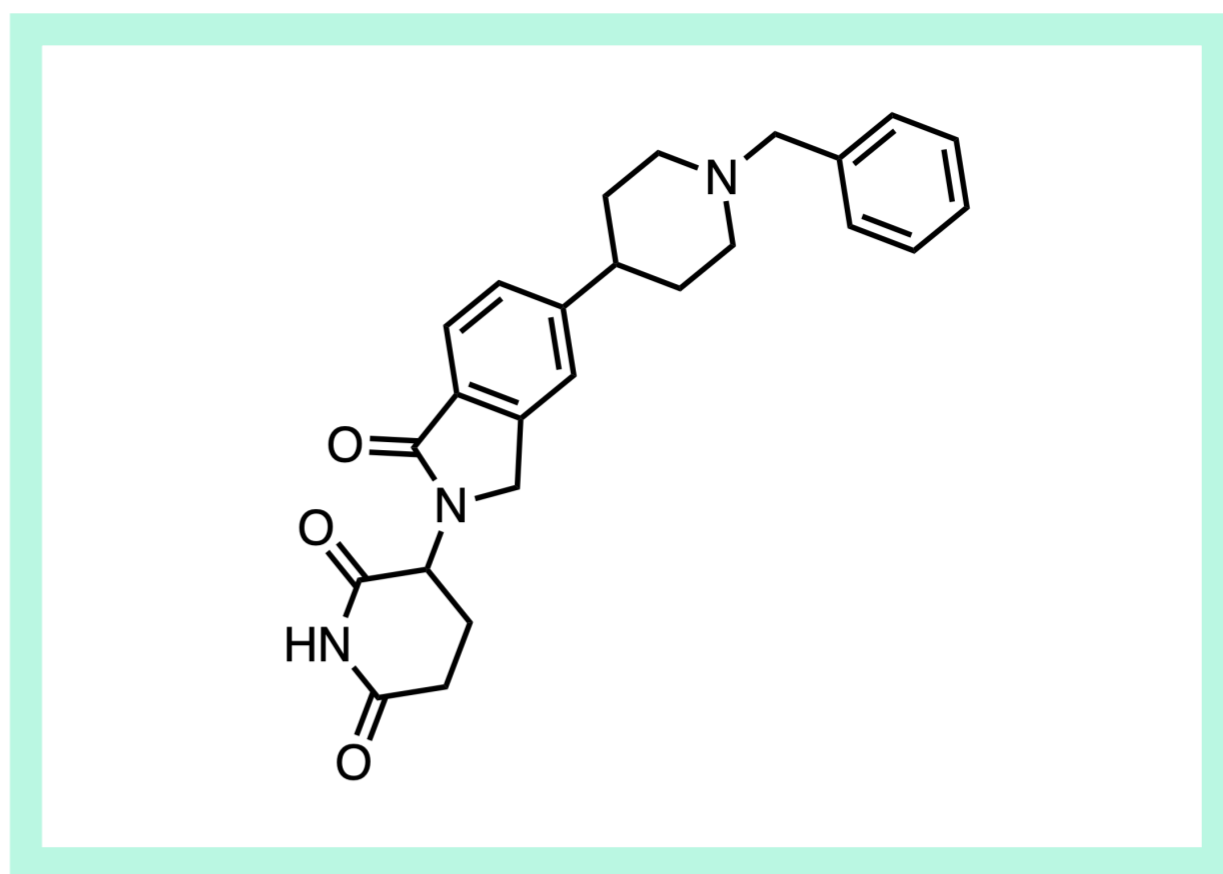
Ph. I/IIb for adv. solid tumors

opt. of pomalidomide analog

Cell Chemical Biology, March 1, 2023

NOVARTIS, CAMBRIDGE, MA

paper DOI: <https://doi.org/10.1016/j.chembiol.2023.02.005>



View Online

Starting with a weaker IKZF1 recruiter without IKZF2 degradation activity. A C(5)-cyclopropyl analog of [lenalidomide](#), compound 1, was chosen as a starting point for optimization based on its weaker IKZF1 recruitment vs. pomalidomide (A_{max} 600% vs. 1,940%) while maintaining a similar levels of IKZF2 recruitment (A_{max} 340% versus 460%). The sensitivity of C(5) to IKZF1/2 selectivity suggested it as an ideal area for optimization, even though compound 1 did not degrade IKZF1 or IKZF2. Phenyl and cyclohexyl ring substitutions gradually increased IKZF2 recruitment, but degradation was not observed until a basic amine was introduced in the form of a piperidine (compound 4).

Remarkable activity improvements from a single benzyl group leads to DKY709. The addition of a benzyl group to the piperidine resulted in NVP-DKY709, with a remarkable improvement in IKZF2 recruitment (A_{max} 1,350%, 400% recruitment at 0.009 μ M) and strong accompanying IKZF2 degradation (D_{max} 53%, DC_{50} 4 nM). DKY709 recruits IKZF1 to CRBN (A_{max} 550%, 400% recruitment at 0.28 μ M) but did not result in IKZF1 degradation up to 50 μ M. No degradation of IKZF2 was observed in CRBN-KO cells, confirming a CRBN-mediated mechanism.

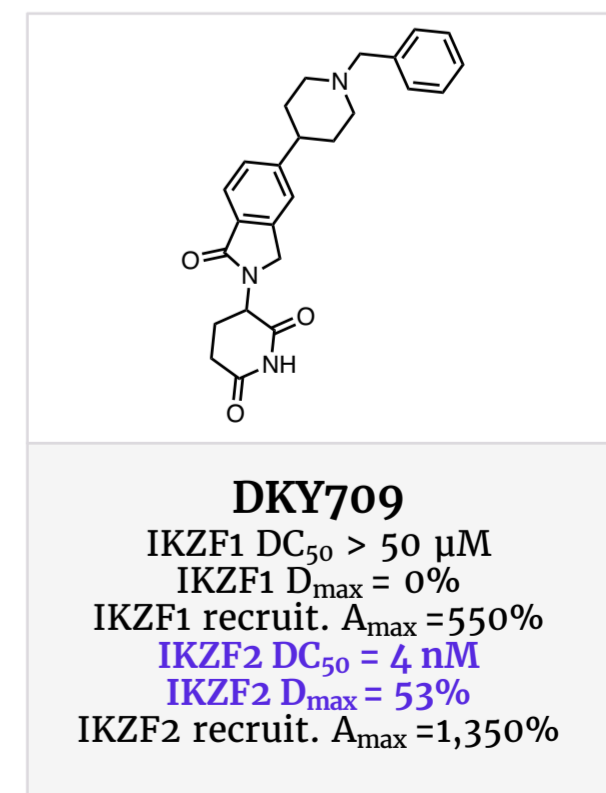
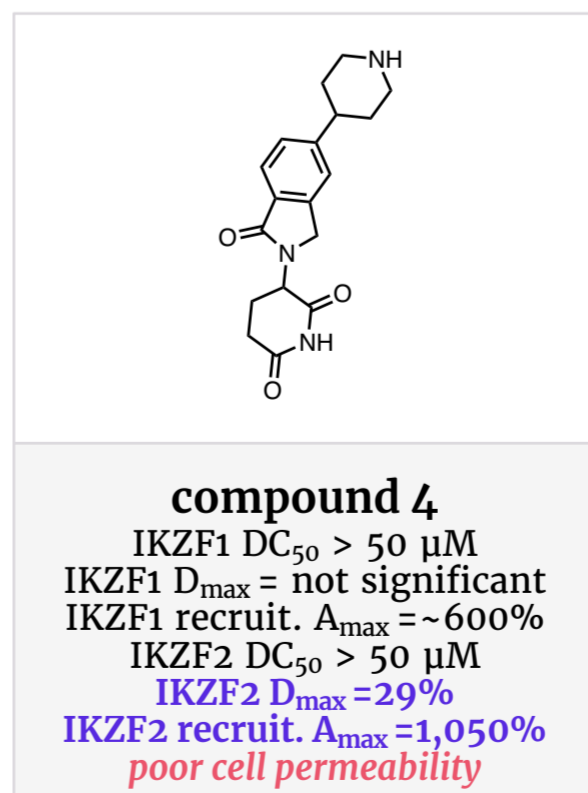
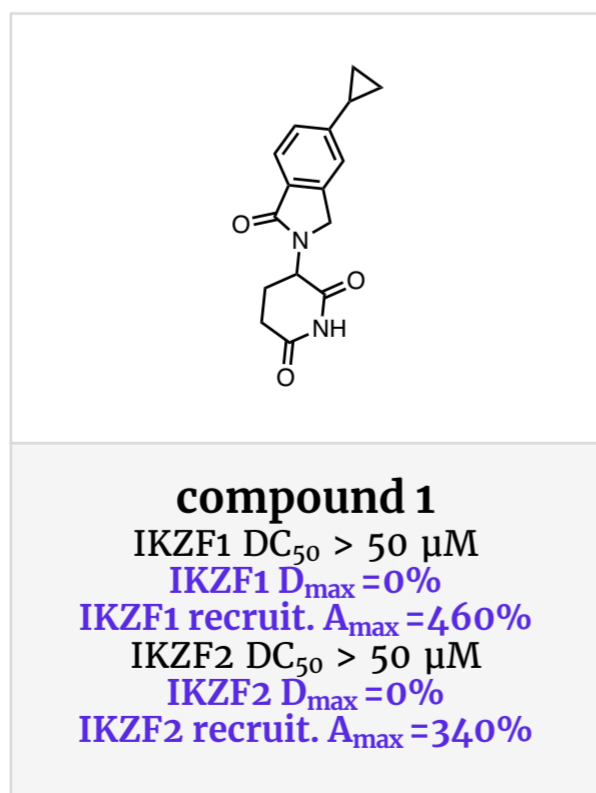
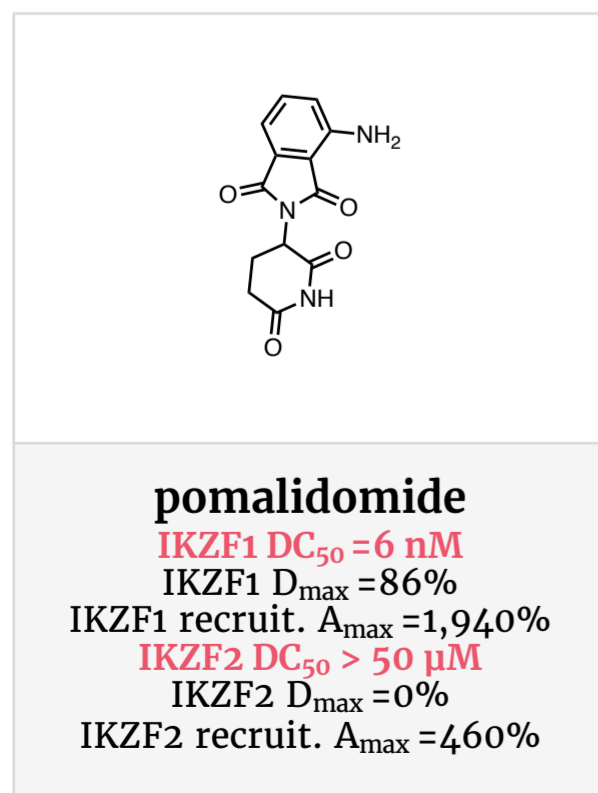
DKY709 is selective across the proteome but hits IKZF4, and SALL4. Quantitative proteomics on Jurkat cells treated with DKY709 showed that only IKZF2 was significantly downregulated among 8,656 quantified proteins. Engineered cellular assays revealed that DKY709 degraded IKZF4 (which also plays a role in T_{reg} function) and the teratogenicity-linked [SALL4](#) (which are not detectable in Jurkat cells), but not the

anti-target GSPT1 whose reduction blocks new protein synthesis (no degradation up to 50 μ M). A summary of preclinical properties of DKY709 appears below:

- CRBN binding IC_{50} = 130 nM
- CRBN cellular engagement IC_{50} = 73 nM
- IKZF2 degradation (ProLabel) DC_{50} = 4 nM, D_{max} = 53%
- IKZF2 CRBN recruitment A_{max} = 1,350%, 400% recruitment at 9 nM
- IKZF2 human primary CD25-enriched T-cells DC_{50} = 11 nM, D_{max} = 89%
- IKZF1 degradation DC_{50} >>50 μ M
- IKZF1 CRBN recruitment A_{max} = 550%, 400% recruitment at 280 nM
- No downregulation of IKZF 1/3/5
- IKZF4 degradation DC_{50} = 13 nM, D_{max} = 21%
- SALL4 degradation (ProLabel) DC_{50} = 2 nM, D_{max} = 55%
- Solubility (pH 6.8) = 255 μ M
- MDCK-LE $P_{app}(A-B)$: 18.2
- In vivo CL (mouse 2 mpk / cyno 0.3 mpk): 18 / 26 mL/min/kg
- In vivo V_{ss} (mouse 2 mpk / cyno 0.3 mpk): 1.9 / 8.6 L/kg
- $t_{1/2,term,IV}$ (mouse 2 mpk / cyno 0.3 mpk): 2.8 / 5.7 h
- C_{max} PO (mouse 3 mpk / cyno 1 mpk): 482 / 41 ng/mL
- F% (mouse 3 mpk / cyno 1 mpk): 53% / 89%

DKY709 decreases T_{reg} immunosuppressive capacity and enhances CD8⁺ T_{eff} cells. Expansion of T_{reg} cells in the presence of DKY709 resulted in >90% IKZF2 protein level reduction and decreased ability of the cells to suppress T_{eff} cells in vitro. Furthermore, primary human T_{eff} cells exhausted in the presence of DKY709 showed an increase in [interferon- \$\gamma\$](#) , which is secreted by activated T_{eff} cells.

Discovery of Selective Molecular Glue Degraders via Recruitment Assays



March 2023

DKY709

IKZF2

oral IKZF2-selective molecular glue degrader

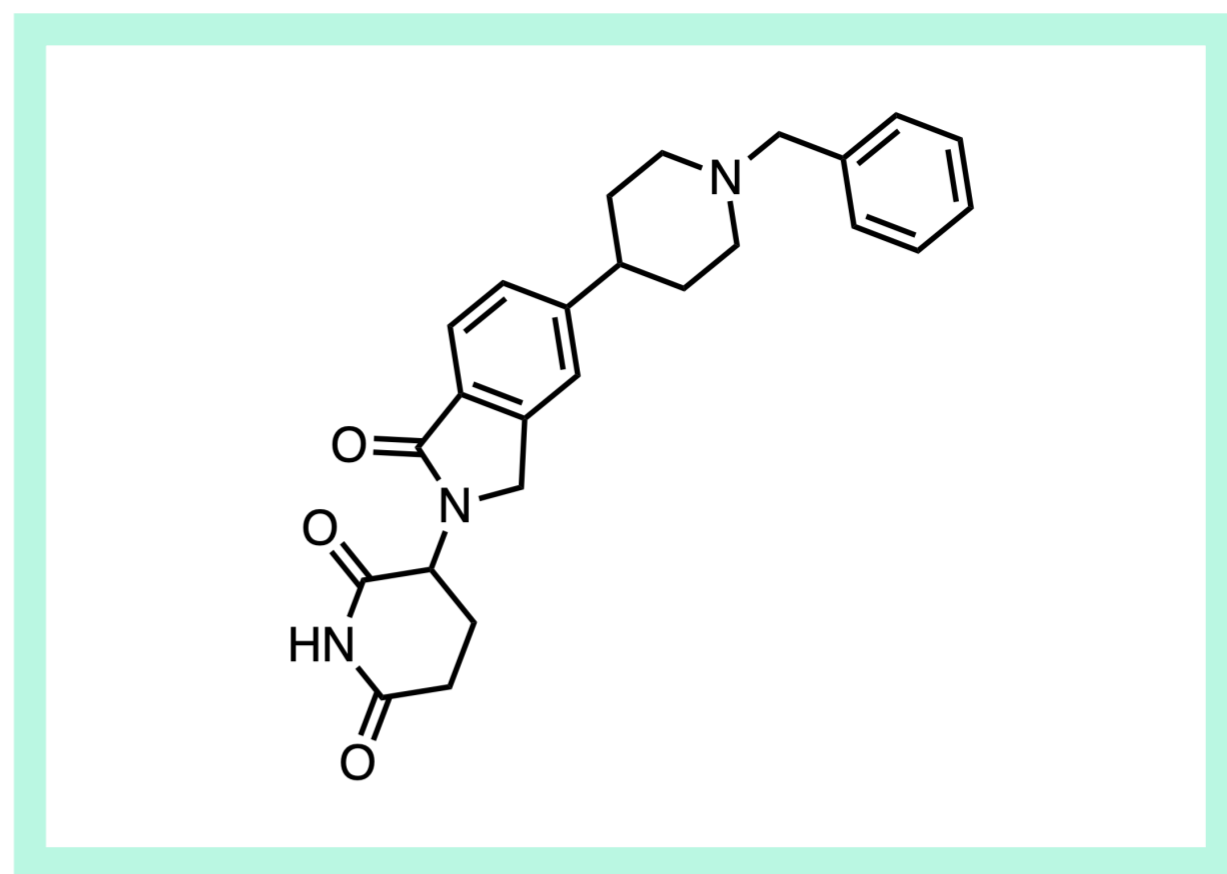
Ph. I/II for adv. solid tumors

opt. of pomalidomide analog

Cell Chemical Biology, March 1, 2023

NOVARTIS, CAMBRIDGE, MA

paper DOI: <https://doi.org/10.1016/j.chembiol.2023.02.005>



View Online

Binding mode. The structures of DKY709:CRBN:IKZF2(ZF2):DDB1 (PDB [7U8F](#)) and DKY709:CRBN:IKZF2(ZF2-3):DDB1 (PDB [8DEY](#)) highlight the salt bridge between the piperidine of DKY709 and Cereblon(E377). The piperidine ring of DKY709 also participates in a CH- π interaction with the Cereblon(H141). This helps to explain the selectivity against IKZF1/3 (in which H141 is a Q) and the lack of selectivity against IKZF4 (which also has a histidine at 141). Surprisingly, the *N*-benzyl group is solvent exposed in the structures. The structure of DDB1:CRBN:DKY709:IKZF2(ZF2-3) is the first disclosed structure highlighting the importance of residues beyond the small-molecule glue-interacting zinc finger domain in the recruitment of transcription factors to CRBN.

DKY709 demonstrates in vivo degradation and immune-boosting activity in non-human primates. IMiD drugs have been shown [not to have activity](#) in [rodents](#), complicating characterization. DKY709 degrades IKZF2 in human, NHP, and rabbit cells, but not in other species including mice, so mice with humanized immune systems were used for in vivo pharmacology. At 100 mpk QD, robust IKZF2 degradation was observed in peripheral T_{reg} cells as well as in tumor cells, and single-agent tumor growth inhibition was observed, though no synergy was detected with anti-PD-1 antibody PDR001. Degradation of IKZF2 in circulating T_{reg}s was also observed in cynos after a single oral dose, with maximum

degradation at 24 h (~90%, 1 mpk). Remarkably, partial degradation was seen as low as 0.01 mpk, highlighting the potentially catalytic nature of the mechanism. Oral DKY709 treatment increased proliferating T cells in the PBMCs after monkey vaccination, highlighting its potential role in boosting immune responses. No toxicology studies have been reported.

In humans, DKY709 leads to sustained IKZF2 degradation with QD oral dosing. In a Ph. I study (NCT03891953), steady-state plasma concentration/time profiles from two patients given 20 mg of DKY709 orally QD showed DKY709 concentrations remained above 50 ng/mL for at least 8 h post dose. This corresponds to unbound concentrations leading to ~80% IKZF2 degradation in human PBMCs in vitro. A profound decrease of IKZF2 in peripheral FOXP3⁺ T cells was rapidly observed with >80% reduction in IKZF2⁺ T_{reg}s within 24 h after the first dose, and >90% degradation at steady state (4-6 weeks) with daily dosing. No safety results have been reported, but the compound appears to have been discontinued by Novartis.

Patents: [Numerous patents](#) describe simple structural variations on the thalidomide core, but DKY709 falls under original patents from Novartis ([WO2019038717A1](#), [US20210309638A1](#)).

March 2023

ACT-777991

CXCR3

oral reversible CXCR3 antagonist

Ph. I in healthy subjects

opt. of known CXCR3 antagonists

J. Med. Chem., March 8, 2023

IDORSIA PHARMACEUTICALS LTD, CH

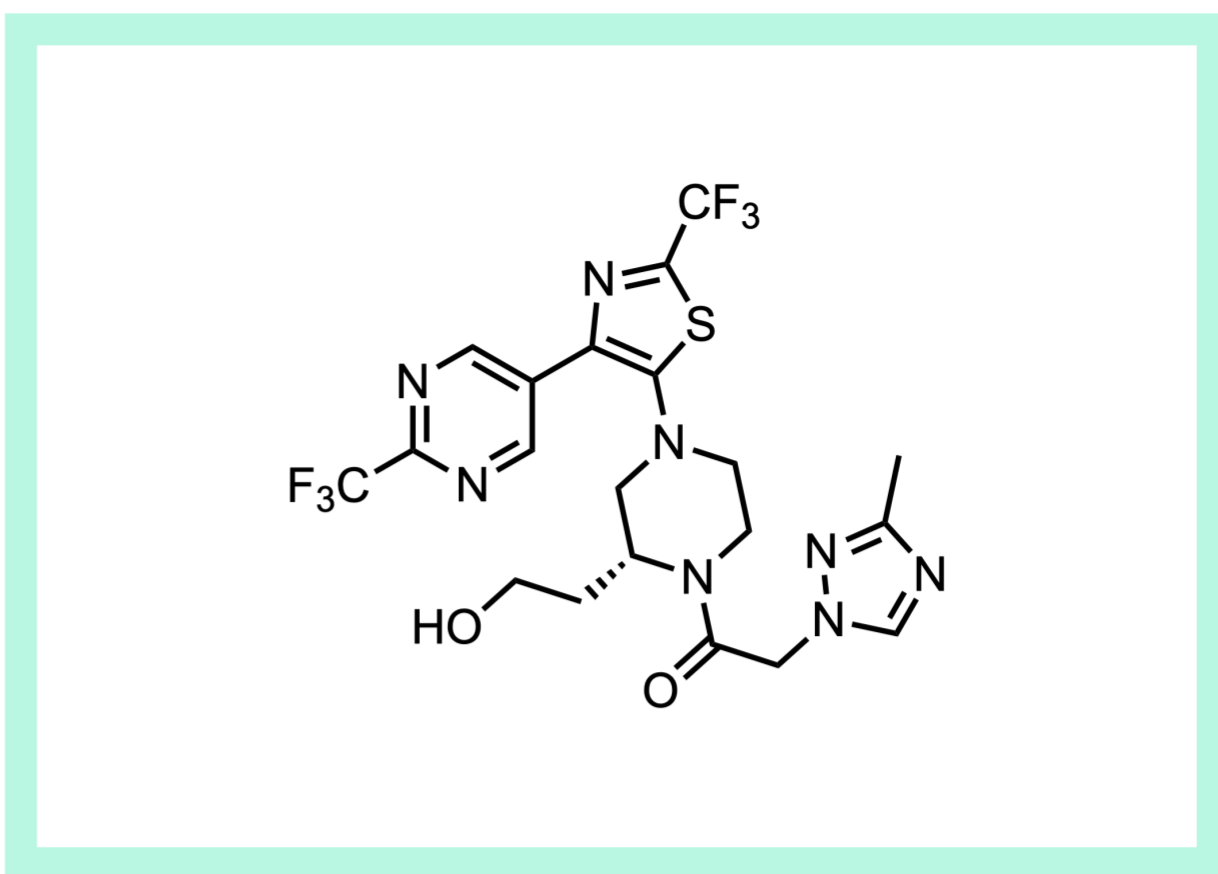
paper DOI:

<https://pubs.acs.org/doi/10.1021/acs.jmedchem.3c00074>

[View Online](#)

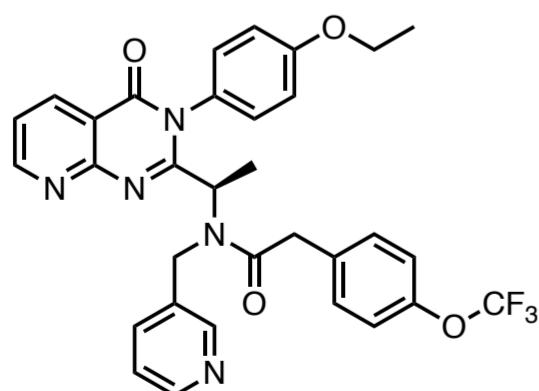
ACT-777991: next-generation CXCR3 antagonist in Phase I trials for Type 1 diabetes. ACT-777991, an oral and insurmountable CXCR3 antagonist discovered by Idorsia (formerly Actelion), is under investigation for the treatment of Type 1 Diabetes (T1D). Despite the complex history of CXCR3 antagonists, ACT-777991 has shown promise with demonstrated in vivo efficacy in T1D mouse models. This compound is the first of its kind to progress to clinical trials since Amgen's AMG 487, which was discontinued due to CYP time-dependent inhibition (TDI) by sequential metabolites. As of May 2022, Phase I results for ACT-777991 are pending, and the asset is listed in [Idorsia's pipeline](#). The advancement of this candidate in T1D, outside of traditional inflammation indications, reflects the industry's continued interest in and evolving understanding of chemokine biology.

CXCR3, an immune response mediator with implications in inflammation and cancer. [C-X-C chemokine receptor type 3 \(CXCR3\)](#), a G-protein-coupled receptor (GPCR), is crucial for immune cell circulation and migration. In the [mid-90s](#), it was found to be upregulated in cells involved in adaptive and innate immunity during inflammation, with [primary expression](#) now known to be on CD4+ and CD8+ T cells. Activated by three ligands, CXCL9 (MIG), CXCL10 (IP-10), and CXCL11 ([ITAC, the most potent](#)), the [CXCR3-CXCL9/10/11 axis](#) is [implicated](#) in various diseases, including [cancer](#), inflammatory diseases, [neurological diseases](#), atherosclerosis, viral infections, and Type 1 diabetes. [CXCL10](#) has been investigated as a target for cancer immunotherapy, while CXCL9 has been found to potentiate the CD8+ T cell-migration in cancer. Both ligands have been studied for their role in autoimmunity, and the role of CXCL9 has remained elusive. The receptor's broad influence underscores its potential as a therapeutic target.

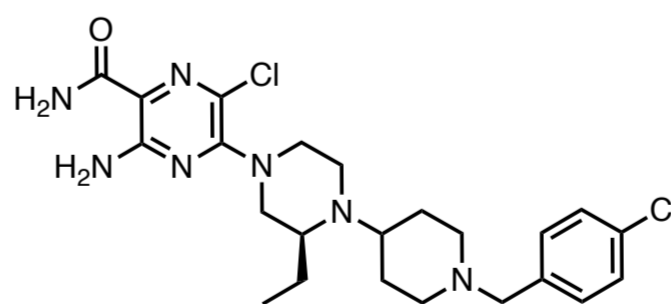


Renewed momentum in CXCR3 antagonist drug development after AMG487's discontinuation. To date, only 2 chemokine receptor drugs have been approved: CCR5 agonist [maraviroc](#) for HIV and CXCR4 antagonist [plerixafor](#) as an immunostimulant in combination with G-CSF for non-Hodgkin's lymphoma. Despite the failure of a [large number of CXCR3 antagonist programs](#) to reach the clinic, interest in this receptor remains, driven by a renewed understanding of chemokine receptor biology and reflected in the [steady rise of CXCR publications](#). Of the 15 classes of identified antagonists, piperazinyl-piperidines (e.g., SCH 546738) and azaquinazolinones (e.g., AMG 487) have been the most optimized, with the latter being the [only one to reach clinical trials](#) until ACT-777991. [Expert opinion](#) in 2016 noted that Amgen 'sneezed' with AMG 487's failure, making other drug developers 'catch a cold' and slow attempts to bring their CXCR3 programs to the clinic. 'The cold' seeped into discovery programs too with a [sharp decline](#) of CXCR3 antagonist patents since 2007, and none in 2012. However, recent patents from Daiichi Sankyo, Sanofi, and Actelion/Idorsia (2016) hint at a potential resurgence in the development of CXCR3 antagonists.

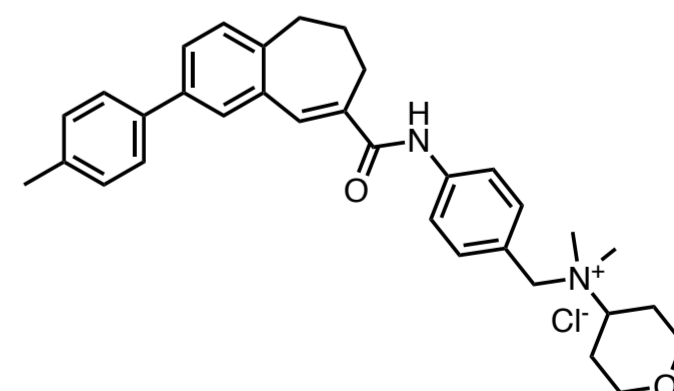
CYP time-dependent inhibition by sequential metabolites caused discontinuation of AMG487, the only small molecule CXCR3 antagonist to reach the clinic. AMG 487, an azaquinazolinone and the [only small molecule CXCR3 antagonist to reach clinical trials](#), was discontinued in Ph. II due to lack of efficacy in psoriasis patients. Despite promising [preclinical potency](#), unexpected pharmacokinetic behavior emerged upon repeated administration, with supraproportional AUC and C_{max} exposure. [Detailed investigation](#) revealed that sequential metabolites of AMG 487 demonstrated competitive and mechanism-based CYP3A4 inhibition, leading to non-linear pharmacokinetics and variable drug exposures. The potential for repeated administration to alter the intrinsic clearance of AMG 487 posed significant development risks, prompting the discontinuation of the program.



AMG 487
oral selective CXCR3 antagonist
CXCR3 IC_{50} = 8.0 nM
discontinued in Ph. II for psoriasis



SCH 546738
oral non-competitive CXCR3 antagonist
CXCR3 K_i = 0.4 nM



TAK-779
CXCR3 antagonist
mCXCR3 IC_{50} (cells) = 369 nM
CCR5 IC_{50} = 1.4 nM
R5 HIV-1 (cells) EC_{50} = 1.2 nM
not developed for HIV due to poor bioavailability

March 2023

ACT-777991

CXCR3

oral reversible CXCR3 antagonist

Ph. I in healthy subjects

opt. of known CXCR3 antagonists

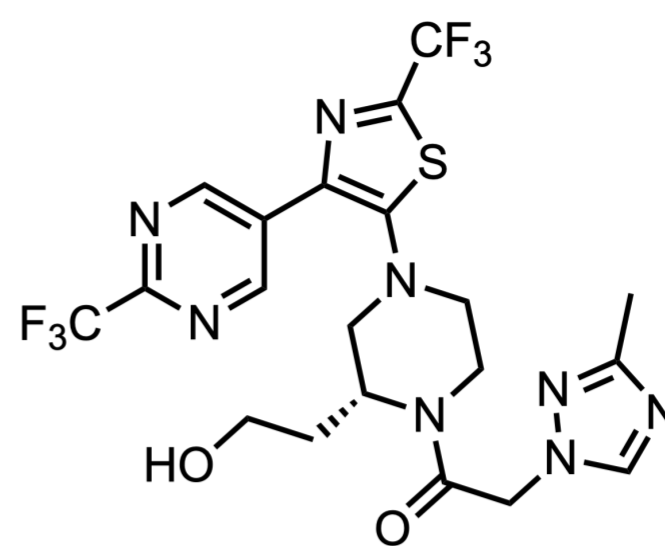
J. Med. Chem., March 8, 2023

IDORSIA PHARMACEUTICALS LTD, CH

paper DOI:

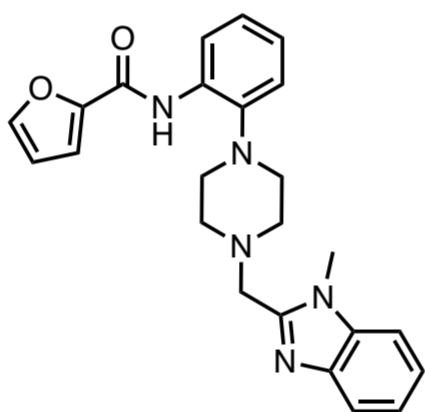
<https://pubs.acs.org/doi/10.1021/acs.jmedchem.3c00074>

[View Online](#)

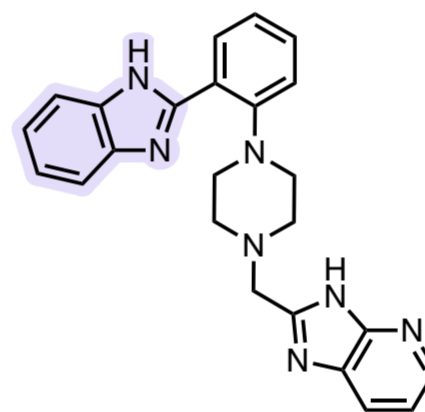


A phenylpiperazine starting point for ACT-777991 from HTS. A phenylpiperazine hit ([compound 1](#)) from a HTS of Actelion-Idorsia's chemical library in a fluorescence-based FLIPR calcium mobilization assay served as the chemistry start for this campaign. Using the CXCL10 ligand as the agonist

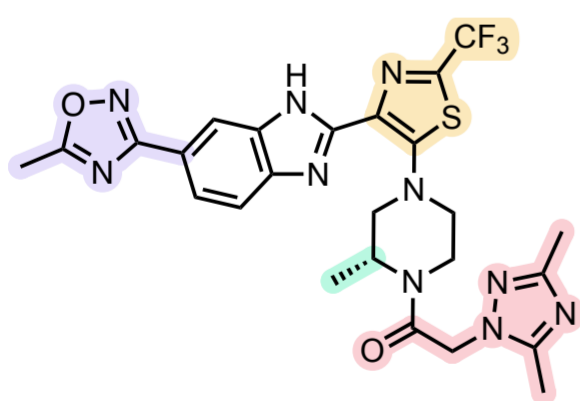
in the assay, the hit demonstrated an IC_{50} of 372 nM. The subsequent hit-to-lead process focused on improving potency with replacements of the furan-2-carboxamide, eventually settling on a benzimidazole with an IC_{50} of 4.3 nM ([compound 3](#), purple).



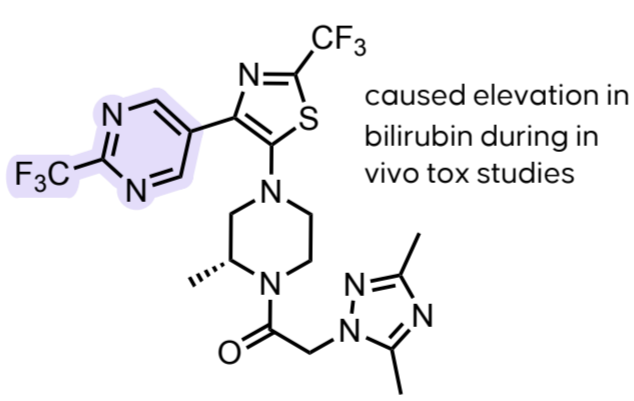
HTS hit 1 (2022 JMC)
FLIPR IC_{50} (CHO-K1) = 372 nM
hERG (QPatch) IC_{50} = 1.4 μ M



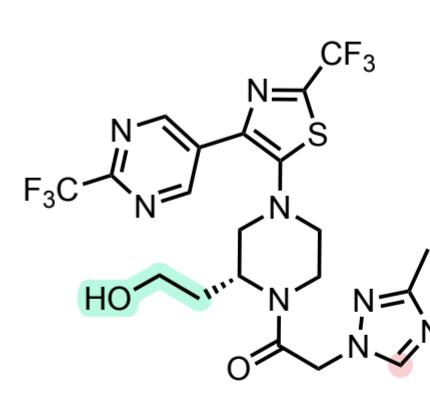
compound 3 (2022 JMC)
FLIPR IC_{50} (CHO-K1) = 4.3 nM
RI IC_{50} (HWB) = 230 nM
hERG (QPatch) IC_{50} = 0.66 μ M



ACT-660602
(compound 1; 9j in 2022 JMC)
FLIPR IC_{50} (CHO-K1) = 2.7 nM
RI IC_{50} (HWB) = 204 nM
hERG IC_{50} > 20 μ M
rCYP2D6 CL_{int} = 0.19 μ L/min/pmol



ACT-672125
(compound 2; 29 in 2022 JMC)
FLIPR IC_{50} (CHO-K1) = 2.5 nM
RI IC_{50} (HWB) = 239 nM
hERG IC_{50} = 18 μ M
rCYP2D6 CL_{int} < 0.04 μ L/min/pmol



ACT-777991
(compound 8a)
RI IC_{50} (HWB) = 56.3 nM
hERG IC_{50} = 26 μ M
rCYP2D6 CL_{int} < 0.04 μ L/min/pmol

March 2023

ACT-777991

CXCR3

oral reversible CXCR3 antagonist

Ph. I in healthy subjects

opt. of known CXCR3 antagonists

J. Med. Chem., March 8, 2023

IDORSIA PHARMACEUTICALS LTD, CH

paper DOI:

<https://pubs.acs.org/doi/10.1021/acs.jmedchem.3c00074>

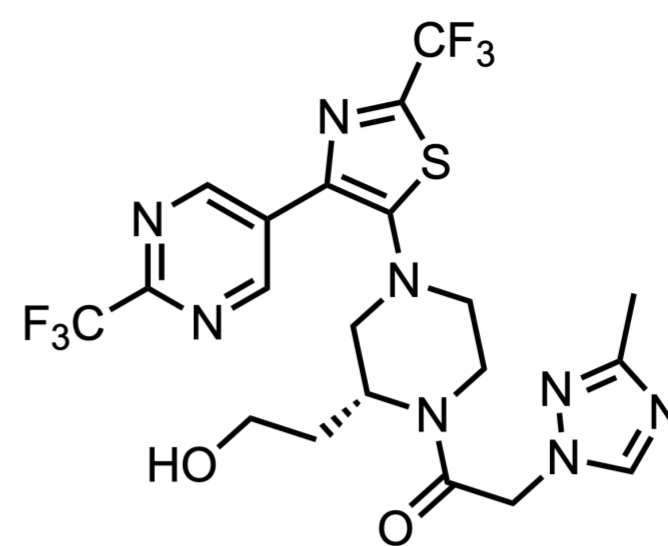
[View Online](#)

Mitigating a pervasive hERG liability by reducing overall molecule lipophilicity. Despite removing the basic amine from the hit, leads with the amide core present in [ACT-672125](#) and [ACT-660602](#) still had significant hERG liabilities. Typical strategies to mitigate hERG like the introduction of a [carboxylic acid](#) led to a loss in CXCR3 affinity.

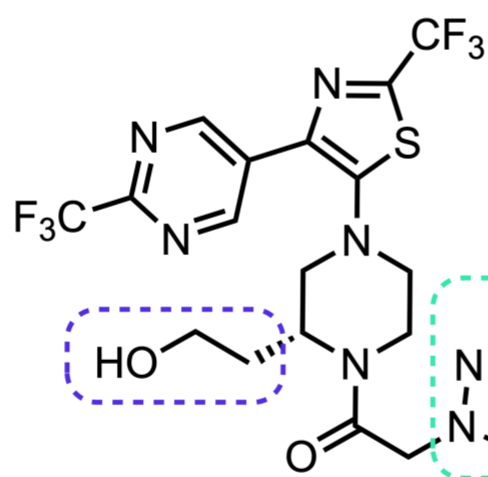
- The discovery of one lead, [ACT-672125](#), was a result of exploring southern aza-benzimidazole replacements (pink), heterocycle-replacements of the phenyl moiety (yellow), and a variety of substitutions on the northern benzimidazole (purple), plus the addition of (*R*)-methyl group on the piperazine (green) to reduce hERG liabilities and maintain/improve potency.
- Another lead discovered in parallel, [ACT-660602](#), was identified following optimization for metabolic stability and addressing the same issues as '2125. The northern substituted benzimidazole was replaced with a 4-trifluoromethyl-pyrimidine (purple) to reduce hERG inhibition, improve

chain length and stereochemistry had no influence on metabolism (purple box). The resultant decrease in lipophilicity for ACT-777991 (8a) improved its unbound fraction in plasma, metabolic stability across species (human, rat, dog) in microsomes and hepatocytes, and reduced in vivo clearance (rat, dog). These findings underline the significance of lipophilicity adjustments in optimizing drug metabolism profiles.

A crystalline API selected to lower the development risk later in the pipeline. The preference for a smaller methyl substituent on the southern heterocycle over larger alkyl substituents in ACT-777991's development was driven by the resulting crystalline solid form. Historically, crystalline forms have shown superior process reproducibility, easier purification and handling, and enhanced stability of the final active pharmaceutical ingredient (API). [Early assessment](#) of solid-state properties in lead compounds is crucial for [risk management](#) in small molecule programs.



- longer piperazine sidechain = higher potency
- stereochem or sidechain length didn't affect CYP2D6 metabolism



- higher solubility
- lower hERG inhibition
- lower CYP2D6/3A4 metabolism

- increasing substituent lipophilicity (e.g., Et-, Pr-, Bu-) increased hERG inhibition
- Me group = crystalline API

ACT-777991

Human CYP2D6 metabolism and bilirubin elevation as key safety issues. While both prior Idorsia molecules ACT-660602 and ACT-672125 demonstrated in vivo efficacy, each had unique issues. '0602 was exclusively metabolized by the [highly polymorphic CYP2D6](#) (in humans), while '2125 caused a concerning [elevation in bilirubin levels](#) in both rat and cynomolgus monkey in vivo tox studies. Thus, [lead optimization](#) efforts focused on increasing potency in the receptor internalization (RI) assay in human blood that the team developed, in addition to achieving a suitable safety profile acceptable for chronic dosing.

Balanced CYP-mediated metabolism achieved through reduction of lipophilicity. Investigations into CYP enzyme contributions to metabolism using individual recombinant CYP enzymes led to a more balanced profile for ACT-777991, with minimized CYP2D6 metabolism. The less lipophilic triazole (vs. pyrazole) and certain substituents on the 5-membered N-heterocycle reduced CYP2D6 and CYP3A4 metabolism (green box), while piperazine side

Binding mode of CXCR3 antagonists not fully understood. While the binding modes of these CXCR3 antagonists from Idorsia have not been reported, [CXCR3-antagonist homology models](#) for virtual screening have been developed. AMG 487 was [predicted to bind](#) in an intrahelical minor pocket of CXCR3, different from the broad-spectrum CCR2/5 and CXCR3 antagonist, TAK-779.

Insurmountable antagonism as a possible avenue to more efficiently control the circulating chemokines during inflammation. While investigating the in vitro pharmacological profile, the team found that increasing concentrations of ACT-777991 reduced the maximal calcium signal (E_{max}) induced by CXCL11, the most potent CXCR3 ligand. This result indicates that ['7991 acts as an insurmountable antagonist](#), which is believed to more efficiently combat the high levels of circulating chemokines for patients with inflammatory disorders. [Insurmountable antagonism](#) is defined as the ability of an antagonist to depress the maximal response for a receptor while also causing rightward shifts of agonist dose-response curves. The phenomenon [may be due to](#) the

March 2023

ACT-777991

CXCR3

oral reversible CXCR3 antagonist

Ph. I in healthy subjects

opt. of known CXCR3 antagonists

J. Med. Chem., March 8, 2023

IDORSIA PHARMACEUTICALS LTD, CH

paper DOI:

<https://pubs.acs.org/doi/10.1021/acs.jmedchem.3c00074>

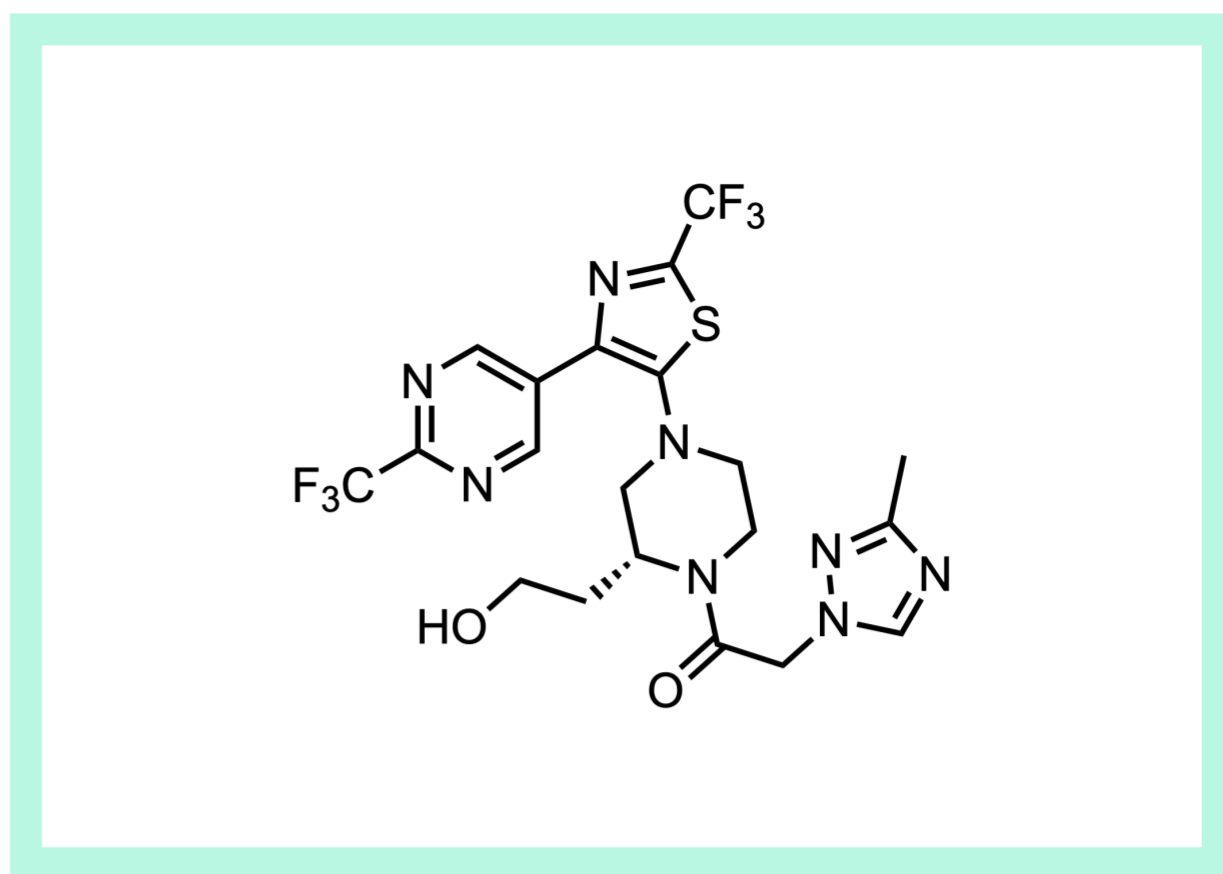
[View Online](#)

longevity of the antagonist-receptor complex, the presence of an allosteric site on the receptor, slow interconversion of receptor conformations, steady removal of the antagonist from specific tissues, among others factors.

- See other March MOTM and insurmountable antagonist, [KW-6356](#), or 2020 MOTM and CXCR7 insurmountable antagonist from Idorsia, [ACT-1004-1239](#), for more on insurmountable antagonism.

Ph. I completed for T1D. The Ph. I trial of 70 healthy subjects was completed in May of last year (2022, [NCT04798209](#)). While the results have not been released, Idorsia has [named](#) a target indication of [recent-onset Type 1 diabetes](#) (T1D) for the molecule. ACT-777991 demonstrated in vivo efficacy for this indication with [reduced blood glucose levels](#) and increased rate of T1D remission when treated in combination with an anti-CD3 antibody in two different T1D mouse models.

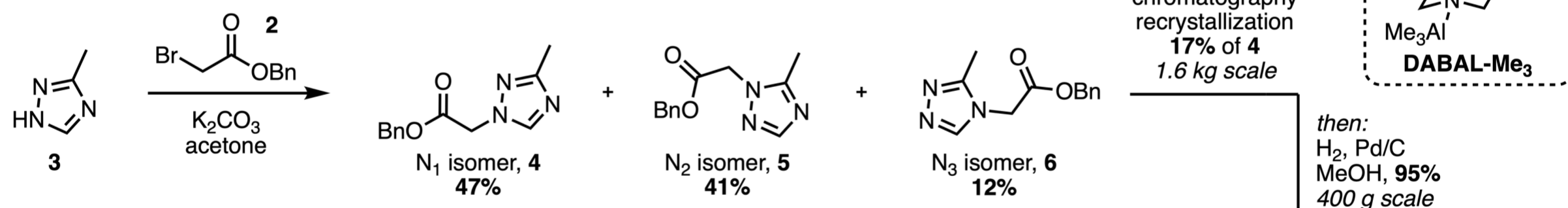
Synthesis-enabled cost-reduction for production on-scale. The [initial route](#) toward the series of compounds investigated in this paper involved



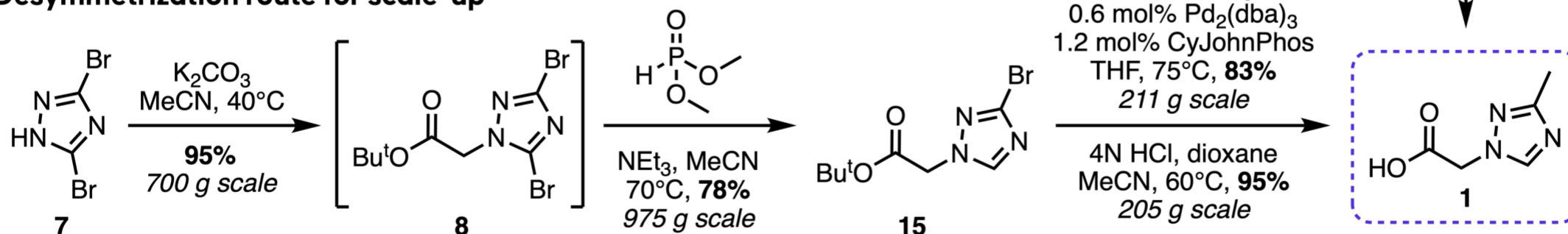
alkylation of the triazole or pyrazole with benzyl bromoacetate for coupling to the piperidine following debenzoylation. However, this strategy suffered from poor *N*-alkylation regioselectivity and required chromatography to isolate the clean regioisomer. Both a de-novo approach of building up the triazole and a desymmetrization route employing a 3,5-dibromo-1H-1,2,4-triazole precursor were [considered for scale-up](#).

The desymmetrization approach improved the overall yield toward southern fragment 1 from 16 to 59%, and enabled a significant ~50% cost savings at only \$8/kg of fragment 1, as compared to \$15/kg for the first generation synthesis. However, the number of isolations increased by one to 3 total (from 2). The de novo approach also required 3 isolations, but at an even lower cost of \$4/kg of 1 (~75% cost savings) and in a 46% overall yield. While the desymmetrization requires use of an expensive Pd₂(dba)₃ catalyst and an uncommon “Me+” source of DABAL-Me₃ that would need to be sourced, the de novo route requires careful safety considerations for the preparation and handling of hydrazine intermediate 17 on-scale.

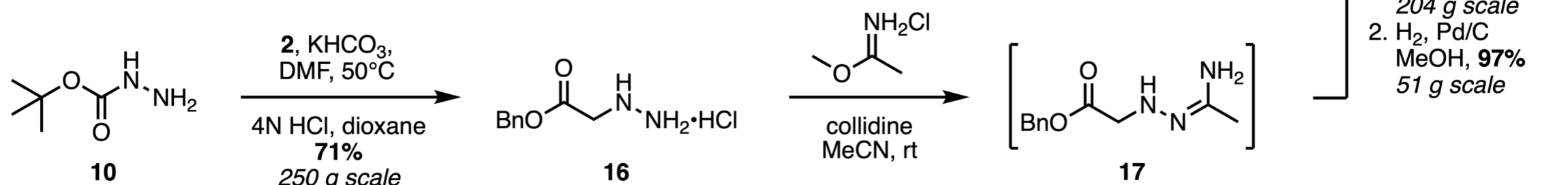
1st-generation med chem route



Desymmetrization route for scale-up



De-novo triazole route for scale-up



March 2023

ACT-777991

CXCR3

oral reversible CXCR3 antagonist

Ph. I in healthy subjects

opt. of known CXCR3 antagonists

J. Med. Chem., March 8, 2023

IDORSIA PHARMACEUTICALS LTD, CH

paper DOI:

<https://pubs.acs.org/doi/10.1021/acs.jmedchem.3c00074>

[View Online](#)

In vitro pharmacology summary for ACT-777991:

- Concentration-dependent inhibition of CXCR3 signaling across species (M/R/D/H, IC_{50} = 1.5–5.3 nM for ligands CXCL9, 10, & 11)
- Binding kinetics: K_d of 4.6 nM
- Reversible binder with fast on/off rates (K_{on} of $6.6 \times 10^6 M^{-1}s^{-1}$ and K_{off} of $0.03 s^{-1}$)
- Functional inhibition in CXCR3-mediated chemotaxis T-cell migration assay (H/M): IC_{50} = 10.5–10.9 nM for T cell migration inhibition toward CXCL11 (chemoattractant) with tritiated '7991 treatment
- CXCR3 receptor internalization assay: IC_{50} of 56 nM for inhibiting receptor internalization (RI) in human whole blood (measured fluorescence of CXCR3-binding antibodies in presence of CXCL10)
- Selectivity for CXCR3 over other chemokine receptors and GPCRs (eg. CCR5, CCR7, CXCR4, CXCR5, CXCR6, FPR1, FPR2, C3aR1, and ChemR23), as well as a panel of 87 potential off-targets at concentrations up to 10 μ M
- Unbound fraction of 10–48% in plasma across all species using ^{14}C -labeled '7991 (at concentrations of 0.1 – 300 μ g/mL in mouse, rat, rabbit, dog and human)
- $\log D_{7.4}$ = 2.3, pK_a = 2.2 (protonation of triazole)
- Solubility @ 37°C: FaSSIF = 718 μ g/mL, FeSSIF = 1252 μ g/mL
- In vitro permeability: (MDCKII cells) P_{app} A-B = 1.5×10^{-6} cm/s

In vivo pharmacology summary for ACT-777991:

- Dose-dependent in vivo efficacy observed in lung inflammation mouse model: mice were dosed (0.006, 0.02, 0.06, 0.2, 0.6, and 2mg/g food) 3 days prior to being exposed to LPS (lipopolysaccharides), which reduced broncho-alveolar lavage (BAL) CD8⁺ T cells (quantified by flow cytometry) and increased CXCR3 expression on CD8⁺ T cells after CXCL10-stimulation
 - Lowest efficacious dose was 0.02 mg/g, with 45% target engagement and evening plasma concentration (C_{trough}) of 99 ng/mL
 - This minimum efficacious concentration used in PBPK modeling predicted human efficacious unbound plasma concentration of 9.9 ng/mL could be achieved with oral dose of 13.5 mg BID or 62 mg QD
- Excellent bioavailability (F, PO) of 80% (rat), 89% (dog), 92% (monkey)
- Low to intermediate clearance (CL) of 9.5 mL/min/kg rat (IV) and dog (IV), and 5.3 for monkey (PO)
- Half life ($t_{1/2}$) of 5.5h (rat), 5.3h (dog), and 4h (monkey)
- Dose-dependent volume of distribution, larger than the total body water: V_{ss} = 1.7–2.7 (rat), 1.2–1.5 (dog), 1.3 (monkey) L/kg

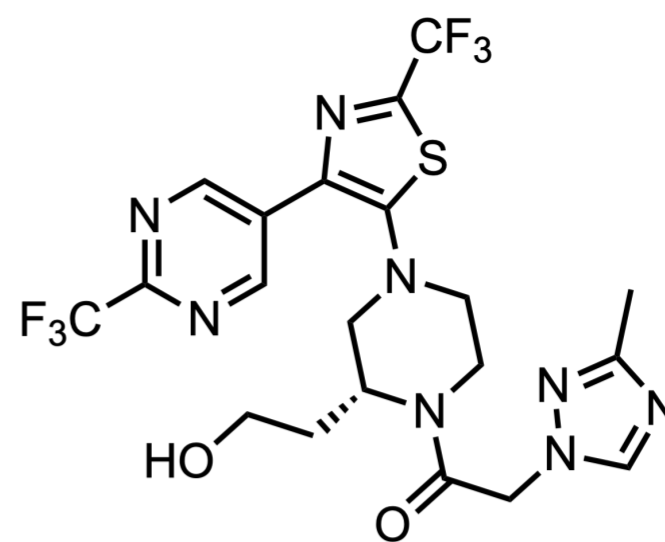
In vitro safety summary:

- No Cyp liability: IC_{50} > 50 μ M for CYP3A4, CYP2C9, and CYP2D6
- No inhibition of human MDR-1/P-gp, OATP1B1, or OATP1B3; but a substrate of MDR-1/P-gp and BCRP
- No reactive metabolite formation (dansyl-glutathione trapping assay)

In vivo safety summary:

- 5–15% dose-dependent QT_c prolongation as compared to vehicle in guinea pigs (IV or PO) and dogs due to hERG inhibition
 - Minimal changes in actual heart rate of dogs indicated that human cardiac risk is low
 - No changes in PR or QRS intervals in either species
- No observed geno- or photo-toxicities allowing for predicted highest safe dose of 140 mg total per day in healthy subjects (AUC ~ 9600 ng·h/mL)

Patents. For ACT-777991: "1-(piperazin-1-yl)-2-([1,2,4]triazol-1-yl)-ethanone derivatives" [WO2015011099A1](#) (2015). For related compounds: "Piperidine cxcr7 receptor modulators" [US20200385373A1](#), [US11306078B2](#) (2020, 2022); "Hydroxyalkyl-piperazine derivatives as cxcr3 receptor modulators" [WO2016113344A1](#) (2016); "(r)-2-methyl-piperazine derivatives as cxcr3 receptor modulators" [WO2016113346A1](#) (2016); "8-(piperazin-1-yl)-1,2,3,4-tetrahydro-isoquinoline derivatives" [WO2015145322A1](#) (2015). "Cxcr7 receptor modulators" [WO2014191929A1](#) (2014) [WO2016087370A1](#) (2016). "4-(benzoimidazol-2-yl)-thiazole compounds and related aza derivatives" [WO2013114332A1](#) (2013); "1-[m-carboxamido(hetero)aryl-methyl]-heterocycl-yl-carboxamide derivatives" [WO2013190508A2](#) / [A3](#) (2013).



Past Molecules

Hall of Fame

2023

[01 January](#)

[02 February](#)

[03 March](#)

2022

[01 January](#)

[02 February](#)

[03 March](#)

[04 April](#)

[05 May](#)

[06 June](#)

[07 July](#)

[08 August](#)

[09 September](#)

[10 October](#)

[11 November](#)

[12 December](#)

2021

[01 January](#)

[02 February](#)

[03 March](#)

[04 April](#)

[05 May](#)

[06 June](#)

[07 July](#)

[08 August](#)

[09 September](#)

[10 October](#)

[11 November](#)

[12 December](#)

2020

[02 February](#)

[03 March](#)

[04 April](#)

[05 May](#)

[06 June](#)

[07 July](#)

[08 August](#)

[09 September](#)

[10 October](#)

[11 November](#)

[12 December](#)

Yearly Nominees

[2020](#)

[2021](#)

[2022](#)

Yearly Winners

[2020](#)

[2021](#)

THANK YOU!

Try Premium

and gain access to hundreds more molecule reviews like this, plus content like:

**Drug Approvals • Tech Reviews • IPO and M&As,
and more features like our sub-structure search.**

sign up for a trial today at
<https://drughunters.com/3WsorHv>

info@drughunter.com